

ISSN 0280-5316
ISRN LUTFD2/TFRT--5825--SE

Model Predictive Control Based Energy Management Algorithm for a Hybrid Excavator

Patrik Thuring

Department of Automatic Control
Lund University
October 2008

Lund University Department of Automatic Control Box 118 SE-221 00 Lund Sweden	<i>Document name</i> MASTER THESIS	
	<i>Date of issue</i> October 2008	
	<i>Document Number</i> ISRN LUTFD2/TFRT--5825--SE	
<i>Author(s)</i> Patrik Thuring	<i>Supervisor</i> Johan Åkesson Automatic Control, Lund Anders Rantzer Automatic Control, Lund (Examiner)	
	<i>Sponsoring organization</i>	
<i>Title and subtitle</i> Model Predictive Control Based Energy Management Algorithm for a Hybrid Excavator (Model Predictive Control baserad energikontrollalgoritm för en hybrid grävmaskin)		
<i>Abstract</i> <p>The Volvo Group has an ambitious plan to efficiencies its construction equipment vehicles with an introduction of a hybrid engine. This Master thesis is based on, as a first approach, to control the energy split in a hybrid construction equipment vehicle (HCEV) with the control strategy Model Predictive Control (MPC). The work is divided into two main parts, where the first one is to create a piece-wise affine system (PWA) of the nonlinear plant and secondly to define the control strategy. Multiple linear models are created from the different mathematical descriptions with the Taylor expansion and then divided in space with polytopes to represent the hybrid dynamics properly. After that, the MPC strategy is to be created and this is done by defining a cost function, where selected variables should follow some trajectory. At each sample, the MPC controller should compute an optimal control signal during the prediction and control horizon to minimize the fuel consumption, make the internal combustion engine run at a favourable rotational speed and save the durability on the battery. The control problem is simulated in Simulink with a pre-defined driving cycle, as can be seen as an artificial user for the HCEV, which generates a power demand that needs to be satisfied.</p>		
<i>Keywords</i>		
<i>Classification system and/or index terms (if any)</i>		
<i>Supplementary bibliographical information</i>		
<i>ISSN and key title</i> 0280-5316		<i>ISBN</i>
<i>Language</i> English	<i>Number of pages</i> 89	<i>Recipient's notes</i>
<i>Security classification</i>		

1. CONTENTS

1.	CONTENTS	2
2.	SUMMARY	4
3.	INTRODUCTION	5
3.1.	Background	5
3.1.1.	Hybrid Construction Equipment Vehicles	5
3.2.	Literature survey	7
3.3.	Motivation to the work.....	8
3.4.	Control goals	9
4.	THEORY AND TOOLS.....	10
4.1.	Piece-wise affine system	10
4.1.1.	Linearization	11
4.1.2.	Polytope	12
4.2.	Model Predictive Control	13
4.2.1.	Simple example.....	14
4.2.2.	Hard constraints	17
4.2.3.	Soft constraints.....	17
4.3.	Model Predictive Control for Piece-wise affine system	18
4.4.	Matlab and Multi-Parametric toolbox	19
4.4.1.	Matlab and Simulink.....	19
4.4.2.	Multi-Parametric toolbox.....	19
4.4.3.	Maple	20
5.	MODELING	21
5.1.	Model description	21
5.2.	Mathematical description of the plant	24
5.2.1.	Evaluation of mappings	30
5.3.	Linearization of system.....	30
5.3.1.	Linearization points.....	31
5.3.2.	Creating Piece-wise affine system	33
5.4.	Sampling time.....	34
5.5.	Handling disturbances	34
5.6.	Model validation	36
5.7.	The linearization of the switches	37
5.7.1.	Pressure difference	37
5.7.2.	Power output from generator	38
5.7.3.	Power output from ESS.....	39
5.8.	Linearization of the plant	40
5.8.3.	PWA 1	41
5.8.3.	PWA 2.....	43
5.8.3.	PWA 3.....	45
6.	MPC SYNTHESIS	48
6.1.	Control objectives.....	48

6.2.	Cost function	49
6.2.1.	Introduction of new control signals	50
6.2.2.	Approach 1: Minimize the fuel consumption	51
6.2.3.	Approach 2: Minimize the losses in the system.....	52
6.3.	Constraints	54
6.3.1.	Physical constraints in the system.....	56
6.4.	Tuning	57
6.5.	Experienced problems.....	58
6.5.1.	MPT limitations	58
6.5.2.	Computational time.....	58
7.	RESULTS.....	59
7.1.	MPC operating (disturbance constant in pred. horizon).....	59
7.1.1.	MPC 1	59
7.1.2.	MPC 2	62
7.1.3.	MPC 3	64
7.1.4.	MPC operating on the nonlinear plant	66
8.	CONCLUSIONS	69
9.	REFERENCES	70
9.1.	References	70
10.	APPENDIX	71
10.1.	Pumps	71
10.2.	Engine system	71
10.3.	Electrical system.....	72
10.4.	Generator	72
10.5.	ESS	72
10.6.	Swing system	73
10.7.	Mapping definitions.....	73
10.8.	Graphical illustration of maps	74
10.9.	Switch.....	77
10.10.	Constraints	78
10.11.	Simulink file on the linearization of the switches.....	79
10.12.	Simulink file for the MPC control	80
10.13.	Coefficients in the jacobian matrices	81

2. SUMMARY

The goal is to control the power split in a Hybrid Construction Machine (HCM) with the control strategy; Model Predictive Control (MPC). This is done by first creating linear models from the mathematical descriptions of the dynamical behaviour of a HCEV. These models are then divided in space to form a Piece-wise affine system as an approximation of a hybrid plant. After the MPC model has been created, the control strategy is to be defined and this is done with a cost function which shall penalize deviations from a set of reference signals, i.e. have the rotational speed be in a specific interval and minimize the fuel consumption. The optimization is applied during the prediction and control horizon in the controller, which introduce the predictive feature in the system. Also, with the use of a MPC controller, physical constraints can be taken into account to simulate the HCM according to reality.

The developed controller is then used in Simulink along with a driving cycle, which generates a power demand from the excavator, to evaluate the controller's performance.

Three models with different approximation levels are evaluated against each other with a simple PI controller operating to choose the most appropriate one. The best one is then used as a PWA model in the MPC controller, where three different MPC control strategies are simulated. These control strategies should be optimized in aspects of low fuel consumption and other dynamical variables.

The results from these control strategies show that the control problem is of a very complex structure and due to limitations on the used toolbox in Matlab, the Multi-parametric toolbox, only an online MPC controller could be created. This lead to a high computational time with a complex controller, i.e. long prediction and control horizon, many linear models in the MPC controller and a short sample interval. Only a short prediction horizon could be used and therefore, the results obtained in this Master thesis are not completely satisfying. For example, indications have been shown that the fuel consumption can be minimized further with a more intelligent controller, i.e. longer prediction horizon.

3. INTRODUCTION

3.1. Background

As with the increasing consumption of petroleum fuel and with the much stricter carbon dioxide (CO₂) policy from governments, greater efforts have been applied to replace our transportation vehicles and hence minimize the fuel consumption. When it comes to hybrid construction equipment vehicles (HCEV), a significant reduction in fuel consumption can be achieved compared to a traditional vehicle due to the fact that the power demand can be divided between both an engine and a battery.

Good preferences for a hybrid construction machine;

- The option of turning on/off the internal combustion engine.
- More favorable working points
- Regenerative power in the system

With the on-going technical development in the hybrid vehicle section, much attention is given to improving the energy control algorithm (ECA) to optimize the energy flow and hence receive lower fuel consumption. One of the Volvo group's biggest competitors, Komatsu, has developed a HCEV that minimizes fuel consumption with 20-40 % [9], but there are expectations in which the fuel consumption can be reduced further with a more intelligent ECA. One of these future thoughts on optimization control strategies is Model Predictive Control which is an intelligent and complex control algorithm.

In Table 1 the key words in this work are highlighted.

Shortage of expression	Meaning
ECA	Energy control algorithm
EGM	Engine mode
EM	Electrical motor
EMA	Energy management algorithm
ESS	Energy storage system
HCEV	Hybrid construction electrical vehicle
ICE	Internal combustion engine
MPC	Model Predictive Control
MPT	Multi-parametric toolbox
SoE	State of energy
SWEM	Swing electrical machine

Table 1. Clarifications on shortage of expressions

3.1.1. Hybrid construction equipment vehicles

The Volvo group has an ambitious plan regarding development of HCEVs. One important challenge when developing such vehicles is to control the energy flows. The control of a hybrid vehicle is more complex compared to a conventional one and the reason is that the power demand is split between a primary power unit (normally an engine) and a secondary power unit (typically a battery). There are quite a lot of differences between a hybrid car and a hybrid construction equipment machine, such as the power demand comes from different actuators, namely the hydraulic pumps and the swing. The actuators are driven through hydraulic and include the *boom cylinder*, *arm cylinder* and *bucket cylinder* in Figure 1 below. Furthermore, the swing is a rotation mechanism that is situated above the undercarriage and makes the upper structure rotates 360 degrees, which also can be seen in Figure 1. This mechanism is electrically driven.

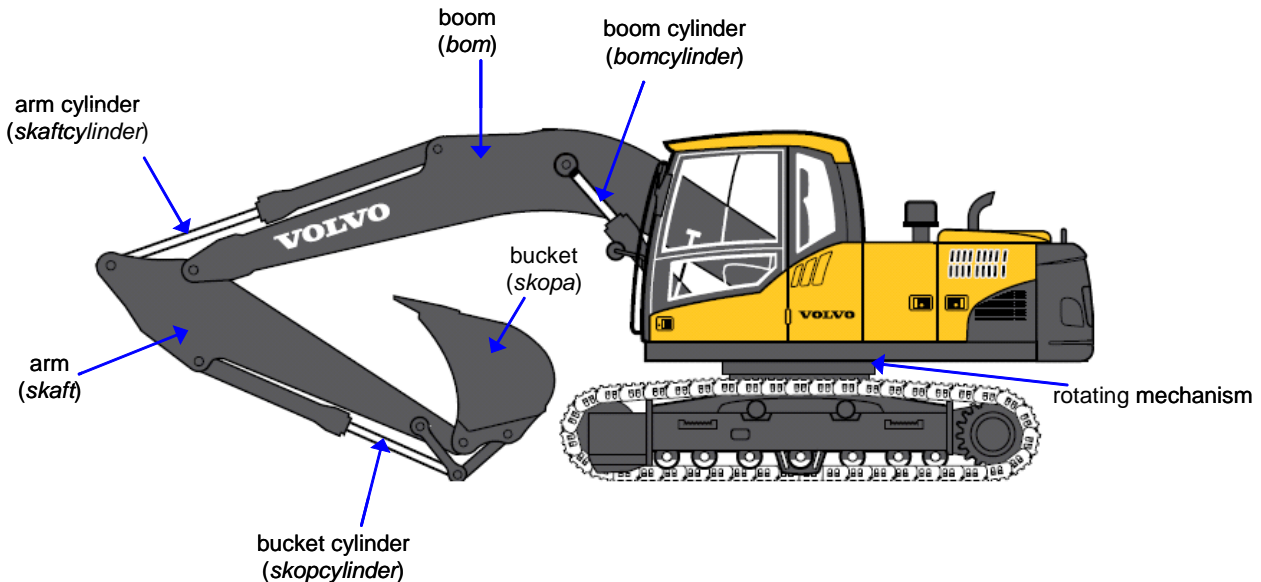


Figure 1. Basic construction of a typical hydraulic excavator

The hydraulic actuators are driven with mechanical power and the swing gets its power demand from an EM that is mounted on the swing. These actuators receive their power demand directly from the ICE or indirectly from the ESS. This is done through a generator, which converts the electrical power to mechanical power. Furthermore, the rotating mechanism in Figure 1 is denoted SWEM and receives its electrical power demand directly from the ESS or indirectly from the generator. In the last case mentioned, the mechanical power is transformed to electrical power needed for the EM. The SWEM can also regenerate energy back to the battery or to the hydraulic actuators through the generator. This is done when the swing rotation mechanism brakes and converts the kinetic energy to electrical energy.

Another difference between an ordinary hybrid vehicle and a HCEV is that the HCEV has several working modes which correspond to different dynamics and different constraints in the system. Furthermore, changes between high and low power is more frequent for an excavator than for a traditional car, which leads to more difficulties in controlling the dynamics in the system.

In Figure 2 a system overview is shown that illustrates the different power demanding units and its suppliers.



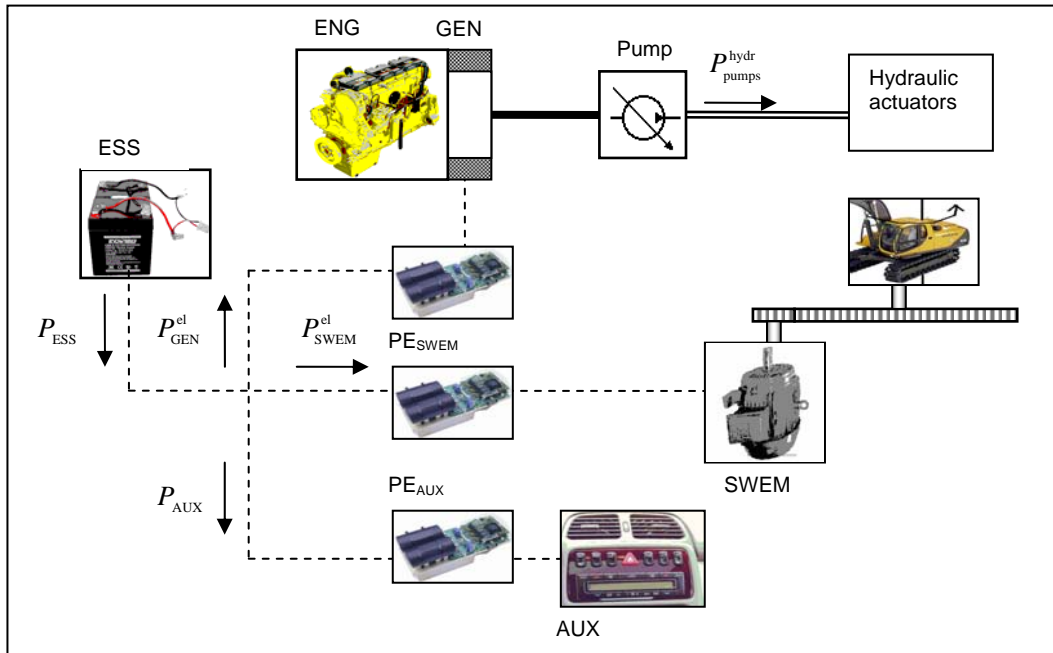


Figure 2. System overview, including power electronics (PE), SWEM stands for swing electric machine and GEN for generator.

The system contains two source of power suppliers, the internal combustion engine (ENG in Figure 2) and the energy storage system (ESS in Figure 2). These two should satisfy the power demanding units, which are the hydraulic actuators (denoted P_{pumps}^{hydr}), the swing electrical machine (denoted P_{SWEM}^{el}) and the power to the AUX (denoted P_{AUX}). In order to convert the mechanical power from the ICE to electrical power (or the opposite), a generator is needed. The generator is mounted directly on the engine as can be seen in Figure 2 and this assumption is made throughout this Master thesis, i.e. the ICE has the same rotational speed as the generator.

As also can be seen in the figure above is the box denoted Hydraulic actuators, which include the boom, arm and bucket cylinders. The rotational mechanism can be seen on the right side in Figure 2, above the SWEM box.

The user interaction in the excavator is replaced with a driving cycle which generates for each work mode a power demand from the hydraulic pumps and from the swing system in a given time interval. A work mode is a predefined session of actions, for example one work mode is called "dig and dump", which digs one scoop and then rotates 90 degrees and then dumps the diggings. For this mentioned session, a mechanical and an electrical power demand are generated in time. The driving cycle is described further in Section 4.1

3.2. Literature survey

From the literature study, it seems that there has been some development regarding hybrid control algorithm for systems similar to this, but not anything where the control algorithm was base on Model Predictive Control (MPC). The whole description of the excavator dynamics and simulation results from a number of working modes where handed out from the beginning of the Thesis work. A lot of the basic work was omitted from that literature but soon after that much more attention was redirected to theory on Model Predictive Control. Some of the most important are displayed below.

In the MPCtools 1.0 – Reference Manual a simple approach on the MPC theory can be found and some easy examples. This is just a basic theory ground for this Thesis because this toolbox is not developed for hybrid systems. The manual can be found in [10].

Most of the theory behind MPC is found in “*Predictive Control with constraints*” [4], which describe different areas of MPC, for example setting up the state-space form and solving predictive control problems. The most important theories on MPC and an easy example are highlighted in Section 4 in this work.

The Multi-Parametric Toolbox is a Matlab program that is developed to describe and simulate a general hybrid system. In this toolbox, there are possibilities to include switches in the system (a more detailed explanation on this can be found in Section 4), which is important for simulation of HCEV. Theory and implementation of a system with such characteristics are documented, with system structures as *linear time-invariant system* (LTI) and what is more interesting in this thesis, *Piecewise Affine system* (PWA). Furthermore, description on how to define different parameters thorough in the regulator can also be found in this toolbox, Multi-Parametric Toolbox (MPT) [7].

The report “Energy management for vehicle power net with flexible electric load demand” [12], which was presented at the 2005 IEEE Conference on Control Applications brings MPC up as a control strategy for a hybrid electrical vehicle. A very basic approach on how MPC should be used as the ECA is presented.

The literature “Computer controlled system” handles computer controlled systems in general. Much theory behind how to discretize systems, choose sampling time etc. Some theory on cost functions can also be found in this book [13].

The document “Conceptual power split control functionally – Power system modeling” [1] is the most important document provided by Volvo Technology. It describes mathematically the HCEV, i.e. for example the generator, the battery etc. and also the system constraints. These equations form a ground for the models used in this work.

“Predictive control for energy management in all/more electric vehicles with multiple energy storage system” [15] is an article from the IEEE which describes a MPC approach for a car with multiple batteries. This article brings up some useful thoughts regarding the control strategy, i.e. describing the cost function and how to define it.

3.3. Motivation to the work

Building real HCEV is very expensive and time demanding, and without extensive preparations, projects can turn out less successive. Therefore system modeling and simulation is mostly necessary in order to produce good products that are competitive on the market.

As a first step to introduce an HCEV base on this EMA from the Volvo group on the market, this report focus on developing a first simulation experiment that includes a model of the system and a MPC regulator that controls the dynamics, and to compare this to other ECA with the same plant.

The following advantages are potentially present when MPC is used in HCEV.

- **MPC as the ECA:** As mentioned earlier in this paper, the literature survey has lead to the conclusion that there have not been any ECA based on MPC reported for system similar to the one present, and this is one of the main driving forces from the Volvo group in this matter. With the introduction of a MPC controller as the ECA, a more intelligent controller is applied compare to, for example, a PI regulator.
 - **MPC characteristics:** With the use of MPC, some new ideas are created in order to control the power split, which are then followed with theoretically and preposterous advantages. The most important ones are multiple input – multiple output and constrains handling. Constrains handling can be achieved as well with an arbitrary ECA with carefully tuning, but to maximizing the performance, the process should run as close as possible towards the constraints in the system without violating them and this can be achieved with the MPC controller.
 - **Avoid high engine speeds:** Because of the predictive feature in MPC, one idea is to completely remove the high engine speed modes that consume very much fuel in the excavator. An illustration of this can be seen in Figure 3, where the prediction horizon is defined as (H_p).
-
-
-

- **Minimize rapid engine power changes:** One strong advantage with the MPC feature is to minimize the rapid power change that can take place when operating the excavator. This is achieved by predicting the future power demand and thus, creating smoother power changes in the system.
- **Real world adaptations:** The regulator can be optimized for real world cycles and not only on predefined driving cycles. This is because the ECA is based on a model described by physical and mechanical equations of an excavator. The ECA can also be adapted for other excavator sizes and types.
- **Fast online** It is possible to create an explicit MPC controller which is much faster than an online base controller due to the use of pre-calculated control laws. During the simulation, investigation is only needed to find the right polytope (see Section 4.1.2) for the current states and inputs to find the appropriate control law. This results in a much faster controller compared to an online controller, where all models must be evaluated during the prediction horizon at each sample.

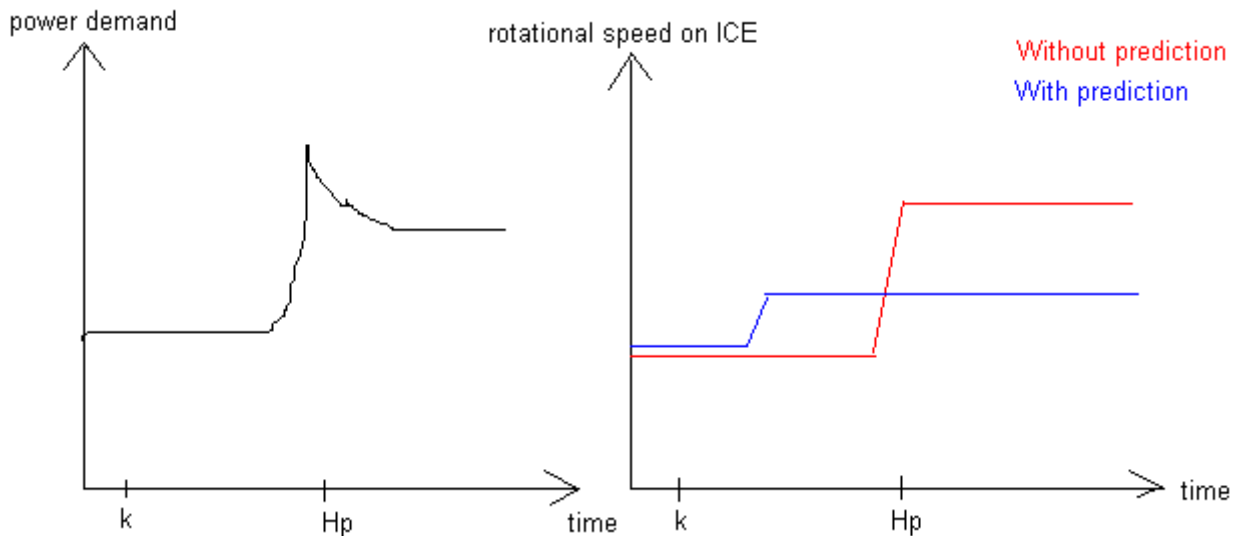


Figure 3. Simple illustration on how the predictive feature can be used in a MPC controller, H_p stands for prediction horizon.

3.4. Control goals

The objective of this work is to control the split between the primary and secondary power unit in a hybrid excavator. The idea is to implement a model predictive control based control-technique with focus on the use of optimal control techniques (finite in the time horizon) in combination with a known driving cycle to derive a control algorithm. The system should at all time satisfy the physical constraints on the included variables in an excavator.

This is done by operating the excavator at a preferable engine mode and at the same time satisfies the power demand in the machine. The two power supplying units, i.e. ICE and the ESS should cooperate and form an optimal power split which minimizes the fuel consumption, but at the same time satisfy the power demand and other constraints in the system.

4. THEORY AND TOOLS

In this section, the used theory and tools are presented and summarized. The theory is divided into three major subsections; Piece-wise affine system (PWA), MPC and MPC for PWA system. After all theory has been described, the used tools are highlighted with a following description.

4.1. Piece-wise affine system

All systems described by hybrid dynamics are nonlinear. Assume that the derivatives in the dynamics (denoted states, x in (1)) are given by a nonlinear function, $f(x, u)$, of the states and some sort of input (denoted u in (1)). Furthermore, the dynamics in the system that is not denoted states or inputs are defined as outputs (y in (2)) and are given by a nonlinear function $g(x, u)$.

$$\dot{x} = f(x, u) \tag{1}$$

$$y = g(x, u) \tag{2}$$

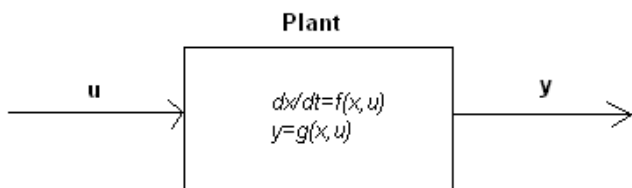


Figure 4. Illustration on a nonlinear plant with inputs (u) and outputs (y).

If the equations above were linear or would be made linear, the result would be a linear model of the dynamics, i.e. a linear model of the plant. Many control problems are based on this plant but with a hybrid system described mathematically, this becomes infeasible.

In a hybrid system, one mathematical description is not sufficient to cover the complete behavior of the hybrid plant and multiple mathematical descriptions are needed. For example, in a hybrid system there exist efficiency factors on the ESS, where the variable changes due to if the ESS should be charged or drained. This leads to multiple mathematical descriptions as shown in (3-4), where the index (i) stands for the different descriptions.

$$\dot{x} = f_{(i)}(x, u) \tag{3}$$

$$y = g_{(i)}(x, u) \tag{4}$$

The illustration on a nonlinear plant with three different models is shown in Figure 5.

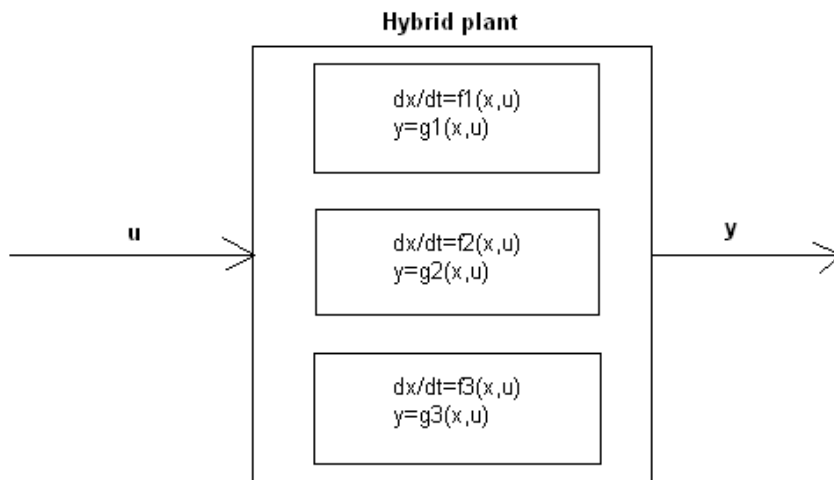


Figure 5. Illustration on a nonlinear hybrid plant with inputs (u) and outputs (y)

If the system above would be linearized, i.e. create multiple linear models from the nonlinear functions, the results would be a piece-wise affine system (PWA).

4.1.1. Linearization

The linearization of the nonlinear functions is done by using the first order Taylor expansion, where the approximation of the nonlinear functions is applied around some specific points in the system. These points are denoted linearization points and form the state-space representations as will be seen further down in this section.

With the Taylor expansion applied to the expressions in (3-4) the result becomes linear equations around a linearization point (x_0, u_0) as shown in (5-6).

$$\dot{x} = f_{(i)}(x, u) \approx f_{(i)}(x_0, u_0) + \frac{\partial f_{(i)}(x_0, u_0)}{\partial x}(x - x_0) + \frac{\partial f_{(i)}(x_0, u_0)}{\partial u}(u - u_0) \quad (5)$$

$$y = g_{(i)}(x, u) \approx g_{(i)}(x_0, u_0) + \frac{\partial g_{(i)}(x_0, u_0)}{\partial x}(x - x_0) + \frac{\partial g_{(i)}(x_0, u_0)}{\partial u}(u - u_0) \quad (6)$$

The linearization points, as can be seen above, are the states and the inputs in the system and these approximate the nonlinear functions (f, g) around constant values. With other words, if a nonlinear function would be linearized around a specific value, the created linear function would be more accurate if the evaluation would be close to the linearization point. This, of course, is also dependent on what grade on the nonlinearity of the function.

The offset terms in (5-6) are not preferable in this approach of PWA system and therefore the expressions are rewritten to (7-8). This is done by multiplying the parentheses and gather all constant terms in one parameter (F, G) , as in (9-10).

$$\dot{x} \approx \frac{\partial f_{(i)}(x_0, u_0)}{\partial x}x + \frac{\partial f_{(i)}(x_0, u_0)}{\partial u}u + F_{(i)} = A_{(i)}x + B_{(i)}u + F_{(i)} \quad (7)$$

$$y \approx \frac{\partial g_{(i)}(x_0, u_0)}{\partial x}x + \frac{\partial g_{(i)}(x_0, u_0)}{\partial u}u + G_{(i)} = C_{(i)}x + D_{(i)}u + G_{(i)} \quad (8)$$

$$F_{(i)} = f_{(i)}(x_0, u_0, d_0) - \frac{\partial f_{(i)}(x_0, u_0, d_0)}{\partial x} \cdot x_0 - \frac{\partial f_{(i)}(x_0, u_0, d_0)}{\partial u} \cdot u_0 \quad (9)$$

$$G_{(i)} = g_{(i)}(x_0, u_0, d_0) - \frac{\partial g_{(i)}(x_0, u_0, d_0)}{\partial x} \cdot x_0 - \frac{\partial g_{(i)}(x_0, u_0, d_0)}{\partial u} \cdot u_0 \quad (10)$$

The result from this rewriting is the well-known state-space form with two constants included. These constants are called the affine terms.

The partial derivatives of the functions $(\partial f, \partial g)$ are gathered together in jacobian matrices, where the elements represent all the thorough partial derivatives evaluated in the linearization points.

An easy example on this is to say that a nonlinear system is described by the equations (e1.1-e1.2);

$$\dot{x} = \sin(x) + u \quad (e1.1)$$

$$y = x + u^2 \quad (e1.2)$$

The system equation in this example is clearly nonlinear and the linear matrices from the first order Taylor expansion become;

$$\dot{x} = \sin(x_0) + u_0 + \cos(x_0) \cdot (x - x_0) + 1 \cdot (u - u_0) = Ax + Bu + F \quad (e1.3)$$

$$y = x_0 + u_0^2 + 1 \cdot (x - x_0) + 2u_0 \cdot (u - u_0) = Cx + Du + G \quad (e1.4)$$

$$\begin{cases} A = \cos(x_0) \\ B = 1 \\ F = \sin(x_0) + u_0 - \cos(x_0) \cdot x_0 - u_0 = \sin(x_0) - \cos(x_0) \\ C = 1 \\ D = 2u_0 \\ G = x_0 + u_0^2 - x_0 - 2u_0^2 = -u_0^2 \end{cases} \quad (\text{e1.5})$$

4.1.2. Polytopes

One could see a Piece-wise affine system as a sort of gain scheduling. Gain scheduling systems, and thus PWA systems are based on multiple models of the plant and where each model describes the dynamics of the plant in a certain region.

This region is built up with a number of polytopes which divides the different state-space representations. Furthermore, these polytopes are defined by the states and the inputs to the system, i.e. for a given value of (x, u) there exists a polytope which is connected to a linear model of the plant around a specific dynamic behavior. In the MPT the creation of these polytopes are made with so called guard lines which define the interval of the region. These are called polytopes and the definition can be found below, which is taken from the *MPT manual* [7].

Polytopic (or, more general, polyhedral) sets are an integral part of multi-parametric programming.

Definition 1 (polyhedron): A convex set $Q \subseteq \mathfrak{R}^n$ given as an intersection of a finite number of closed half-spaces;

$$Q = \{x \in \mathfrak{R}^n \mid Q^x x \leq Q^c\}, \text{ is called } \textit{polyhedron}. \quad (11)$$

Definition 2 (polytope): A bounded polyhedron $\mathfrak{S} \subset \mathfrak{R}^n$

$$\mathfrak{S} = \{x \in \mathfrak{R}^n \mid P^x x \leq P^c\}, \text{ is called } \textit{polytope}. \quad (12)$$

The theory behind polytope can be found in [7], but as a short summary and in this case, polytopes represent different subspaces in the definition area for the states and inputs. When the system dynamics are in a specific polytope, then there exists a linear representation of the plant which describes the dynamics approximately. Also, polytopes are always limited in there definition area and convex.

The dynamical behavior of a general class of system is captured by relations of the following form in the MPT (notice here the discrete time);

$$\begin{aligned} x(k+1) &= A_i x(k) + B_i u(k) + f_i \\ y(k) &= C_i x(k) + D_i u(k) + g_i \end{aligned} \quad (13)$$

Each dynamics (i) is active in a polyhedral partition bounded by the so-called guard lines;

$$\textit{guard}X_i x(k) + \textit{guard}U_i u(k) \leq \textit{guard}C_i \quad (14)$$

For each (i) there exists a specific state-space representation defined by these guard lines in (14).

In this work, the dimension of the whole definition area for the polytopes is of an order 7 (three states and four inputs as will be defined later on).

How these polytopes are divided in space is of course impossible to show graphically but as for comprehension an easy example is studied.

Assume there exists a system with only two states and the different dynamics only depend on the value of these states, i.e. in (14) $\textit{guard}U_i = [0 \ 0]$. In Figure 6 three polytope have been plotted to illustrate where the different models are active. If x_1 (x_1 in Figure 6) has a value in $3 \leq x_1 \leq 7$ and x_2 (x_2 in Figure

6) has a value in $0 \leq x_2 \leq 10$, then “model 1” is active (area colored red in Figure 6). Furthermore, if the states are in the set $7 \leq x_1 \leq 10$ and $0 \leq x_2 \leq 10$, then “model 2” is active (area colored green). At last, if the values of the states are in the interval $0 \leq x_1 \leq 3$ and $0 \leq x_2 \leq 10$ “Model 3” is active (area colored blue).

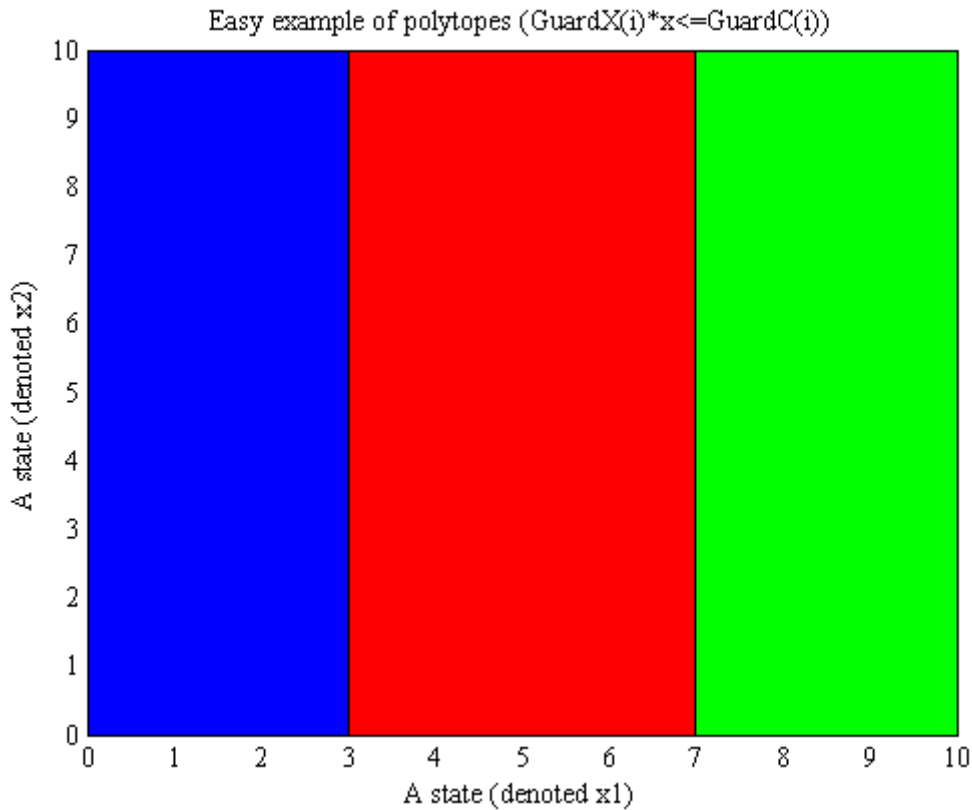


Figure 6. An example of 3 polytopes which describes different dynamics in a plant.

4.2. Model predictive control

The method Model Predictive Control (MPC), which shall be the applied control algorithm, has some very good aspects that suit this problem well, see Section 3.4. MPC is of nature very good when handling multiple-inputs multiple-outputs (MIMO) and take constraints on inputs, states and outputs into account. The control strategy in the MPC approach is that it uses a receding control horizon. This is because the MPC controller solves, at each sampling instant, a finite horizon optimal control problem. The calculated control signals in this way are used differently compare to other control strategies, the first value of the resulting optimal control variable solution is applied to the plant and the rest are discarded. Then the same procedure is repeated at the next sampling interval with the prediction horizon shifted one step ahead, as with the strategy implies, i.e. receding control horizon.

A short theoretical explanation on MPC follows, but a more detailed version can be found in [4]. The MPC algorithm uses a so called prediction horizon and a control horizon to compute an optimal control signal. As stated before, a finite horizon optimal control problem is computed at each sample and the first control signal calculated is then applied to the plant while the rest are discarded, and then the procedure starts all over again at the next sampling interval. The idea is shown in Figure 7, where the controlled output (\hat{z}) should follow some reference signal (r). Notice also that H_p stands for prediction horizon and H_u stands for control horizon. The prediction of the controlled variables (\hat{z}) is performed over an interval with length H_p samples. Furthermore, the predicted control variables (\hat{u}) are predicted during the length of the control horizon and after that it stays fixed during the rest of the prediction

horizon. The complexity in the system increases rapidly when the control horizon is increased. This is because the decision variables in the optimization problem increase with H_u . In most cases the control horizon is smaller than the prediction horizon ($H_u < H_p$).

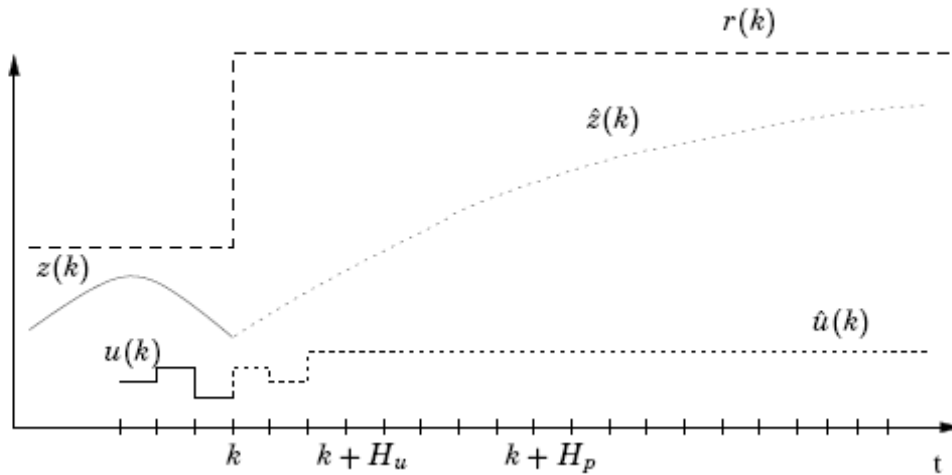


Figure 7. Illustration of the idea of MPC. Here $r(k)$ is the set point trajectory, $z(k)$ represents the controlled output and $u(k)$ the control signal. The graphical illustration is taken from [10].

In Figure 7 the controlled outputs are denoted (z), but in this work the controlled outputs are denoted (y).

The optimization calculation in the MPC algorithm includes a cost function which is to be minimized and the general expression for this is stated as followed;

$$J(k) = \sum_{i=H_w}^{H_p+H_w-1} \left\| \hat{y}(k+i|k) - r(k+i|k) \right\|_Q^2 + \sum_{i=0}^{H_u-1} \left\| \Delta u(k+i|k) \right\|_R^2 \quad (15)$$

Here $\hat{y}(k+i|k)$ are the predicted controlled outputs at time k and $\Delta u(k+i|k)$ are the predicted control increments at time k , and the matrices $Q \geq 0$ and $R > 0$ are weighting matrices. The weighting matrices are assumed to be constant in the prediction horizon. The parameter denoted (H_w) in (15) defines the first sample included in prediction horizon. This feature makes it possible to shift the control horizon when solving the optimal control problem. In this work, this parameter is set to one ($H_w = 1$), i.e. the prediction starts one sample ahead from the current one.

The cost function defined in (15) penalize deviations of the controlled variables as well as variations in the control signal. A quadratic norm is used in the function, which is the most common approach. This cost function in combination with a linear system yields a finite horizon LQ problem.

4.2.1. A simple example on MPC

A simple example on how the MPC calculations proceed is shown in this subsection. In this example, the input to the system is on the form ($\Delta u(k)$), which is the increments of the control signal instead of the ordinary control signal ($u(k)$). This is because it is much easier to show how the MPC strategy works theoretically. Notice that in the presented problem in this work, the control approach is done with the ordinary control signal, but in general, the increment form is more common.

Assume a state-space system described by the simple form in (e2.1). This system represents a double integrator in discrete time. A physical comprehension of this kind of system is for instance problem based on vehicle steering control.

$$x(k+1) = \begin{bmatrix} 1 & 1 \\ 0 & 1 \end{bmatrix} \cdot x(k) + \begin{bmatrix} 1 \\ 0.5 \end{bmatrix} \cdot \Delta u(k) = Ax(k) + B\Delta u(k) \quad (\text{e2.1})$$

$$y(k) = \begin{bmatrix} 1 & 0 \\ 0 & 1 \end{bmatrix} \cdot x(k) + \begin{bmatrix} 0 \\ 0 \end{bmatrix} \cdot \Delta u(k) = Cx(k)$$

Notice that this state-space form is an example and the throughout elements in the matrices are not based on any dynamical behavior.

In this example we use a basic cost function which controls the outputs (y) to a reference trajectory and the increment inputs should forced to zero. Also in the cost function below we say that the prediction horizon is 2 and the control horizon is 1. Notice that the horizon units are in number of samples.

$$V(k) = \sum_{i=1}^2 \|\hat{y}(k+i|k) - r(k+i)\|_Q^2 + \sum_{i=0}^0 \|\Delta \hat{u}(k+i|k)\|_R^2 \quad (\text{e2.2})$$

Now the cost function could be rewritten so that the sums are replaced by vectors and the quadratic norm;

$$V(k) = (Y(k) - I(k))^T \cdot Q_e \cdot (Y(k) - I(k)) + \Delta U(k)^T \cdot R_e \cdot \Delta U(k) \quad (\text{e2.3})$$

Where $Y(k)$ is a vector containing the predicted output signals from the current sample to the second predicted sample ($H_p = 2$) and $\Delta U(k)$ contains the predicted control signal from the current sample to the first sample ($H_u = 1$).

$Y(k) = \begin{bmatrix} \hat{y}(k+1|k) \\ \hat{y}(k+2|k) \end{bmatrix}$, $\Delta U(k) = [\Delta \hat{u}(k|k)]$, Notice here that for example $\hat{y}(k+1|k)$ denotes the predicted output one sample ahead from the current sample.

Assume further that the reference vector is constant in time; i.e. $r(k+1|k) = r(k+2|k) = \begin{bmatrix} 5 \\ 10 \end{bmatrix}$,

$I(k) = \begin{bmatrix} r(k+1|k) \\ r(k+1|k) \end{bmatrix}$ and the weighting matrices are $Q = \begin{bmatrix} 1 & 0 \\ 0 & 1 \end{bmatrix}$ and $R = [0.1]$, i.e. penalize the outputs equally and the input less. This means that deviations from the outputs are controlled harder than the increments on the control signal.

The weighting matrices must also be extended when the cost function is rewritten as followed;

$$Q_e = \begin{bmatrix} Q & 0 \\ 0 & Q \end{bmatrix} \text{ and } R_e = [R].$$

Now the predicted outputs are replaced by the help of the linear equations stated in (e2.1). This is done by shifting (e2.1) in time to get expressions for $\hat{y}(k+1|k)$ and $\hat{y}(k+2|k)$ as function of the current state and the predictive control signals in time;

$$\begin{aligned} \hat{y}(k+1|k) &= Cx(k+1) = CAx(k) + CB\Delta \hat{u}(k|k) \\ \hat{y}(k+2|k) &= Cx(k+2) = CAx(k+1) + CB\Delta \hat{u}(k+1|k) = \\ &= CA^2x(k) + CAB\Delta \hat{u}(k|k) \end{aligned}$$

This leads to a new expression for the output vector in the prediction horizon;

$$Y(k) = \Psi \cdot x(k) + \Theta \cdot \Delta U(k) \quad (\text{e2.4})$$

$$\text{, where } \Psi = \begin{bmatrix} CA \\ CA^2 \end{bmatrix} \text{ and } \Theta = \begin{bmatrix} CB \\ CAB \end{bmatrix}.$$

Now an expression is created that represents a 'tracking error', meaning the difference between the future target trajectory and the 'free response'. With other words, the response that would occur over the prediction horizon if the extended control vector ($\Delta U_e(k)$) is set to zero.

$$\varepsilon(k) = I(k) - \Psi \cdot x(k) \quad (\text{e2.5})$$

Assume that the current state is given by; $x(k) = \begin{bmatrix} 2 \\ 4 \end{bmatrix}$, then the equation (e2.5) can be calculated;

$$\varepsilon(k) = \begin{bmatrix} 5 \\ 10 \\ 5 \\ 10 \end{bmatrix} - \begin{bmatrix} 1 & 1 \\ 0 & 1 \\ 1 & 2 \\ 0 & 1 \end{bmatrix} \cdot \begin{bmatrix} 2 \\ 4 \end{bmatrix} = \begin{bmatrix} -1 \\ 6 \\ -5 \\ 6 \end{bmatrix}.$$

If this error would be zero ($\varepsilon(k) = 0$), then the correct optimal control signal would be zero ($\Delta U_e(k) = 0$), but this is not the case right now apparently. If the outputs were following the reference, then no change in the control signal should occur.

The cost function in (e2.2) could now be rewritten with the use of (e2.4) and (e2.5) as;

$$\begin{aligned} V(k) &= [(\Psi(k) \cdot x(k))^T + (\Theta \cdot \Delta U(k))^T - (\Psi(k) \cdot x(k))^T - (\varepsilon(k))^T] Q_e [\Psi(k) \cdot x(k) + \Theta \cdot \Delta U(k) - \Psi(k) \cdot x(k) - \varepsilon(k)] \\ &+ \Delta U(k)^T \cdot R_e \cdot \Delta U(k) = [\Delta U(k)^T \cdot \Theta^T - \varepsilon(k)^T] Q_e [\Theta \cdot \Delta U(k) - \varepsilon(k)] + \Delta U(k)^T \cdot R_e \cdot \Delta U(k) = \\ &= \varepsilon(k)^T Q_e \varepsilon(k) - 2\Delta U(k)^T \Theta^T Q_e \varepsilon(k) + \Delta U(k)^T [\Theta^T Q_e \Theta + R_e] \Delta U(k) \end{aligned}$$

A simplification on the cost function derived above results in a quadratic equation;

$$V(k) = const - \Delta U(k)^T \Gamma + \Delta U(k)^T H \Delta U(k) \quad (e2.6)$$

In this quadratic equation (e.6) the parameters are defined as followed;

$$const = \varepsilon(k)^T Q_e \varepsilon(k) = \begin{bmatrix} -1 \\ 6 \\ -5 \\ 6 \end{bmatrix}^T \cdot \begin{bmatrix} 1 & 0 & 0 & 0 \\ 0 & 1 & 0 & 0 \\ 0 & 0 & 1 & 0 \\ 0 & 0 & 0 & 1 \end{bmatrix} \cdot \begin{bmatrix} -1 \\ 6 \\ -5 \\ 6 \end{bmatrix} = 98$$

$$\Gamma = 2\Theta^T Q_e \varepsilon(k) = 2 \cdot \begin{bmatrix} 1 \\ 0.5 \\ 1.5 \\ 0.5 \end{bmatrix}^T \cdot \begin{bmatrix} 1 & 0 & 0 & 0 \\ 0 & 1 & 0 & 0 \\ 0 & 0 & 1 & 0 \\ 0 & 0 & 0 & 1 \end{bmatrix} \cdot \begin{bmatrix} -1 \\ 6 \\ -5 \\ 6 \end{bmatrix} = -5$$

$$H = \Theta^T Q \Theta + R = \begin{bmatrix} 1 \\ 0.5 \\ 1.5 \\ 0.5 \end{bmatrix}^T \begin{bmatrix} 1 & 0 & 0 & 0 \\ 0 & 1 & 0 & 0 \\ 0 & 0 & 1 & 0 \\ 0 & 0 & 0 & 1 \end{bmatrix} \begin{bmatrix} 1 \\ 0.5 \\ 1.5 \\ 0.5 \end{bmatrix} + 0.1 = 3.85$$

This finally brings the equation (e2.6) to a convenient expression (e2.7);

$$V(k) = 0 \rightarrow 0 = 98 - 5\Delta u(k | k) + 3.85\Delta u(k | k)^2 \quad (e2.7)$$

The purpose was to minimize the cost function in (e2.2) and therefore a minimum should be found for the function stated in (e2.7). This is done by finding the gradient of $V(k)$ in (e2.7) and set it to zero. The derivation is done with aspects on the control variable ($\Delta u(k | k)$) and the result can be seen in (e2.8).

$$\nabla_{\Delta u(k|k)} V(k) = -5 + 3.85 \cdot 2 \cdot \Delta u(k | k) = -5 + 7.7 \cdot \Delta u(k | k) = 0 \quad (e2.8)$$

The optimal incremented control signal that is sent to the plant in this sample is equal to (e2.9);

$$\Delta u(k | k) = 0.6494 \quad (e2.9)$$

This signal must be manipulated before entering the plant to form the ordinary control signal ($u(k | k)$).

The calculation in (e2.8) becomes very simple because of the short prediction horizon and the short control horizon. If a larger problem should be calculated, a least-square method is applied to find the optimal control signal which forces the function as close as possible to its minimum, but at the same time satisfy all constraints in the system.

To guarantee that a minimum is achieved for the cost function, the second derivative is investigated. If the second derivative of a function is greater than zero, a minimum is found. Differentiating the gradient $\nabla_{\Delta u(k|k)} V(k)$ again with respect to $\Delta u(k|k)$ gives the second derivative of the function, as can be seen in (e2.10). All matrices are kept as symbols to show the conditions for a minimum on the cost function.

$$\frac{\partial^2 V}{\partial \Delta u(k|k)^2} = 2H = 2(\Theta^T Q \Theta + R) \quad (\text{e2.10})$$

If we assume that the weighting matrices are $Q \geq 0$ and $R > 0$, then this guarantees a minimum for the cost function.

4.2.2. Hard constraints

Defining constraints is an essential part of the MPC control strategy and it is this that makes the MPC approach such a favorable ECA. In a hybrid system there exist dynamics that need to be bounded in some certain limits, which is based on physical limitations. There are two kinds of constraints, hard constraints and soft constraints. In this first subsection the hard constraints are defined and after that the soft constraints are introduced.

According to the physical limitations on the dynamics, much of the thorough variables in the system are bounded with hard constraints. In the MPT toolbox constraints can be defined on the states, inputs and outputs. The meaning of hard constraints is to bound parameters in the system in specific regions and really makes sure that those variables are constrained by physical boundaries.

The cost function introduced in the previously subsection (15) should be minimized in the prediction horizon but at the same time satisfy all the constraints in a system. The constraints in the MPC approach are generally on the control signals and the outputs, but with the use of the MPT toolbox constraints on the states are also introduced, these are defined in (16).

$$\begin{aligned} x_{\min} &\leq x(k) \leq x_{\max} \\ y_{\min} &\leq y(k) \leq y_{\max} \\ u_{\min} &\leq u(k) \leq u_{\max} \\ \Delta u_{\min} &\leq u(k) - u(k-1) \leq \Delta u_{\max} \end{aligned} \quad (16)$$

Hard constraints are, as the name implies, constraints that need to be fulfilled at all time, i.e. the values of the states, inputs and outputs must be in the defined intervals when the optimal control problem is calculated.

4.2.3. Soft constraint

Soft constraints are more generous constraints than hard constraints. These constraints make the hard constraints to be violated at all time but the violated variable is added in the cost function with a weighting value to bring it back into the right interval. An example is shown in Figure 8, where the variable in the simulation has a soft constraint and this is violated as the figure implies.

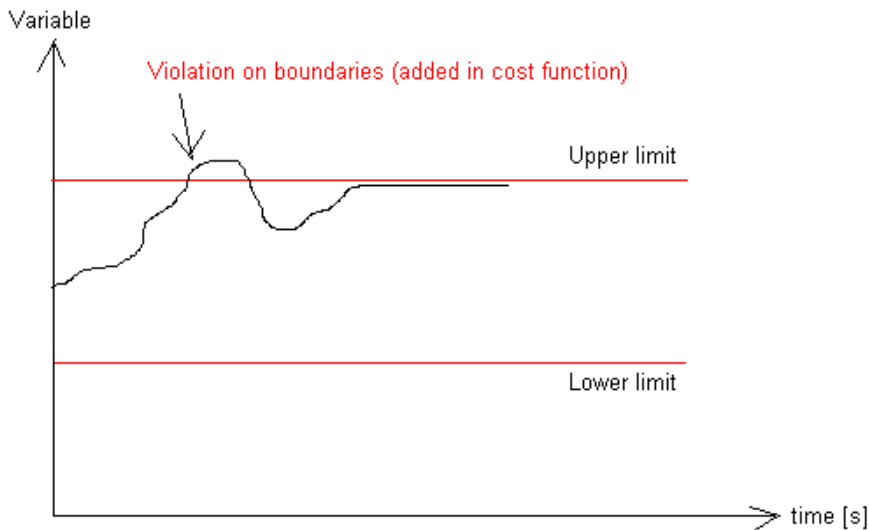


Figure 8. Shows the parameter with soft constraints and if the boundaries are violated, this parameter is added in the cost function to bring it back in the right interval.

One could see the soft constraints penalty as same as the variables in the ordinary cost function (15), which penalize deviations from a reference value. This reference value is the boundary value on the variable and if this variable exceeds the border further, it leads to a greater value to minimize.

4.3. Model predictive control for piece-wise affine system

Model predictive control for PWA system has a higher complexity than a MPC based on a LTI system. In a LTI system the MPC is only applied to one plant model compare to a PWA system, where the optimization problem is computed for all included linear models. At each sample, when an optimal control signal should be calculated, the MPC controller must calculate an optimal control signal for each combination of linear models in the PWA system. Notice here that this involves an online MPC controller, which is used in this work. Motivation on this can be found further down in this work, at Section 6. The best combination of the linear models produces the optimal control which is applied to the plant. For example, if a PWA system is defined by six linear models and the prediction horizon is set to two, the MPC controller must calculate $6^2 = 36$ different control signals before choosing the best. In this example mentioned, the worst case scenario is presented, but this never occurs. This is because some of the combinations become redundant and can be discarded.

Then again, the computational time increases rapidly with aspects to the prediction horizon, control horizon and the amount of linear models in the PWA system. The sampling time is also highly depended on the computational time, which can be easily understood; due to at each sample, an optimal control signal should be calculated. These parameters are very important to be considered before developing a MPC controller. With the choice of a MPC controller where the PWA model includes many linear models and a long prediction horizon, the result becomes better when controlling a nonlinear plant, logically. But this also leads to an increase in computational time. A trade off must be made between how well the PWA system should approximate the nonlinear plant, how good the MPC controller should be (pred. horizon, ctl horizon) and how much CPU capacity is available (computational time).

The constraints in a PWA system is defined as same as in a LTI system, i.e. the constraints are defined as constant values for the different variables.

4.4. Matlab and Multi-parametric toolbox

All modeling and simulations are performed in the computer program Matlab [16] and more specific Simulink, which is a simulation tool. With the MPC as the ECA and the hybrid dynamics in the system, a toolbox with these preferences should be used and this is denoted Multi-Parametric Toolbox (MPT). In the following section a summary on the Matlab commands and the used features in MPT are highlighted.

4.4.1. Matlab and simulink

The software Matlab is a mathematical and simulation program, which is used throughout this work. In Matlab there exist a great number of different toolboxes and subprograms that handle different kind of control problems. The toolbox used for this hybrid system is the MPT in combination with Simulink. In simulink the user can simulate the behavior when the ECA is applied to the plant and evaluate the results graphically.

4.4.2. Multi-parametric toolbox

The MPTs [7] purpose is to handle system where the mathematical description is changing due to the dynamic, i.e. for example hybrid system. Two different kind of system are compatible in the MPT. These are LTI (linear time-invariant) system and PWA system. As stated before, the PWA system is the one used in this work.

As a summary, the used tools to create a MPC regulator for a PWA can be divided into two major parts. The first part is to define the PWA system as the theory implies in Section 4.1. This is done through creating linear models of the nonlinear plant and divides them by help of guard lines. The constraints in the system are also defined here. Only constant constraints can be defined in MPT and this could lead to a limitation when handling this kind of system, more on this in Section 5.

The second major part when creating the controller is to define the problem structure. This involves defining prediction horizon, norm, weighting matrices etc.

When these two parts have been defined, the MPC controller can be created. This controller can be either an explicit or an online controller. An explicit controller precalculates controllaws offline and then connects them to certain polytopes. This alternative has a faster computation time then the online regulator, due to the online regulator needs to calculate all matrices at every sample.

The MPT toolbox is compatible with the use of soft constraints and has some features that can be defined regarding these constraints. When creating the soft constraints, it is necessary to define penalty value on the violation. It is the same strategy here as in the ordinary cost function theory, that a higher value on the penalty results in higher value in the cost function due to the violation and forces the variable faster into the right boundaries.

One could also set an above (or below) limit on the violated soft constraints so that violation on the soft constraints are penalized, but when the second limit is reach, this constraint works as a hard constraint that can not be violated. This can be seen in Figure 9.

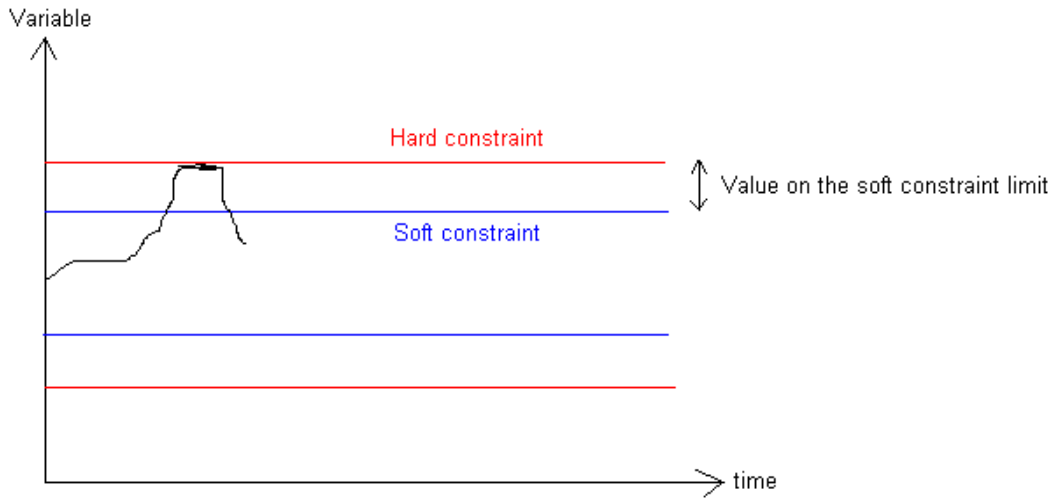


Figure 9. Describing the limit value on soft constraints before it becomes hard constraints. More detailed theory can be found in the MPT use manual [7]

4.4.3. Maple

The mathematical program Maple [17] is also used in this work and is needed when the nonlinear functions should be derivated. When the functions becomes complicated and include many variables, an easy and convenient way is to let Maple calculate the different partial derivatives in the system.



5. MODELING

The first part of the modeling section states the general model description of the plant and driving cycle. After this, it describes the mathematical description of the plant and how to accomplish linear representations of the system due to different linearization points and different dynamics. The two last parts describe handling of disturbances in the system and the linear model validated to the nonlinear plant.

5.1. Model description

When working with simulations based on physical systems, models must be developed to work as a substitute for the real world behavior. Generally, all models are approximations of the real dynamical behavior and it is of great importance to have a model which behaves as similar to its reality. There are basically two main things that must be introduced in order to create a control structure and these are the plant and the regulator. The plant defines the complete system and how it behaves, i.e. includes the ICE, generator and ESS dynamics. This could be denoted a model, because it is an approximation of the real world behavior.

A regulator must exist to control the plant and its dynamics. The outputs from the plant that are needed in the control strategy are then used as a feedback to the regulator which then calculates a control signal. For example, assume that the outputs are the fuel consumption, rotational speed and the power demand. These should be sent to the regulator to compute a control signal based on the values of these outputs which then shall be applied to the plant.

Furthermore, in this case, a driving cycle is also introduced to create runnable simulations and this generates the power demand in the excavator and is a sort of input to the plant. One could see the driving cycle as an artificial operator in the excavator, i.e. perform different task with the vehicle. An illustration can be seen in Figure 10.

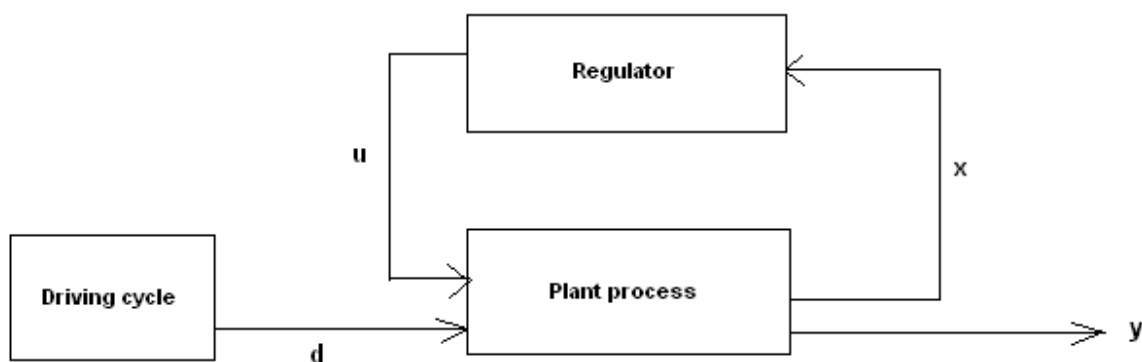


Figure 10. Description of the process, where the inputs are denoted (u), the disturbances (d) and outputs (y).

The control signal should control the plant as stated before and this means that this signal should tell how much the ICE and the generator must produce in power to satisfy the power demand in the excavator, and indirectly how much power that would be withdrawn from the ESS. The control signal should describe the torque on the ICE (T_{Eng}) and the torque on the generator (T_{Gen}). The driving cycle should describe the power demand which stand for the power from the hydraulic pumps and the electrical swing.

To clarify the procedure, at each sampling instant in the simulation a value of how much power the excavator needs is created and sent to the plant along with a control signal based on previous sample.

These input signals are then used to calculate all output signals, where some of those are then sent back to the regulator to perform a new control signal, i.e. to control the excavator preferably.

There exist two kinds of power in the system, mechanical power and electrical power. Mechanical power is the power needed for the arms and bucket illustrated in Figure 1. The ICE and the generator can both produce mechanical power which is then send to the hydraulic pumps. Here the mechanical power becomes hydraulic power to satisfy the hydraulic actuators.

The electrical power can be supplied both from the generator and the ESS. The creation of electrical power is possible because the mechanical power produced by the ICE can be converted to electrical power by the generator. There are two different electrical power demanders in the system; the swing system and the AUX system. After the electrical power has been withdrawn, it is sent both to the SWEM, where it is converted to mechanical power in order to rotate the upper part of the excavator and to the constant electrical power demand from the AUX system. This could work on the other way around as well, i.e. the swing system could produce electrical power when the upper part of the excavator is braking. When the excavator is braking, mechanical power is produced in the swing system which is then converted by the SWEM to electrical power. This electrical power could both be used to recharge the ESS or to operate the hydraulic actuators with the help of the generator.

The driving cycle gives a power demand for the pumps and the swing. A complete driving cycle can be seen in Figure 11. The power demand for the pumps is always greater then zero (no regenerative energy here) and is always mechanical power. The swing power sign however, can change if the rotation brakes. When the swing is producing electrical power (negative value on the SW_power in Figure 11) the excavator rotational mechanism is braking, which leads to that this part becomes a power supplier. If the sign on SW_power is positive in Figure 11 the swing system needs power to operate the rotating mechanism, which in this case comes from the electrical power on the ESS or the generator.

What can also be seen in Figure 11 are the different work modes and there characteristics. For example, when the power demands from both the Pumps and Swing are close to zero, the idling work mode is operating. Another characteristic work mode is if the Swing power is negative, then a mode with much motions on the rotation mechanism in the HCEV is operating, which is "dig and dump". When the excavator is traveling, the rotational mechanism is fixed and this can be seen in the driving cycle as only a power demand from the pumps.



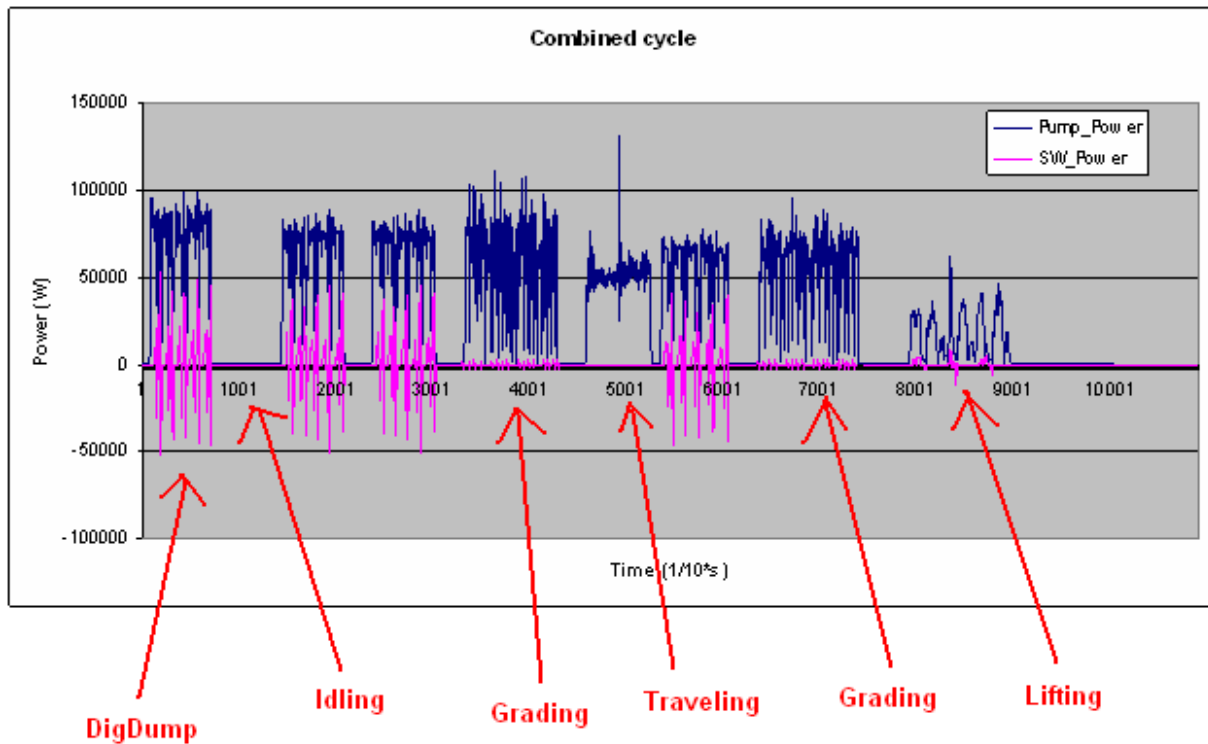


Figure 11. Combined cycle with the power demand from Pumps and the swing. In the beginning (0-80 s) work mode DigDump is present. In the end (800-900 s) work mode Lifting is present. In the middle (350-450 s) the work mode Grading is present, which is characterized by a Swing power close to zero and high power demand on the pumps. The graph is taken from [6].

In Figure 12 below, a linear model of the real plant must be established in order to create a MPC regulator and in our case, multiple linear models must be determined due to different nonlinear dynamics in the mathematical hybrid system. This illustration also shows that the first control signal computed is applied to the plant.

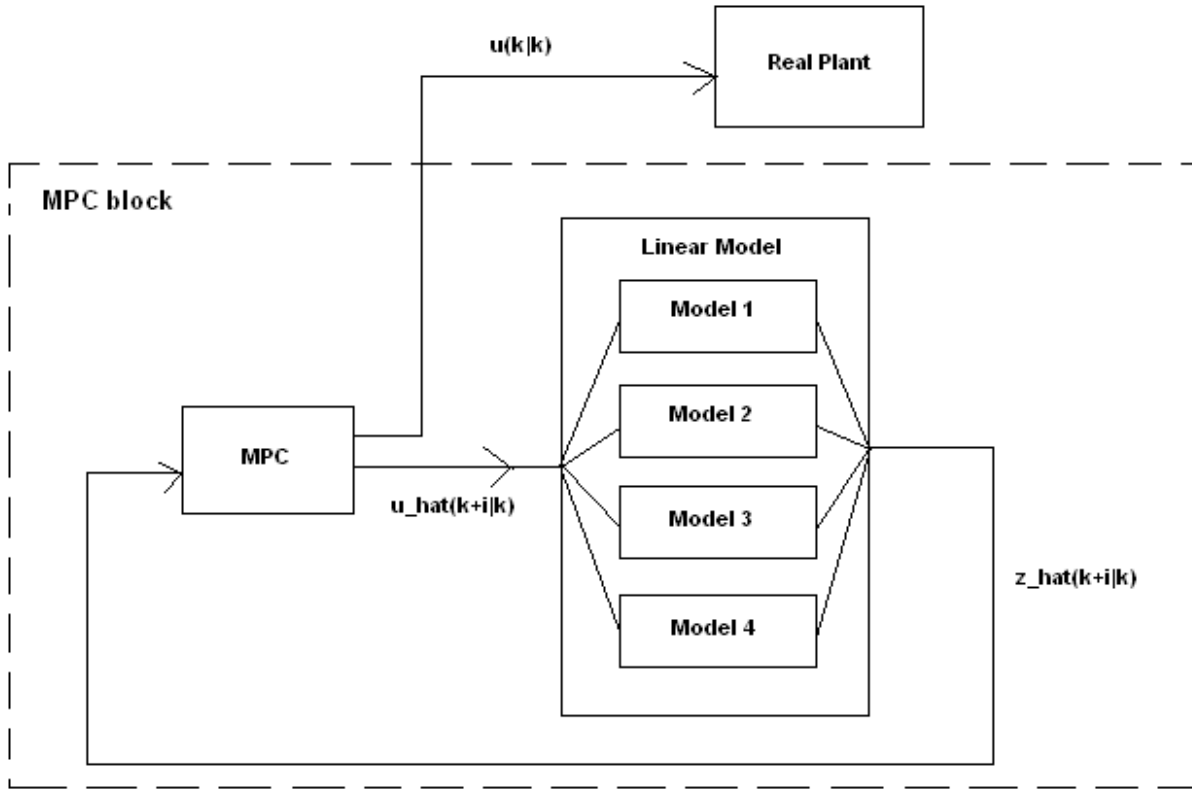


Figure 12. Description of the MPC regulator. The optimal control signal $u(k|k)$ is applied to the plant

With this known, an optimal power split should be applied in order to minimize fuel consumption, minimize component wear and of course not sacrifice work performance. All of these specifications can not be optimal at the same time, so a trade off must be introduced to get a satisfying result. This demands a lot of attention and it is a decision based on many variables.

5.2. Mathematical description of the plant

The MPC algorithm demands a state-space representation of the system in order for it to be implemented and establish this description is compulsory. Mathematically, the states of the system are defined as time derivative functions of the states themselves and the inputs. Equation (17) describes this, where the states are denoted \bar{x} and the inputs are \bar{u} and \bar{d} . The outputs of the process can be seen in (18), which is a function of states and the inputs.

$$\dot{\bar{x}} = A\bar{x} + B\bar{u} + B_d\bar{d} \quad (17)$$

$$y = C\bar{x} + D\bar{u} + D_d\bar{d} \quad (18)$$

When deriving a state-space form as seen above, the identification of the states must be done. This is accomplished through investigation of the expressions in Appendix 10.1-10.6 that involves time derivatives. There are a total number of four time derivative expressions in Appendix 10.1-10.6 and these are the rotational acceleration on the ICE, change in the ICE pressure, change in the battery level and the rate of flow of diesel. The first three mentioned describe the dynamics in the system but the rate of flow of the diesel describes the fuel consumption in the system, which only tells how much diesel the excavator consumes. Therefore, the rate of fuel becomes an output signal which depends on how much the ICE produces.

The states are defined below (19).

$$x = \begin{Bmatrix} \omega_{ENG} \\ p_{boost} \\ SoE \end{Bmatrix} \quad (19)$$

Some variables are distinguished from start and those are the control signals and the disturbances, which are the inputs to the process. The signal that comes from the regulator and thus, the signal that controls the process, is introduced in (20), where the engine torque (T_{ENG}) and generator torque (T_{GEN}) corresponds to how much the internal combustion engine (ICE) and the generator shall produce, respectively. The last signal in the control vector is *isengon* and this *Boolean* signal describes if the ICE should be on/off. This signal however, is in the initial approach removed from the model to have a less complicated problem structure.

$$u = \begin{Bmatrix} T_{ENG} \\ T_{GEN} \\ (isengon) \end{Bmatrix} \quad (20)$$

As mentioned above, there are some disturbances that are included as inputs to the process. In Section 4 there is a driving cycle that generates power demand for the pumps and the swing, and these signals are introduced as known disturbances. These are not actual disturbances; one could see them as input signals that need to be satisfied. We define this disturbance representation in (21) and clarify that SWEM = swing electrical motor.

$$d = \begin{Bmatrix} P_{pumps}^{mech}(t) \\ P_{SWEM}^{el}(t) \end{Bmatrix} \quad (21)$$

In order to simulate and develop an ECA for the HCEV, a model needs to be created from real dynamics in a HCEV. The model must be built on a mathematical theory that describes most of the dynamics in the system. Some dynamical features are ignored to simplify the control problem. In Table 2, the most important parameters and variables are summarized.

Parameter	Physical description	Unit []
ω_{ENG}	Engine rotational speed	[rad/s]
T_{ENG}	Engine torque	[Nm]
T_{boost}	Turboboost torque	[Nm]
T_{GEN}	Generator torque	[Nm]
T_{pumps}	Pumps actuator torque	[Nm]
dp	Pressure difference in ICE	[Pa]
I_{ENG}	Engine inertia (Constant)	[kg*m ²]
p_{boost}	Turbo pressure	[Pa]
K_{corr}	Correction factor on gas law (Constant)	[1]
φ_{ESS}	Efficiency factor on battery	[1]
E_{ESS}^{max}	Maximum energy in battery	[J]
SoE	Level of energy in battery	[1]
P_{ESS}	Electrical power output from battery	[W]
P_{GEN}^{el}	Electrical power output from generator	[W]
P_{AUX}	Electrical power from radio, etc. (Constant)	[W]
P_{SWEM}^{el}	Electrical power from SWEM	[W]

φ_{GEN}	Efficiency factor on generator	[1]
P_{ESS}^{loss}	Power losses in battery	[W]
N_{cell}^{ser}	Number of battery cells in series (Constant)	[1]
N_{cell}^{par}	Number of battery cells in parallel (Constant)	[1]
R_{cell}	Resistance in a cell	[Ω]

Table 2. Thorough parameters and variables in the MPC approach.

With all states, inputs and disturbances identified, the next goal is to form the linear equation stated in (17). This equation is a linear function of the states, the inputs and the disturbances. In (22-24) the three time derivative functions of the states can be seen.

$$\dot{\omega}_{ENG} = \begin{cases} \frac{(T_{ENG} + T_{boost} + T_{GEN} - T_{pumps})}{I_{ENG}} & (dp > 0) \\ \frac{(T_{ENG} + T_{GEN} - T_{pumps})}{I_{ENG}} & (dp \leq 0) \end{cases} \quad (22)$$

$$\dot{p}_{boost} = \begin{cases} \frac{dp}{getboosttimeconstA(\omega_{ENG})} - \frac{K_{corr} \cdot \dot{\omega}_{ENG} \cdot P_{boost}}{\omega_{ENG}} & (dp > 0) \\ \frac{dp}{getboosttimeconstB(\omega_{ENG})} - \frac{K_{corr} \cdot \dot{\omega}_{ENG} \cdot P_{boost}}{\omega_{ENG}} & (dp \leq 0) \end{cases} \quad (23)$$

$$S\dot{O}E = \begin{cases} -\frac{\varphi_{ESS} \cdot P_{ESS}}{E_{ESSmax}} & (P_{ESS} < 0) \quad charge \\ -\frac{P_{ESS}}{\varphi_{ESS} \cdot E_{ESSmax}} & (P_{ESS} \geq 0) \quad discharge \end{cases} \quad (24)$$

There is some work to be done in order to have all the expressions above as functions of only the states and the inputs.

The time derivative of the rotational speed is represented by the mechanical law which says that the sum of torque divided with the engine inertia is equal to the rotational acceleration. Engine torque, turboboost torque, generator torque and hydraulic pumps torque constitute the sum of torque if the pressure difference is greater than zero (dp). Otherwise, if it is negative, the generated turboboost torque becomes zero and this is because the pressure difference is defined as the difference between the steady state turboboost and the current turboboost at a specific time (26). For example, if the current turboboost is less than the steady state boost, this means that the turbo has not enough pressure to develop its maximal torque and there will be a torque loss in the system.

On the other hand, if the current boost is higher than the steady state boost, assumptions are made that the maximal torque is generated the whole time if this condition holds, which is a good approximation.

This change in the mathematical description due to different variables (dp, P_{ESS} etc.) is denoted a switch.

For example, if at first, the pressure difference is greater then zero and at the next sample the variables have been changed so the pressure difference changes sign, then a new mathematical description is active.

For (22), the torque for the turboboost and the torque for the pumps must be replaced. The equation for T_{boost} is stated as follows;

$$T_{boost} = -k_1(\omega_{ENG}) \cdot dp^2 - k_2(\omega_{ENG}) \cdot dp, \text{ where } k_1(\omega_{ENG}) \text{ and } k_2(\omega_{ENG}) \text{ are maps.} \quad (25)$$

Using the equation for the pressure difference, the turboboost torque can be expressed with only the desirable variables;

$$dp = getboost(T_{ENG}, \omega_{ENG}) - p_{boost}, \text{ where } getboost(T_{ENG}, \omega_{ENG}) \text{ is a map.} \quad (26)$$

At last, the generated torque from the hydraulic pumps is replaced with equation (27);

$$T_{pumps} = \begin{cases} 0 & (isengon = False \Leftrightarrow Eng = off) \\ \frac{P_{pumps}}{\omega_{ENG}} & (isengon = True \Leftrightarrow Eng = on) \end{cases} \quad (27)$$

If (25), (26) and (27) is substituted into (22), the result becomes a function of only the states and the inputs, which is presented further down in this section at (21).

The rewriting of the time derivative on the turbo pressure (23) are made by substituting dp and $\dot{\omega}_{ENG}$. Due to the derivation of the rotational acceleration, equation (39) can be derived by the combination of (38) and (21).

The last expression, which describes the time derivative of the SoE , includes two variables that needs to be replaced and these are the power in the battery (P_{ESS}) and the efficiency in the battery (φ_{ESS}). To derive an expression for (40) the law of Kirchoff is used. The sum of all currents in the system can be defined as;

$$I_{ESS} - I_{GEN} - I_{AUX} - I_{SWEM} = 0 \quad (28)$$

Where I_{ESS} , I_{GEN} , I_{aux} , I_{SWEM} are the battery current, generator current, AUX current and Swing electrical machinery current, respectively. This is illustrated in Figure 13.

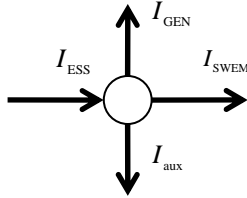


Figure 13. Currents in electric node.

This equation can be changed to an expression for the sum of power from the different actuators through the equation on the rate of energy transfer;

$$I = \frac{P}{U} \text{ where } P \text{ is denoted the power and } U \text{ the voltage.} \quad (29)$$

These combined form the sum of the powers (Notice also that the voltage is the same in Figure 12 and can be cancelled);

$$P_{ESS} - P_{GEN}^{el} - P_{AUX} - P_{SWEM}^{el} = 0 \quad (30)$$

Now the only parameter that needs to be substituted is the electrical generator power;

$$P_{GEN}^{el} = \begin{cases} P_{GEN}^{mech} \cdot \varphi_{GEN} & (motor \text{ operation} : P_{GEN} > 0) \\ \frac{P_{GEN}^{mech}}{\varphi_{GEN}} & (generator \text{ operation} : P_{GEN} \leq 0) \end{cases} \quad (31)$$

, where $\varphi_{GEN} = getgeneff(\omega_{ENG}, T_{GEN})$ is a map.

The expression for the mechanical generator power is used to replace the variable in (31);

$$P_{GEN}^{mech} = T_{GEN} \cdot \omega_{GEN} = T_{GEN} \cdot \omega_{ENG} \quad (32)$$

(This is possible due to no gear ratio between the generator and the engine, i.e. ICE mounted directly on generator).

To conclude, the result of combining equations (30), (31) and (32) becomes;

$$P_{ESS} = T_{GEN} \cdot \omega_{ENG} \cdot getgeneff(\omega_{ENG}, T_{GEN}) + P_{AUX} + P_{SWEM}^{el} \quad (33)$$

The last variable substitution is the efficiency of the battery (φ_{ESS}), which can be seen in (34).

$$\varphi_{ESS}(P_{ESS}, \eta_{ESS}) \approx \begin{cases} 1/\eta_{ESS} & (P_{ESS} > 0 \Leftrightarrow \text{discharge mode}) \\ \eta_{ESS} & (P_{ESS} < 0 \Leftrightarrow \text{charge mode}) \end{cases} \quad (34)$$

The η_{ESS} is defined by a few equations below (35)-(37);

$$\eta_{ESS} = \frac{|P_{ESS}| - |P_{ESS}^{loss}|}{|P_{ESS}|} \quad (35)$$

$$P_{ESS}^{loss} = R_{ESS} \cdot \left(\frac{P_{ESS}}{U_{ESS}} \right)^2, \text{ where } U_{ESS} = \text{getucell}(SoE) \cdot N_{cell}^{ser} \text{ is a map on the battery voltage.} \quad (36)$$

$$R_{ESS} = \frac{N_{cell}^{ser}}{N_{cell}^{par}} \cdot R_{cell} \quad (37)$$

Through these substitutions the three time derivatives states can be defined as nonlinear functions depended on states, inputs and disturbances (38)-(40). Notice here that the mathematical description changes due to some certain condition.

$$\dot{x}_1 = \begin{cases} (u_1 - \Omega_6(x_1) \cdot (\Omega_3(x_1, u_1) - x_2)^2 - \Omega_7(x_1) \cdot (\Omega_3(x_1, u_1) - x_2) + u_2 - \frac{d_1}{x_1}) / I_{ENG} & (dp > 0) \\ (u_1 + u_2 - \frac{d_1}{x_1}) / I_{ENG} & (dp \leq 0) \end{cases} \quad (38)$$

$$\dot{x}_2 = \begin{cases} \frac{\Omega_3(x_1, u_1) - x_2}{\Omega_1(x_1)} - \frac{K_{corr} \cdot x_2}{x_1 \cdot I_{ENG}} \cdot (u_1 - \Omega_6(x_1) \cdot (\Omega_3(x_1, u_1) - x_2)^2 - \Omega_7(x_1) \cdot (\Omega_3(x_1, u_1) - x_2) + u_2 - \frac{d_1}{x_1}) & (dp > 0) \\ -\Omega_7(x_1) \cdot (\Omega_3(x_1, u_1) - x_2) + u_2 - \frac{d_1}{x_1} & (dp > 0) \\ \frac{\Omega_3(x_1, u_1) - x_2}{\Omega_2(x_1)} - \frac{K_{corr} \cdot x_2}{x_1 \cdot I_{ENG}} \cdot (u_1 + u_2 - \frac{d_1}{x_1}) & (dp \leq 0) \end{cases} \quad (39)$$

$$\dot{x}_3 = \begin{cases} \frac{(u_2 \cdot x_1 \cdot \Omega_5(x_1, u_2) + P_{AUX} + d_2)}{(1 - \frac{R_{cell}}{N_{cell}^{par} \cdot N_{cell}^{ser} \cdot \Omega_{10}(x_3)^2} \cdot (u_2 \cdot x_1 \cdot \Omega_5(x_1, u_2) + P_{AUX} + d_2)) \cdot E_{ESS}^{max}} - ((u_2 \cdot x_1 \cdot \Omega_5(x_1, u_2) + P_{AUX} + d_2) \cdot (1 + \frac{R_{cell}}{N_{cell}^{par} \cdot N_{cell}^{ser} \cdot \Omega_{10}(x_3)^2} \cdot (u_2 \cdot x_1 \cdot \Omega_5(x_1, u_2) + P_{AUX} + d_2))) / E_{ESS}^{max}} & (*) \\ \frac{(\frac{u_2 \cdot x_1}{\Omega_5(x_1, u_2)} + P_{AUX} + d_2)}{(1 - \frac{R_{cell}}{N_{cell}^{par} \cdot N_{cell}^{ser} \cdot \Omega_{10}(x_3)^2} \cdot (\frac{u_2 \cdot x_1}{\Omega_5(x_1, u_2)} + P_{AUX} + d_2)) \cdot E_{ESS}^{max}} - ((\frac{u_2 \cdot x_1}{\Omega_5(x_1, u_2)} + P_{AUX} + d_2) \cdot (1 + \frac{R_{cell}}{N_{cell}^{par} \cdot N_{cell}^{ser} \cdot \Omega_{10}(x_3)^2} \cdot (\frac{u_2 \cdot x_1}{\Omega_5(x_1, u_2)} + P_{AUX} + d_2))) \cdot E_{ESS}^{max}} & (**) \\ \frac{(\frac{u_2 \cdot x_1}{\Omega_5(x_1, u_2)} + P_{AUX} + d_2)}{(1 - \frac{R_{cell}}{N_{cell}^{par} \cdot N_{cell}^{ser} \cdot \Omega_{10}(x_3)^2} \cdot (\frac{u_2 \cdot x_1}{\Omega_5(x_1, u_2)} + P_{AUX} + d_2)) \cdot E_{ESS}^{max}} - ((\frac{u_2 \cdot x_1}{\Omega_5(x_1, u_2)} + P_{AUX} + d_2) \cdot (1 + \frac{R_{cell}}{N_{cell}^{par} \cdot N_{cell}^{ser} \cdot \Omega_{10}(x_3)^2} \cdot (\frac{u_2 \cdot x_1}{\Omega_5(x_1, u_2)} + P_{AUX} + d_2))) \cdot E_{ESS}^{max}} & (***) \\ \frac{(\frac{u_2 \cdot x_1}{\Omega_5(x_1, u_2)} + P_{AUX} + d_2)}{(1 - \frac{R_{cell}}{N_{cell}^{par} \cdot N_{cell}^{ser} \cdot \Omega_{10}(x_3)^2} \cdot (\frac{u_2 \cdot x_1}{\Omega_5(x_1, u_2)} + P_{AUX} + d_2)) \cdot E_{ESS}^{max}} - ((\frac{u_2 \cdot x_1}{\Omega_5(x_1, u_2)} + P_{AUX} + d_2) \cdot (1 + \frac{R_{cell}}{N_{cell}^{par} \cdot N_{cell}^{ser} \cdot \Omega_{10}(x_3)^2} \cdot (\frac{u_2 \cdot x_1}{\Omega_5(x_1, u_2)} + P_{AUX} + d_2))) \cdot E_{ESS}^{max}} & (***) \end{cases} \quad (40)$$

As can be seen in (38)-(40), the mathematical description contains switches. The expressions changes for example if the generator is operating as an engine (generates torque) or as a generator (transform mechanical power to electrical power). Additional theory can be found in [8].

As above, the outputs must be a function of only the states and the inputs. A straight-forward algebra combination from the expressions in Appendix 10.1 leads to the eleven outputs expressions in equation (41)-(51).

The output vector contains both all states and inputs, but also new signals that need to be controlled or constrained.

This output signal represents the first state in the model which is the rotational speed on the ICE.

$$y_1 = \omega_{ENG} = x_1 \quad (41)$$

The second output signal is the first control signal in the system, i.e. torque on the ICE.

$$y_2 = T_{ENG} = u_1 \quad (42)$$

The torque loss in the ICE due to the turbo boost is represented by the T_{boost} . As can be seen in the equation below, this variable is always negative or zero (torque loss), with the assumption made before. Notice here that the turbo boost torque is equal to zero when the pressure difference is equal or less than zero.

$$y_3 = T_{boost} = \begin{cases} -\Omega_6(x_1) \cdot (\Omega_3(x_1, u_1) - x_2)^2 - \Omega_7(x_1) \cdot (\Omega_3(x_1, u_1) - x_2) & (dp > 0) \\ 0 & (dp \leq 0) \end{cases} \quad (43)$$

The fourth output is the second state and represents the pressure in the ICE.

$$y_4 = P_{boost} = x_2 \quad (44)$$

The fifth output is the torque on the pumps and it is given by the known disturbance from the hydraulic pumps (d_1), i.e. the mechanical power demand, and the rotational speed on the ICE. If the feature engine on/off is introduced, then this variable must be divided into two expressions.

$$y_5 = T_{pumps} = \begin{cases} 0 & (isengon = false) \\ \frac{d_1}{x_1} & (isengon = true) \end{cases} \quad (45)$$

When the states were defined there existed a time derivative function which was not defined as a state. This signal becomes an output signal instead and represents a map on how much the excavator consumes in diesel fuel. Notice that the signal is given in [mg/s]. If the engine is off the fuel consumption becomes zero.

$$y_6 = \dot{m}_{fuel} = \begin{cases} 0 & (isengon = false) \\ \Omega_{11}(u_1, x_1) & (isengon = true) \end{cases} \quad (46)$$

The power output from the ESS is denoted P_{ESS} and this is the seventh output in the model. Due to the efficiency factor on the generator (transform mech. power to elec. power or vice versa) this expression is divided into two different equations. Notice also that if P_{ESS} is negative, then power is flows into the ESS.

$$y_7 = P_{ESS} = \begin{cases} d_2 + P_{AUX} + u_2 \cdot x_1 \cdot \Omega_5(x_1, u_2) & (if P_{GEN} \leq 0) \\ d_2 + P_{AUX} + \frac{u_2 \cdot x_1}{\Omega_5(x_1, u_2)} & (if P_{GEN} > 0) \end{cases} \quad (47)$$

The eighth output is the last state, i.e. the SoE.

$$y_8 = SoE = x_3 \quad (48)$$

The efficiency factor on the ESS is divided into four different equations due to if the generator is working as a motor or a generator, but also because the introductions of the absolute sign in (19). This results in an expression if the value inside the absolute sign is positive and another one if it is negative.

$$y_9 = \eta_{ESS} = \begin{cases} 1 - \frac{R_{cell}}{N_{cell}^{ser} \cdot N_{cell}^{par} \cdot \Omega_{10}(x_3)^2} \cdot (d_2 + P_{AUX} + u_2 \cdot x_1 \cdot \Omega_5(x_1, u_2)) & (*) \\ 1 + \frac{R_{cell}}{N_{cell}^{ser} \cdot N_{cell}^{par} \cdot \Omega_{10}(x_3)^2} \cdot (d_2 + P_{AUX} + u_2 \cdot x_1 \cdot \Omega_5(x_1, u_2)) & (**) \\ 1 - \frac{R_{cell}}{N_{cell}^{ser} \cdot N_{cell}^{par} \cdot \Omega_{10}(x_3)^2} \cdot (d_2 + P_{AUX} + \frac{u_2 \cdot x_1}{\Omega_5(x_1, u_2)}) & (***) \\ 1 + \frac{R_{cell}}{N_{cell}^{ser} \cdot N_{cell}^{par} \cdot \Omega_{10}(x_3)^2} \cdot (d_2 + P_{AUX} + \frac{u_2 \cdot x_1}{\Omega_5(x_1, u_2)}) & (***) \end{cases} \quad (49)$$

The total power demand in the system is denoted P_{DEM} and is the sum of the power demand from the hydraulic pumps, the SWEM and the constant auxiliary power.

$$y_{10} = P_{DEM} = d_1 + d_2 + P_{AUX} \quad (50)$$

Last output in the model is the generator torque, which is the second control signal. This signal could both be positive and negative depended on if the generator should provide mechanical power or electrical power.

$$y_{11} = T_{GEN} = u_2 \quad (51)$$

(*) $P_{GEN} \leq 0$ and $P_{ESS} > 0$

(**) $P_{GEN} \leq 0$ and $P_{ESS} \leq 0$

(***) $P_{GEN} > 0$ and $P_{ESS} > 0$

(****) $P_{GEN} > 0$ and $P_{ESS} \leq 0$

5.2.1. Evaluation of the mappings

The functions denoted omegas, Ω_n , in the equations in the previous section represent the different maps in the system. The definitions of the maps can be found in Appendix 10.7 and includes both 1-dimensional functions as well as 2-dimensional functions.

These maps are created from data achieved from tests with a real HCEV and are then interpolated to create functions, which are approximations of the real behavior of the dynamics. Numerical methods were applied to create these functions from data sheets. These were premade when this thesis work started.

As high-lighted in the next section, when the system must be linearized, the derivative of the functions must be evaluated and therefore the maps must also be differentiable. This is done with a toolbox in Matlab called the Spline toolbox. This toolbox creates an interpolated function from data with some very nice features compare to for example interpolation function *interp1*. The most important features for this work is the spline commands *fnval* and *fnder*, which evaluates the function for a given input value and derivates the interpolated function, which are needed when the nonlinear plant should be linearized. Due to the Taylor expansion described in Section 4.1, all the nonlinear expressions must be partial derivated with aspect to all included variables, which is done with the command *fnder*. Furthermore, when these functions have been derivated, the linearization points shall be evaluated to create the linear matrices in the state-space form and the command *fnval* does this. This leads to a very convenient way when handling the nonlinear maps and the linearization of the plant.

The spline functions can also be plotted with the command *fnplt*. The maps plotted in this way can be seen in Appendix 9.9.

5.3. Linearization of the system

As seen in equations (38)-(40) and (41)-(51), this state-space representation is very much nonlinear, discontinuous with several maps included. The next step towards obtaining a suitable MPC model is to apply some approximations in order to achieve a PWA representation of the process.

This is done with the previously stated Taylor expansion applied to all the time derivative state functions and the output functions. The results are multiple partial derivatives of the included functions in the state-space form which is evaluated in the linearization points.

All matrices in (52)-(53) become Jacobin matrices where each and every element comprehends to a partial derivative with respect to a particular variable and all of these can be seen in Appendix 9.8. The elements in the created matrices are denoted $a_1 \dots a_9$ for the A matrix, $b_1 \dots b_6$ for the B matrix etc in (52-53).

For example, if the first state is set to $\dot{x}_1 = f_1$, then the first element in the A matrix is defined as

$$a_1 = \frac{\partial}{\partial x_1}(f_1(x_0, u_0, d_0)) \text{ and next } a_2 = \frac{\partial}{\partial x_2}(f_1(x_0, u_0, d_0)) \text{ and so forth.}$$

As can be seen in the nonlinear state-space representation in (38-51), most of the equations are fairly complicated, and with the risk of human error, all derivatives were calculated with the assistance of the computer algebra program *Maple*.

This finally gives the linear state-space system in (52)-(53).

$$\dot{x} = \begin{bmatrix} \dot{\omega}_{ENG} \\ \dot{P}_{boost} \\ \dot{SoE} \end{bmatrix} = \begin{bmatrix} a_{11} & a_{12} & 0 \\ a_{21} & a_{22} & 0 \\ a_{31} & 0 & a_{33} \end{bmatrix} x + \begin{bmatrix} b_{11} & b_{12} \\ b_{21} & b_{22} \\ 0 & b_{32} \end{bmatrix} u + \begin{bmatrix} bd_{11} & 0 \\ bd_{21} & 0 \\ 0 & bd_{32} \end{bmatrix} d + F_{(i)} \quad (52)$$

$$y = \begin{bmatrix} \omega_{ENG} \\ T_{ENG} \\ T_{boost} \\ P_{boost} \\ T_{pumps} \\ m_{fuel} \\ P_{ESS} \\ SoE \\ \eta_{ESS} \\ P_{DEM} \\ T_{GEN} \end{bmatrix} = \begin{bmatrix} c_{11} & 0 & 0 \\ 0 & 0 & 0 \\ c_{31} & c_{32} & 0 \\ 0 & c_{42} & 0 \\ c_{51} & 0 & 0 \\ c_{61} & 0 & 0 \\ c_{71} & 0 & 0 \\ 0 & 0 & c_{83} \\ c_{91} & 0 & c_{93} \\ 0 & 0 & 0 \\ 0 & 0 & 0 \end{bmatrix} x + \begin{bmatrix} 0 & 0 \\ d_{21} & 0 \\ d_{31} & 0 \\ 0 & 0 \\ 0 & 0 \\ d_{61} & 0 \\ 0 & d_{72} \\ 0 & 0 \\ 0 & d_{92} \\ 0 & 0 \\ 0 & d_{112} \end{bmatrix} u + \begin{bmatrix} 0 & 0 \\ 0 & 0 \\ 0 & 0 \\ 0 & 0 \\ dd_{51} & 0 \\ 0 & 0 \\ 0 & dd_{72} \\ 0 & 0 \\ 0 & dd_{92} \\ dd_{101} & dd_{102} \\ 0 & 0 \end{bmatrix} d + G_{(i)} \quad (53)$$

Because of the system dynamics change due to the switches stated in equations (38)-(40) and (41)-(51), most of the elements in the matrices obviously changes as well.

As summary, the process is approximated with several linear representation due to different condition, for example if the pressure difference is greater or smaller than zero, i.e. $dp > 0$ or $dp \leq 0$ and due to the nonlinearities in the system. These nonlinearities represent the nonlinear maps and all other nonlinear dynamic in the state and the output functions.

5.3.1. Linearization points

When the task is to linearize a system and thus create a state-space form, the most common and natural way is to approximate the dynamics around a stationary point. A stationary point is a point in a function where the value of the function becomes zero (or close to it). In continuous time this means that the derivative is zero (the functions is the derivatives) and in discrete time the value at the next sampling time is equal to the previously.

This is not a good approach to the problem presented, due to how the mathematical descriptions of the dynamics are defined. As stated before, there are several switches in the hybrid system and these comprehend each to a certain operating mode. When linearizing a nonlinear system with switches included, the description on where the linearization points should be, becomes very important. This is because if this hybrid system would be linearized around a stationary point, then by definition, the linear functions are linearized around a point that results in a zero in the nonlinear functions. Recall from the Section 5.2, these switches occurs when for example dp is close to zero. After a little investigation it is fairly straightforward to see that in the equation below taken from (23), the function goes to zero if $dp \rightarrow 0$ and if $\dot{\omega} \rightarrow 0$. Because $\dot{\omega}$ is one of the functions that should be evaluated around a stationary point and thus is zero, results in the variable dp to be close to zero in order to achieve a stationary point for this function.

$$\lim_{\dot{\omega} \rightarrow 0, dp \rightarrow 0} (\dot{P}_{boost}) = \lim_{\dot{\omega} \rightarrow 0, dp \rightarrow 0} \frac{dp}{getboosttimeconstA(\omega_{ENG})} - \frac{K_{corr} \cdot \dot{\omega}_{ENG} \cdot P_{boost}}{\omega_{ENG}} = 0$$

If dp is close to zero the dynamic lies very close to a switch because of the condition ($dp > 0$ or $dp \leq 0$).

The third state equation (24) also brings out the same problem. This is because the switch ($P_{ESS} \geq 0$ or $P_{ESS} < 0$) is included in the numerator in the $S\dot{o}E$ and leads to a stationary point that it is close to a switch. This can be seen below where the state function $S\dot{o}E$ becomes zero if the variable $P_{ESS} = 0$, i.e. close to a switch.

$$\lim_{P_{ESS} \rightarrow 0} (S\dot{o}E) = \lim_{P_{ESS} \rightarrow 0} \left(-\frac{\varphi_{ESS} \cdot P_{ESS}}{E_{ESS\ max}} \right) = 0$$

In Figure 13 an illustration on this problem is shown.

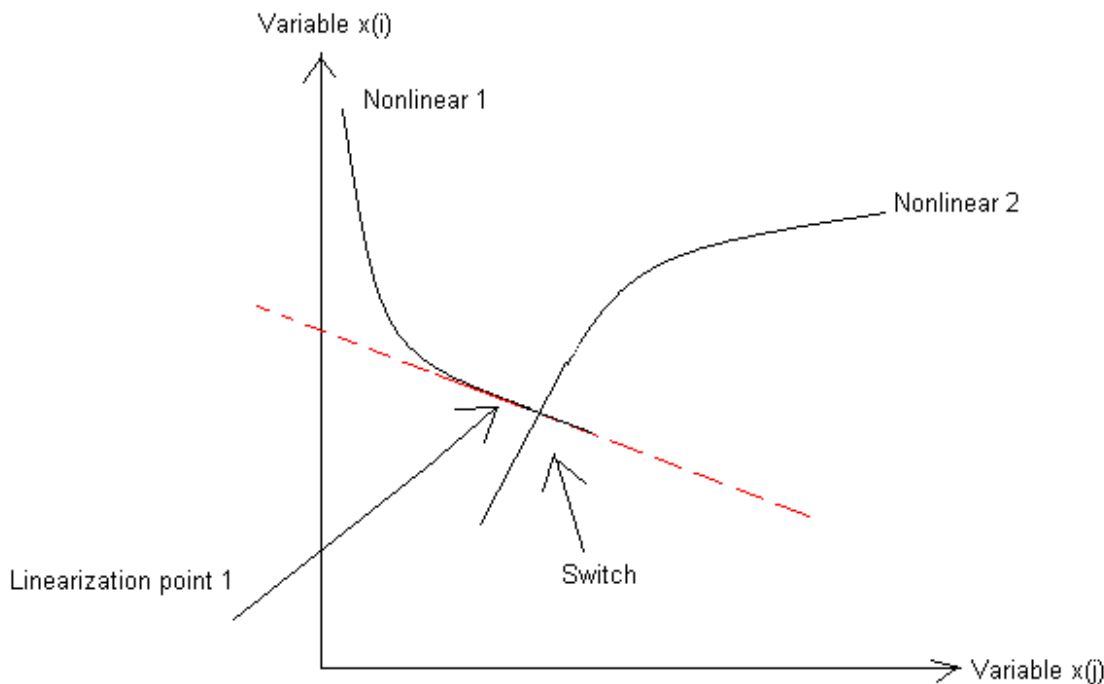


Figure 14. Illustration on a bad choice of linearization point.

The solution to this problem stated here is to linearize around a non stationary point and after that manipulate the Taylor expansion with a constant in order to get the desirable form in (17)-(18) and not be close to any switch. The constant is the one presented in (9), i.e. $f_{(i)}(x_0, u_0, d_0)$ and this is why it is more convenient in general to linearizes the nonlinear functions around stationary points due to the fact that $f_{(i)}(x_0, u_0, d_0) = 0$.

The problem now remains to get feasible and satisfying linear models that describe the different dynamics of the system.

When handling problems connected to the MPC approach, the most excessive work is to create a complete approximate model that describes the plant in a satisfying way. Due to the nonlinear preferences of the maps and the included expressions in the state-space equations the plant should be linearized around multiple points to create an acceptable approximation. But with the increase of linear models in the PWA system, the computation time becomes greater and a trade off must be introduced between achieving a good approximation of the plant and at the same time not to increase the complexity too much.

5.3.2. Creating PWA system

A good model of the plant is essential in order to achieve reasonable results and choosing polytopes is probably the most important part to accomplish this. As for this work, the mission was to develop linear models that describe the plant for only the presented driving cycle in Figure 11. To decide the number of linear models in the system, and thus set the approximate level in the simulations are a little bit of a “try and error” method. However, some things can be established from the beginning to simplify the approach, for example, between what boundaries the variables are defined due to physical constraints.

The goal is to minimize the number of models and at the same time get as good linear representation of the plant as possible. To achieve this objective, investigations must be made on all the maps and the switches to see where the number of switching nonlinearities occurs.

- **Physical constraints:** The included variables in the state-space representation have all physical constraints that describe in what interval these variables can occur. For example, the control signal T_{Eng} can not be negative due to the physical constraint on the ICE. Another example is the state, turbo pressure (p_{boost}), which also can not be negative because this is physical impossible.
- **Nonlinear maps:** All the maps in Appendix 10.7 are included in the mathematical description which defines the plant. So in order to get a feasible approximation of the plant, these nonlinear functions must be studied in order to decide how many linear functions to introduce. In Appendix 10.8 the maps have been plotted and there are a total of eight maps.
- **Switches:** There are several switches included in the system that describes the change from a mathematical expression to another. These are important to understand in order to know where the most nonlinear properties occur and thus how the system should be linearized. Because of the fact that the guard lines in the MPT toolbox are defined as linear, these switches must be linearized as well. The switches can be found in Appendix 10.9 and the total number of switches is four. If all switches are introduced in the dynamics (the boolean variable *isengon* not included) there could be eight different combinations of mathematical descriptions in the system.

Different combinations of switches

```

if (dp >=0){
    if (PGen<0){
        if (PESS>0){
            Switch 1
        }else{
            Switch 2
        }
    }else{
        if (PESS>0){
            Switch 3
        }else{
            Switch 4
        }
    }
}

```

```

}else{
    if (PGen<0){
        if (PESS>0){
            Switch 5
        }else{
            Switch 6
        }
    }else{
        if (PESS>0){
            Switch 7
        }else{
            Switch 8
        }
    }
}

```

Figure 15. The different conditions on the switches in the system.

It is important to have as few linear models as possible in the MPC regulator and therefore it is of high priority to investigate if all switches are introduced in the presented driving cycle. As can be seen in Figure 15, that if all the mathematical descriptions are included, it would lead to at least sixteen linear models in the PWA system and then all of these nonlinear descriptions must be linearized maybe around two points, which doubles the amount of models to thirty-two. So for starters, the option to turn on/off engine is removed.

It is very hard from the beginning to know if all the mathematical descriptions should be included, but a closer look at the condition of the switches leads to some simplifications. The equation that defines the output power from the battery (P_{ESS} , (33)) includes the parameter (P_{Gen} , (32)) and both of these define each a switch, as can be realized in Figure 14. The switches denoted 4 and 8 are highly unlikely to occur because of the reason that if P_{Gen} is positive, it takes a great negative value on P_{SWEM} to cancel both P_{Gen} and $P_{AUX} = 12500W$ together. The equation from (33) is shown below with the inequality that it should be greater than zero.

$$P_{ESS} > 0 \leftrightarrow P_{Gen}^{el} + P_{AUX} + P_{SWEM}^{el} > 0, \text{ if } [P_{AUX} = 12500, P_{Gen}^{el} > 0] \rightarrow P_{SWEM}^{el} > P_{AUX} + P_{Gen}^{el}$$

Therefore, due to the unlikely occurrences of *switch 4* and *switch 8*, these are cancelled when creating the PWA system.

5.4. Sampling time

The sampling time is a crucial parameter when creating PWA system as an approximation of the plant. A PWA system created from the mathematical equations given in Section 5.2 is given in continuous time. The MPC controller needs a discrete PWA model and therefore, the continuous PWA system must be discretized. This is done with a sampling time which approximates the continuous dynamic in the system to a discrete system. With a smaller sampling time, i.e. sample the system in more points, a more correct creation of the continuous dynamics is made in discrete time, but also a more computational depended problem.

After some “try and error” and simulation experience of the system, the sampling time was set to 0.5 seconds and this holds throughout the master thesis.

5.5. Handling of disturbances

The influence of disturbances is of great importance in this control problem. As stated before, the disturbance represents the power demand from the pumps and the swing, which must be fulfilled at all time during the simulation and is introduced as an input signal along with the control signal to the plant.

This however results in a problem when defining the model of the plant with the MPT toolbox. The Toolbox is only capable of handling a constant disturbance on state update equations and not on the outputs. It is essential to include the influence of the power demand (P_{pumps}, P_{SWEM}) both in the state update equations and the output equations. To develop a model without introducing the disturbances could perhaps work sometime in general, but in this case that is an impossibility. The reason is that this disturbance is so vital to the system and magnitude is so great on this signal ($0 < P_{pumps} < 10^5$ W, $-5 \cdot 10^4 < P_{SWEM} < 5 \cdot 10^4$ W), that it would take an almost impossible robust controller to handle this behavior. So the conclusion is that it must be included in the model setup and this is done by extending the state vector with the disturbances.

There is an option of state feedback in the toolbox which opens up a possibility to include the disturbance in the model. This is possible if the state vector is extended with the disturbance as can be seen in (54). With the help of state feedback this model can describe the same equations for the dynamics as with the model when the disturbances are introduced as inputs to the plant, i.e. included in the control signal vector.

$$x = \begin{Bmatrix} \omega_{ENG} \\ pboost \\ SoE \\ P_{pumps} \\ P_{SWEM} \end{Bmatrix} \quad (54)$$

When defining the disturbances as states in the system, a decision on how these should be updated from one sample to the next in discrete time (or in the continuous case how the time derivative must be made). As a first stage in this approach the disturbance in the model is assumed to be constant during the prediction horizon, i.e. the values of (d_1, d_2) are constant when computing the optimal control problem. With the extension on the state vector, an extension of the state-space matrices follows;

$$\begin{Bmatrix} \dot{\bar{x}} \\ \dot{d} \end{Bmatrix} = \begin{bmatrix} A & Bd \\ 0 & 0 \end{bmatrix} \cdot \bar{x} + \begin{bmatrix} B \\ 0 \end{bmatrix} \cdot \bar{u} + \begin{bmatrix} F \\ 0 \end{bmatrix} \quad (55)$$

$$\bar{y} = [C \quad Dd] \cdot \bar{x} + D \cdot \bar{u} + G \quad (56)$$

With this strategy and with the help of state feedback, the power demand can be included in the model and a graphical illustration of the approach can be found in Figure 16.

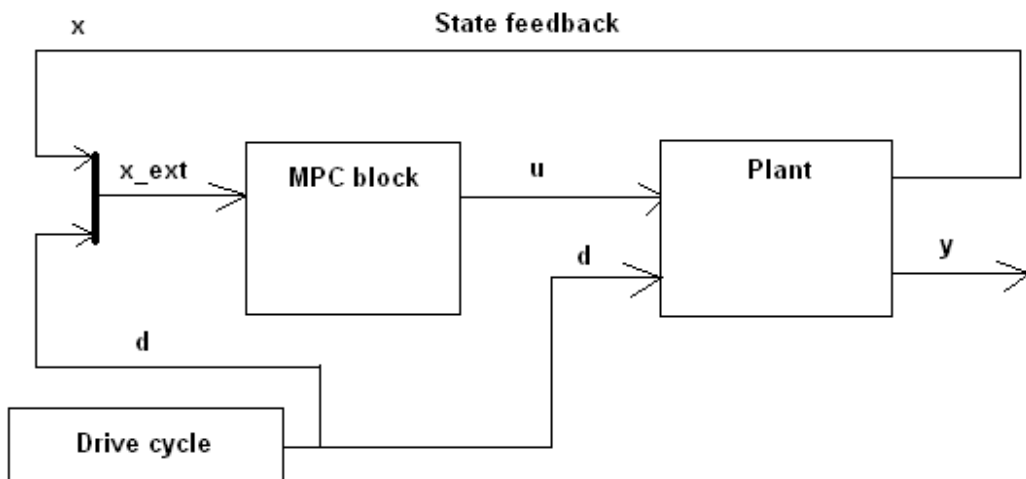


Figure 16. Graphical illustration on the extended state vector approach. The parameter denoted x_{ext} represents the extended state (54).

5.6. Model validation

In the first three sections (6.1-6.3), results are presented for the linearized switches and the models included in the dynamics. In these sections the simulations have been generated by a premade simple regulator constructed by Jonas Hellgren at Volvo Technology with the driving cycle presented in Section 4.2. With the unknown number of linear models in the PWA system, the linearization of the nonlinear dynamics in the system was made with different approximation levels. Then these different PWA systems were evaluated against each other to investigate what level of nonlinearities existed. Three models have been stated in Table 3 with different level of approximation. The first one, (PWA 1) has six switches included and as stated before in Section 5.3.2, the total number of switches was eight, but then two of those were cancelled. Furthermore, in this PWA model, the nonlinear functions and maps were linearized around two points. The approximate level is the lowest for this model.

The model denoted PWA 2 has also all switches included but only linearized around one point. This model should be more approximated than PWA 1, due to the linear representation of the nonlinear functions and maps are more poorly approximated.

Last model to evaluate is the PWA 3 model and this model has only three switches included. The explanation on why there only exist three switches here is because the turbo dynamics in the ICE are completely ignored. With this assumption the switch denoted dp is removed and results in only two expressions that defines the switches in this PWA system.

<i>PWA model</i>	Number of models	Number of states
PWA 1: 6 switches and 2 linear points	12	7
PWA 2: 6 switches and 1 linear point	6	7
PWA 3: 3 switches and 1 linear point (no turbo)	3	6

Table 3. Defining the different PWA systems.

In the first experiment, i.e. the linearization of the switches, the simulink file used can be seen in Appendix 10.10. To the very left in this figure the driving cycle is generated which produce the power demand from the pumps and from the swing, but also the EGM signal. In the center of this simulink file, the nonlinear plant is located and this box generates all the necessary outputs from given values of the inputs, i.e. the power demand and the control signals from the regulator. The outputs mentioned are the values of the nonlinear switch functions.

The premade regulator in these linearization experiments is of a very simple nature. With the outputs know from the plant, the torque on the generator is calculated as followed;

$$T_{Gen} = - \frac{(1000 \cdot (SoE_{ref} - SoE))^2 + P_{AUX} + 0.5 \cdot (P_{SWEM}^{el} > 0) \cdot P_{SWEM}^{el}}{\max(10, \omega_{Eng})} \quad (57)$$

The control strategy for this regulator and thus in this expression is that the first part of (57) is controlling deviations from a reference level in the battery. This reference level is set to $SoE_{ref} = 0.5$ and says that the HCEV should have a current power capacity around half of a fully charged battery. If there exist a large deviation from this reference trajectory, the control signal on the generator (T_{Gen}) becomes larger and this means that more mechanical power is transformed into electrical power to charge the battery. The second term in (57) is very straight forward and it represents that the generator should satisfy the constant power to the electrical system in the HCEV.

Finally, the last term handles the power from the swing system and it says that if the power from the SWEM is greater then zero (i.e. a power demand from the swing system), then half of that power should be satisfied by the generator.

The denominator in (57) is the rotational speed on the generator which is the same as for the ICE to create the torque signal.

After the torque on the generator has been calculated, the torque on the ICE is calculated in a fairly easy way as can be seen in (58). It takes the difference between the generated torque on the pumps and the torque losses due to the turbo boost and the calculated torque on the generator.

$$T_{Eng}^{ref} = T_{pumps} - T_{boost} - T_{Gen} \quad (58)$$

Now the complete control signal is calculated, but due to the fact that the ICE can not achieve a desirable torque simultaneously, a torque reference signal on the ICE is created as in (58). This reference signal combined with a reference signal on the engine rotational speed is included to control the engine modes.

The linearization of the switches

In Figure 14 the definition of all the switches in the system can be seen. There are three switches from the dynamics that form different combinations of mathematical descriptions and those are the pressure difference (dp), the power output from the generator (P_{Gen}) and the power output from the battery (P_{ESS}).

As stated in a previous section (5.3.2) these switches must also be linearized in order for the MPT toolbox to divide the different linear models.

5.6.1. Pressure difference

The equation for the pressure difference can be found in Section 5.2 in equation (26). The nonlinear preference here is the nonlinear map which defines the steady-state boost pressure ($\Omega_3(\omega_{Eng}, T_{Eng})$) and this map can be seen in Appendix 9.8.1. This map thus also the pressure difference expression is linearized around two points and can be seen below.

The nonlinear pressure difference is calculated with the predefined map which describes the steady-state pressure boost. For a given value on the rotational speed (ω_{Eng}) and the torque on the engine (T_{Eng}), a value on the steady-state pressure boost can be achieved and then this value is subtracted with the value of the current pressure in the engine (p_{boost}) during the simulation. At the same time a linear representation of the pressure difference is calculated with the form shown in (59).

$$dp_{linear} = (k_{dp})_1 \cdot x_1 + (k_{dp})_2 \cdot u_1 + m_{dp} \quad (59)$$

In the table below the linear equation parameters are shown and the nonlinear pressure difference function is divided into two linear equations. These two are used when PWA 1 model is evaluated and this is because all functions are linearized around two points. For PWA 2 and PWA 3, only *linear part 1* in Table 4 is used.

Pressure difference model	x_1^0	u_1^0	$(k_{dp})_1$	$(k_{dp})_2$	m_{dp}
Linear part 1	200	250	0.9156	0.2963	-81.0342
Linear part 2	200	500	0.6561	0.2691	-6.4689

Table 4. Describes the linearization points and the linear equation parameter values for the pressure difference function

In Figure 17 the results from a simulation with the defined simple regulator is shown and with both linear parts from Table 4 operating.

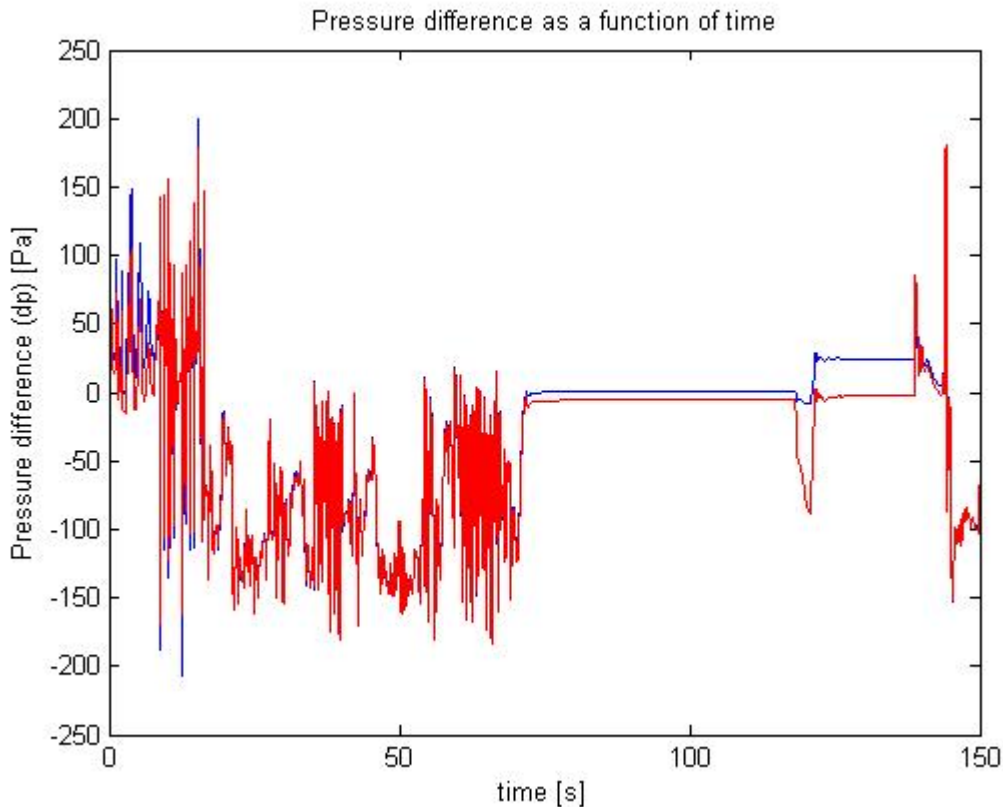


Figure 17. The pressure difference for the nonlinear representation (blue) and the linear representation (red), two linear points.

The linear curve (red in Figure 17) follows the nonlinear curve (blue in Figure 17) very well but in the end of this simulation there occurs an offset error. This is probably due to a value on ω_{Eng} and T_{Eng} that diverge a lot from the linearization points. Besides this, the result is satisfying with the use of two linearization points for this nonlinear function.

5.6.2. Power output from generator

The nonlinear equation for the power output on the generator (P_{Gen}) is defined in (32). This parameter defines the second switch in the system and more physically, describes if the generator should work as a motor (transform electrical power to mechanical power) or work as a generator (transform mechanical power to electrical power). If the power output on the generator is greater than zero, the generator is operating as a motor and if the power output is equal or smaller than zero, the generator transforms mechanical power to electrical power, i.e. work as a generator.

The linearization on this nonlinear function (P_{Gen}) can be seen in Table 5 and is divided into two linear equation for PWA 1 and the *Linear part 1* for PWA 2 and PWA 3.

P_{Gen} model	x_1^0	u_2^0	$(k_{Pgen})_1$	$(k_{Pgen})_2$	m_{Pgen}
Linear part 1	200	-100	-150	200	30000
Linear part 2	200	-200	-300	200	60000

Table 5. Describes the linearization points and the linear equation parameter values for the power output from the generator function.

The power output from the generator for the nonlinear and the linear representation can be seen in Figure 18.

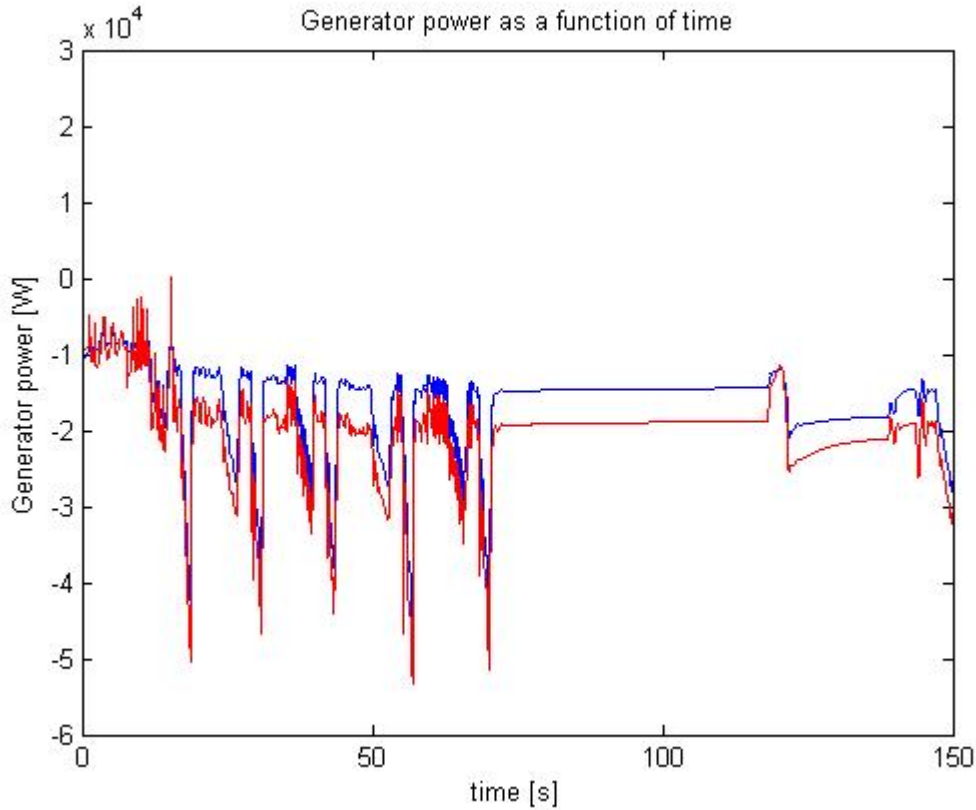


Figure 18. The power output from the generator for the nonlinear representation (blue) and the linear representation (red), two linear points.

This graph also shows (Figure 18) an offset error from the nonlinear function. The difference between this approximation error and the one in the previously graph (Figure 17), is that the offset error occur during a great part of the simulation. This mean that the dynamical behavior of the generator is harder to approximate with two points compared to the pressure difference switch.

5.6.3. Power output from ESS

The definition on the last switch is the power output from the ESS (P_{ESS}) and this function can be found in Section 5.2 (33) and here below;

$$P_{ESS} = T_{GEN} \cdot \omega_{ENG} \cdot getgeneff(\omega_{ENG}, T_{GEN}) + P_{AUX} + P_{SWEM}^{el} \quad (60)$$

Due to the fact that the power on the AUX system is constant and that the power from the SWEM is known, the only nonlinearity in equation (60) is the power output from the generator. This switch is defined as if the P_{ESS} is greater or smaller then zero, and physically if the battery should withdraw electrical power from the battery or charge the battery.

The linearization should only be applied to the first term of the equation which is almost as same as the linearization on the second switch (power output on the generator (P_{Gen}^{mech})). The difference is the efficiency factor on the generator and this function, as can be seen in *Appendix 9.8.6*, is very nonlinear.

The linear equations on the nonlinear function can be seen in Table 6. Both the nonlinear and the linear representation are plotted in Figure 18.

P_{ESS} model	x_1^0	u_2^0	$(k_{Pgen})_1$	$(k_{Pgen})_2$	m_{Pgen}
Linear part 1	200	-100	-136.1086	160.2034	$2.5143 \cdot 10^4$
Linear part 2	200	-200	-280.6985	174.9874	$5.4478 \cdot 10^4$

(A.1) Describes the linearization points and the linear equation parameter values for the power output from the ESS function.

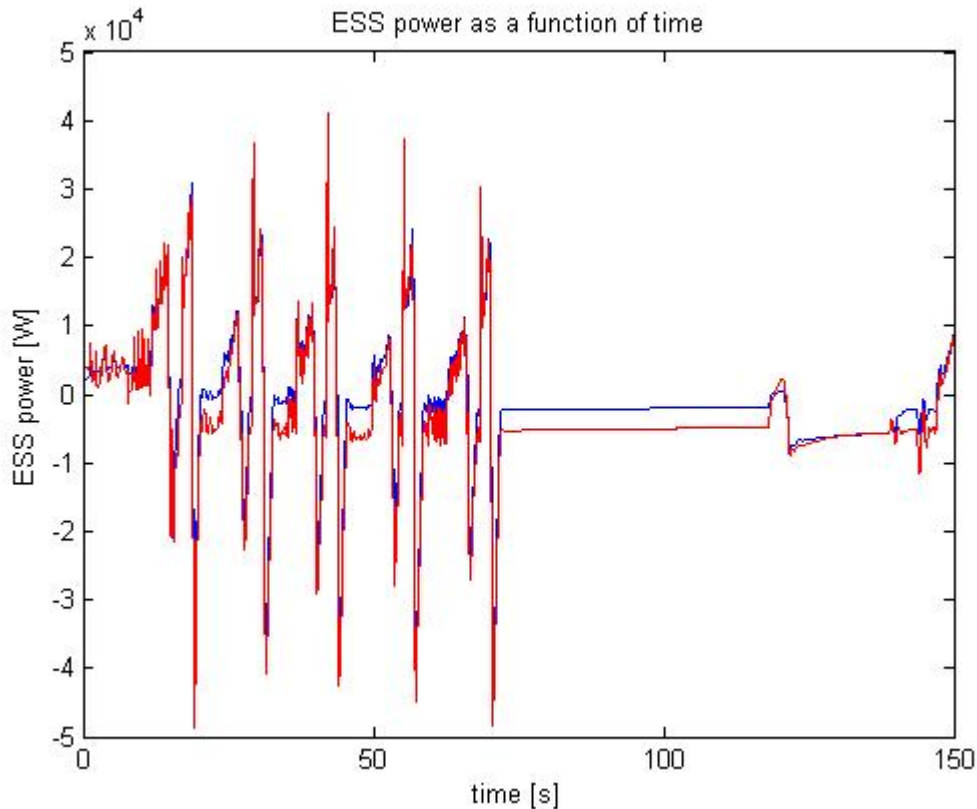


Figure 19. The power output from the ESS for the nonlinear representation (blue) and the linear representation (red), two linear points.

The linear curve follows the rapid changes of the P_{ESS} in Figure 19, but when the dynamic is near constant, an offset error occur.

In almost all switches that are approximated, an offset error can be seen when the dynamic is constant in time. This behavior depends probably on when the switch dynamic is constant in time, the linearization points are far from the current operating values.

Linearization of the plant

As stated before, different linear models with different approximate levels are created and evaluated against each other. When the linearization points were defined, a great part of the strategy was through investigation of the nonlinear functions and maps. This lead to approximate values on the linear points, but after that, some “try and error” methods was applied to construct the PWA systems.

The evaluation of the different PWA system was made with the simple PI-regulator defined in the beginning of Section 5.6. Due to this, the result from these simulations has a good probability to be satisfying when the MPC controller is introduced as well, but not certain. This is because the MPC controller has a different control strategy then the PI-regulator, which means that the system dynamics are in other regions. For example, the simple structure in the used PI-regulator leads to that the generator can not work as an engine in the simulations ($P_{gen} > 0$) and therefore a lot of dynamical behavior is not tested. In these three systems evaluated, the linearization points for the rotational speed on the engine and the battery level have been set to $x_1^0 = 200$, $x_3^0 = 0.5$. Only the work mode “dig and dump” is simulated in this work (0-100 s) and this work mode correspond to an engine mode (EGM) which has constraints defining the rotational speed around 200 rad/s. The battery level should also be in some strict limits and vary around 0.5.

Some different sampling intervals were tested in these simulations and it was shown that a sampling time equal to 0.5s was too large and made the regulator unable to control the system. But with a sampling time of 0.1s the PWA systems could be controlled likewise as the nonlinear plant.

5.6.4. PWA 1

The system denoted PWA 1 has twelve linear models, i.e. six switches and two different linearization points for the torque on the ICE. This is the most complex PWA system evaluated and should show best result regarding approximation of the plant.

The linearization points for the twelve models can be seen in Table 6. Notice here that each and every one of the first six linear models describes the switches (*switch 1-3* and *switch 5-7* in Figure 15). The last six also describes the switches but in a different linearization point.

PWA Model

Model nr	x_1^0	x_2^0	x_3^0	u_1^0	u_2^0	d_1^0	d_2^0
Mod (1)	200	100	0.5	100	-50	50000	10000
Mod (2)	200	100	0.5	100	-120	10000	0
Mod (3)	200	100	0.5	100	100	10000	10000
Mod (4)	200	200	0.5	100	-50	10000	10000
Mod (5)	200	200	0.5	100	-120	10000	0
Mod (6)	200	200	0.5	100	50	10000	10000
Mod (7)	200	200	0.5	600	-200	50000	50000
Mod (8)	200	200	0.5	600	-200	50000	0
Mod (9)	200	200	0.5	600	200	50000	10000
Mod (10)	200	300	0.5	600	-200	50000	50000
Mod (11)	200	300	0.5	600	-200	50000	0
Mod (12)	200	300	0.5	600	200	50000	10000

Table 6. The complete PWA 1 system.

In Figure 20 the result is shown when the nonlinear and the linear model for the rotational speed on the ICE are controlled by the simple PI-regulator. Figure 21 and 22 shows the same for the boost pressure in the ICE and the battery level, respectively.

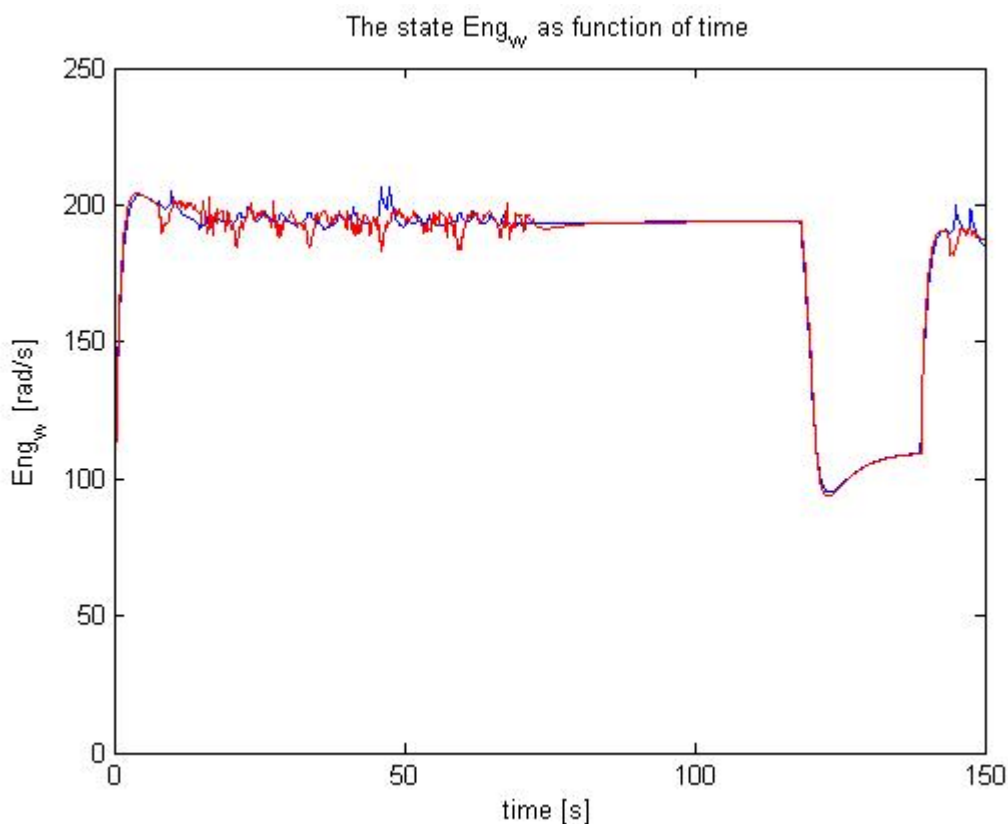


Figure 20. The ω_{ENG} dynamic for the nonlinear PWA 1 representation (blue) and the linear PWA 1 representation (red).

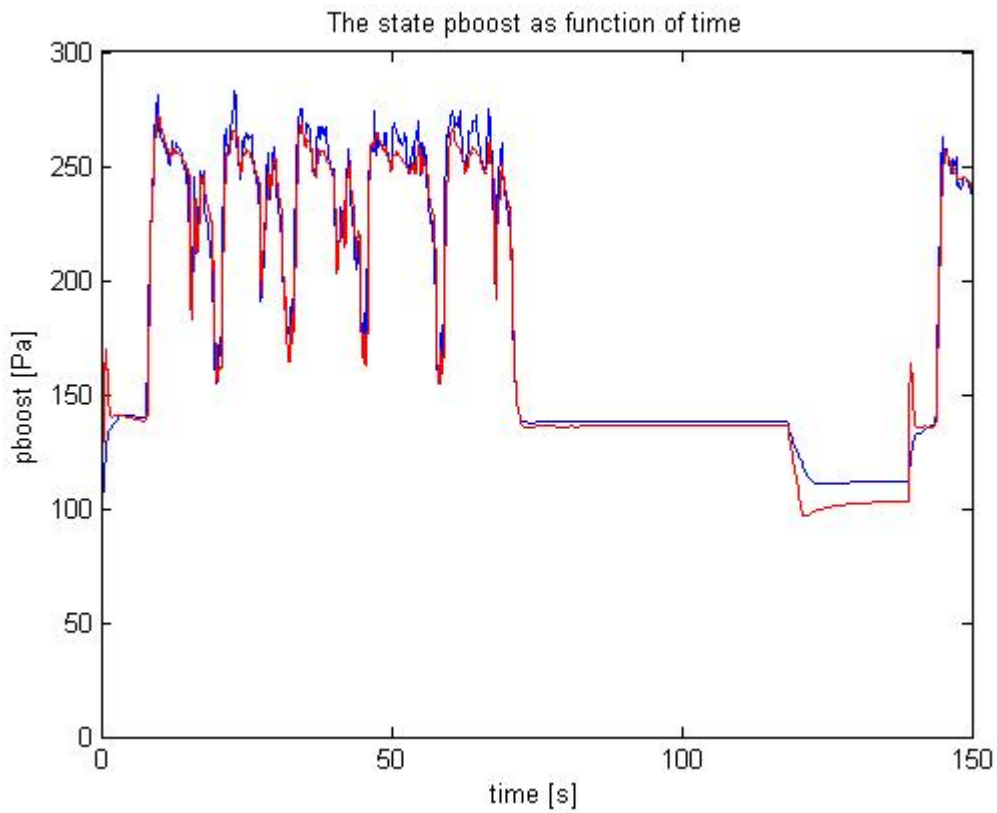


Figure 21. The pboost dynamic for the nonlinear PWA 1 representation (blue) and the linear PWA 1 representation (red).

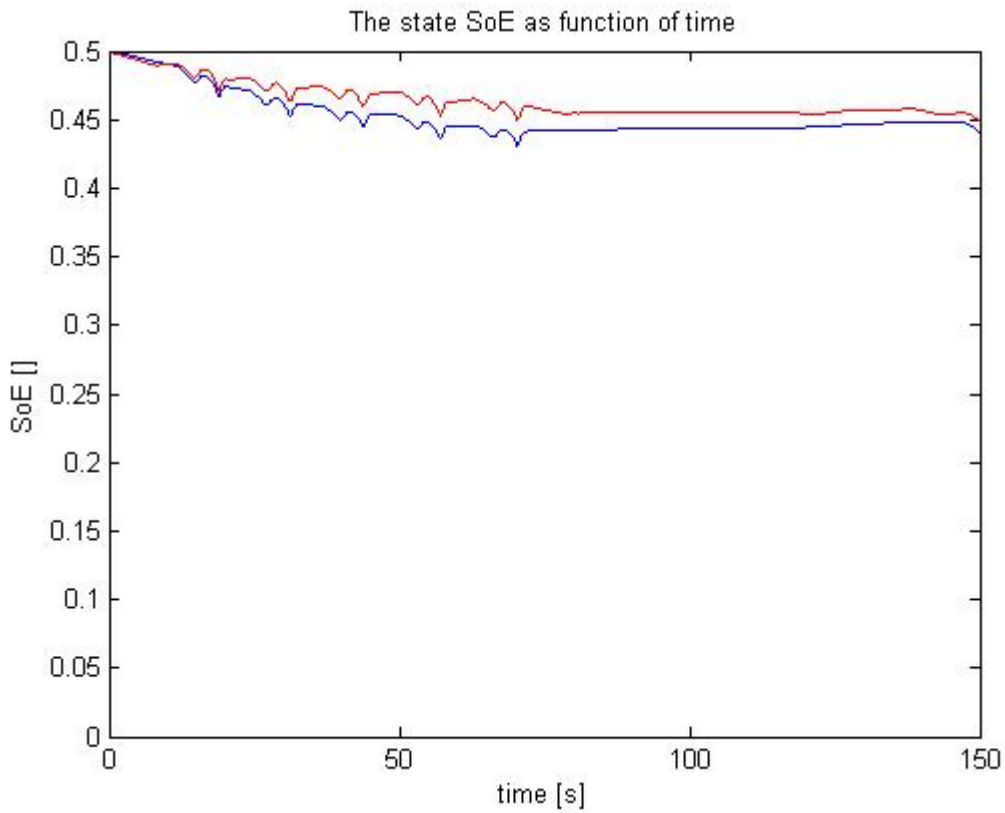


Figure 22. The SoE dynamic for the nonlinear PWA 1 representation (blue) and the linear PWA 1 representation (red).

The conclusions from these three graphs are fairly satisfying. In Figure 20 it can be seen that the linear representation on the rotational speed follows the nonlinear function very well. The reference trajectory for this signal is equal to 200 rad/s the first 120 seconds of the simulation (specific EGM) and after that, the EGM switches and the reference trajectory gets a new value. It is a little strange that after a new reference trajectory has been introduced in the system, which lies far away from the linearization point (200 rad/s), the linear curve follows the nonlinear curve almost with the same precision as in the first 0-100 seconds in the simulation. One explanation is probably that one of the control strategies in the used regulator controls the rotational speed to its reference and therefore makes the PWA system close to the plant.

The boost pressure in the ICE is shown in Figure 21 with satisfying results for the first 120 seconds of the simulations. After this time, a new work mode (and also an EGM) is introduced, which leads to a poorer approximation of the plant. The explanation on why the pressure curve is poorer than the rotational speed curve in Figure 20 after 120 seconds is that the control strategy here ignores the value of the pressure compare to the rotational speed.

The last graph (Figure 22) shows the battery level and here the results are not so satisfying. The linear curve lies above the nonlinear curve during the simulation with a 3-4 % average wrong. Much attention has been made here to tune the linearization points to achieve a better result on the *SoE*, but without any success. The reason why it deviates a lot between the linear and the nonlinear functions for the battery level is the complex structure of the mathematical description. The dynamical behavior of *SoE* includes multiple switches and many nonlinearities, such as maps and nonlinear expressions. This leads to a harder task when linearizing the variable with a small number of points.

5.6.5. PWA 2

The PWA 2 system is built up with six linear models, where each describing a switch in the plant (*switch no: 1-3, 5-7*). Only one set of linearization points are used and the approximation level should be higher here than for the PWA 1 system.

In Table 7 the parameters for the linearized system can be found.

Model nr	x_1^0	x_2^0	x_3^0	u_1^0	u_2^0	d_1^0	d_2^0
Mod (1)	200	150	0.5	500	-300	50000	50000
Mod (2)	200	150	0.5	500	-300	50000	0
Mod (3)	200	150	0.5	500	300	50000	10000
Mod (4)	200	300	0.5	500	-300	50000	50000
Mod (5)	200	300	0.5	500	-300	50000	0
Mod (6)	200	300	0.5	500	300	50000	10000

Table 7. The complete PWA 2 system.

The following three graphs show the linear and nonlinear representation of the rotational speed, pressure difference and battery level, respectively. These are denoted Figure 23-25.

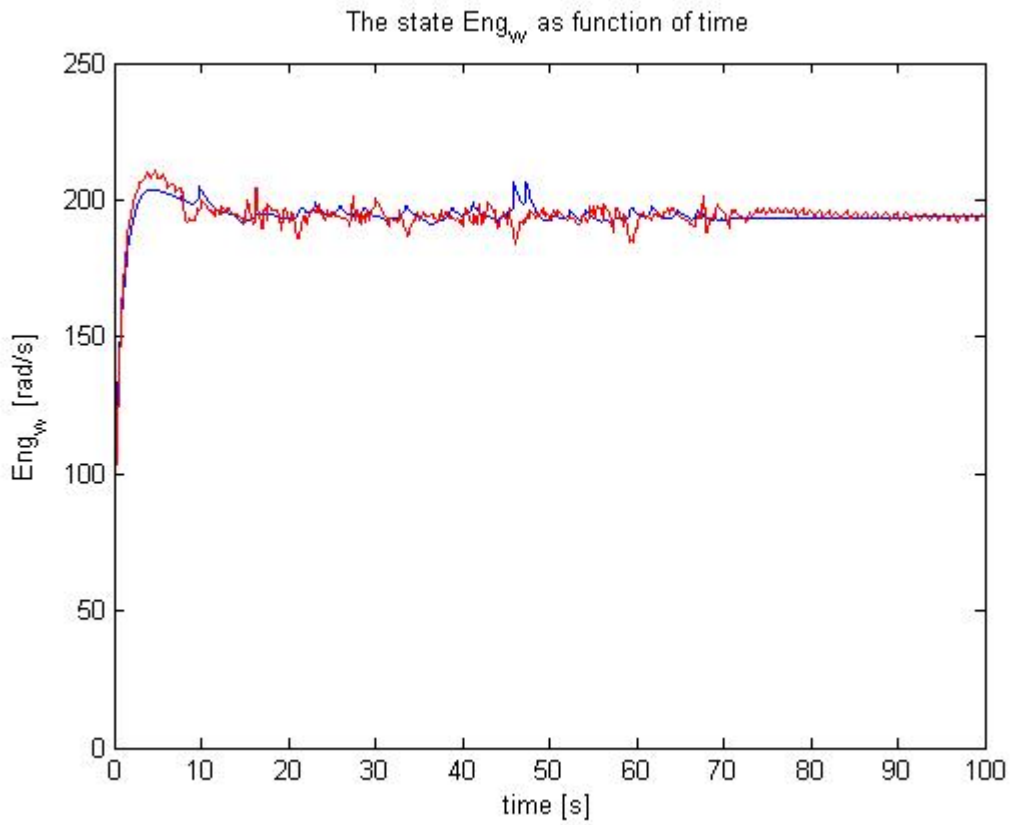


Figure 23. The ω_{ENG} dynamic for the nonlinear PWA 2 representation (blue) and the linear PWA 2 representation (red).

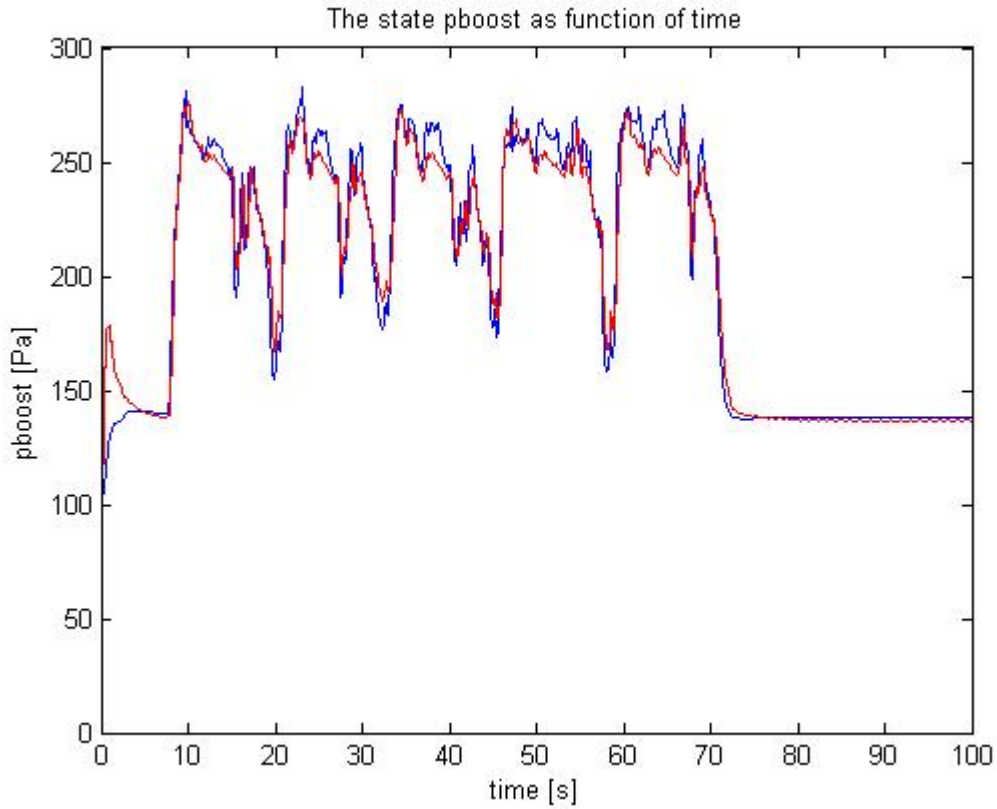


Figure 24. The pboost dynamic for the nonlinear PWA 2 representation (blue) and the linear PWA 2 representation (red).

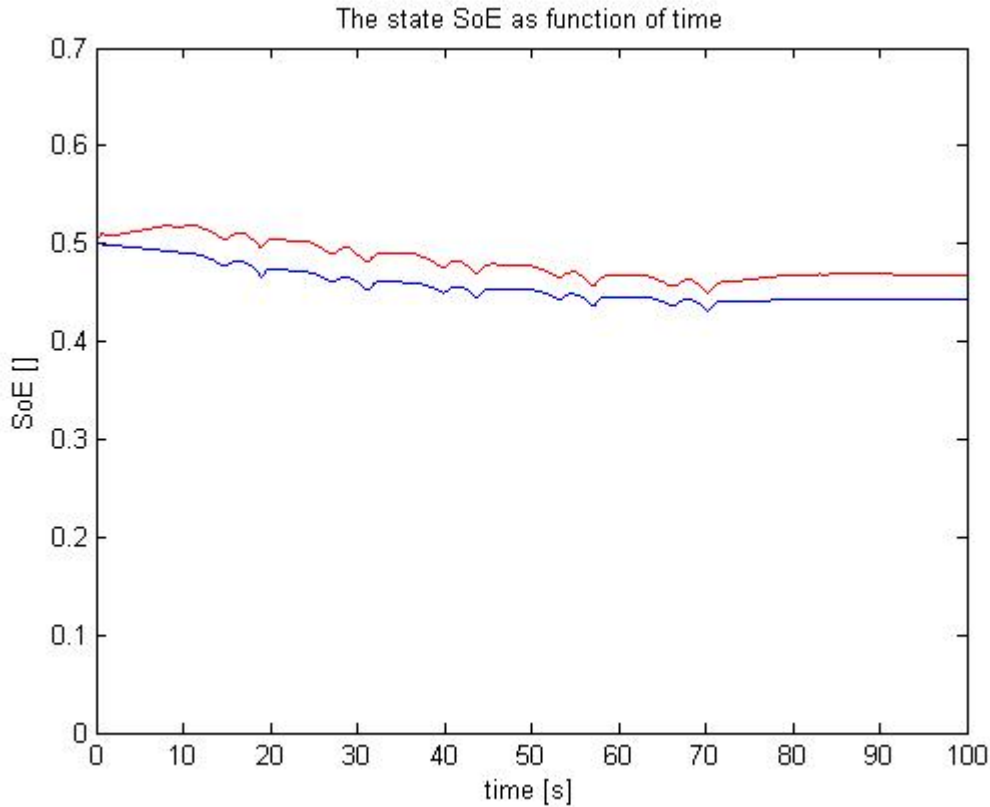


Figure 25. The SoE dynamic for the nonlinear PWA 2 representation (blue) and the linear PWA 2 representation (red).

The results from the PWA 2 system are very the same as for PWA 1, but with some difference in the battery level, which is poorer in PWA 2. This is some proof that the approximation of the dynamical behavior for the battery level becomes worse if less linearization points are used. Notice that the difference between the linear and the nonlinear representation in Figure 25 is the greatest in the beginning of the simulation. This can be explained with the value of the generator torque ($T_{Gen} = u_2$), which has a low value during the first 10-20 seconds of the simulation. That is why PWA 1 shows a better result than PWA 2, due to different linearization sets in PWA 2 (one set has a low value on u_2).

5.6.6. PWA 3 (No turbo dynamic)

The last model evaluated is denoted PWA 3. In this model the turbo dynamics have been omitted, i.e. there are not any torque losses in the ICE due to not completely developed steady state pressure. When the turbo dynamic is remove, which is a state in the ordinary description, some switches can also be removed which depends on the pressure. Also the new model has one less state equation to approximate. In Figure 15, the switch defined as dp (pressure difference) is removed and this results in three different switches. This model is linearized around one set of points, but with all three switches included as can be seen in Table 8. The switches are the one denoted in Figure 15 as *switch 1-3*.

Model nr	x_1^0	x_3^0	u_1^0	u_2^0	d_1^0	d_2^0
Mod (1)	200	0.5	500	-300	50000	50000
Mod (2)	200	0.5	500	-300	50000	0
Mod (3)	200	0.5	500	300	50000	10000

Table 8. The complete PWA 3 system (no turbo dynamic)

Likewise as previously, the states are plotted with the linear and the nonlinear representation in Figure 26-27. Notice here that there only exist two states and therefore also two plots.

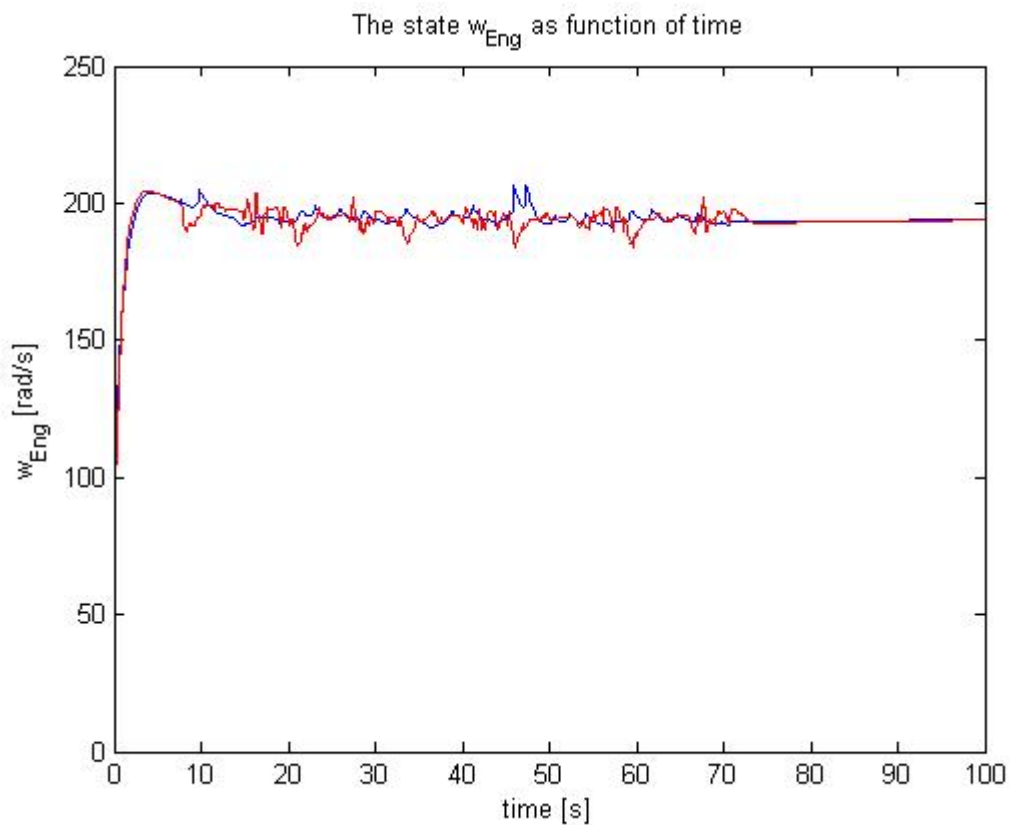


Figure 26. The ω_{ENG} dynamic for the nonlinear PWA 3 representation (blue) and the linear PWA 3 representation (red). No turbo dynamic.

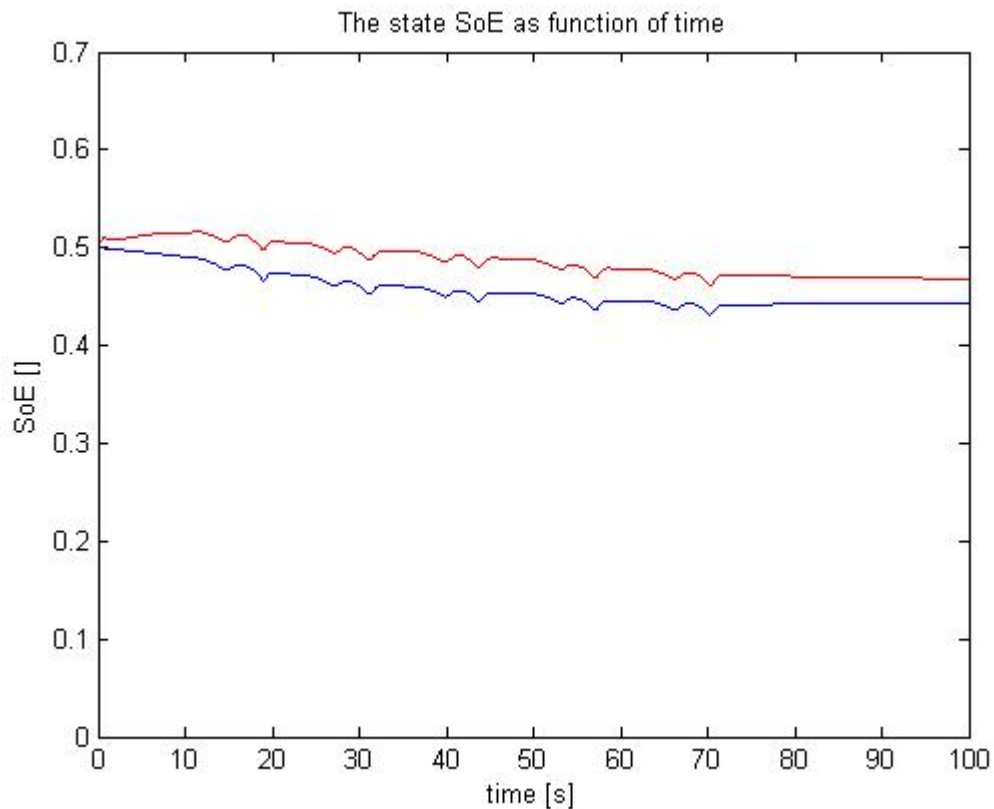


Figure 27. The SoE dynamic for the nonlinear PWA 3 representation (blue) and the linear PWA 3 representation (red). No turbo dynamic.

There are some notifying results with PWA 3 compare to the PWA 2 system. It appears that the turbo dynamic has very little impact on the ICE for these graphs. If Figure 26 is studied, the appearance is very similar to the rotational speed in the PWA 2 system (Figure 23). According to this, the approximation of removing the turbo dynamics in the plant system does not result in any major changes during this simulation.

The simulation results with this system should not be trusted entirely, due to the limited set of dynamical behavior that follows from the used regulator.

When all switches are introduced and the values of the variables in the system can be set to anywhere in the definition area, then the result of the approximations would become poorer.

6. MPC SYNTHESIS

In Section 6, the control objectives are defined as well as the creation of the MPC controller, which means for example defining the PWA system for the MPC controller, defining the cost function and the constraints in the system.

6.1. Control objectives

In all hybrid systems there exist many efficiency factors on most of the dynamics, i.e. the generator has one efficiency factor when operating as a motor and another when operating as a generator. Likewise it is for the SWEM and for the ESS. The best EMA for a hybrid system is when the efficiency factors are used optimally. A diesel engine, which is the one in this excavator's ICE, has a very low efficiency factor and there exist a lot of losses when the engine produces mechanical power. On the other hand, a battery has a much higher factor compared to the diesel engine. A basic strategy for the EMA is to use the battery as a power supplier instead of the ICE when the excavator is operating. But this can not be done continuously because the ESS would then be drained which in turn affects the durability of the battery in a negative way. The level of power in the ESS is denoted SoE (state of energy) and this level should be kept in some specific interval.

Some other things to keep in mind when describing the EMA is to satisfy the power demand from the pumps and the swing with the appropriate power from the ICE and the ESS at all time. In other words, the power given by the driving cycle must be fulfilled by the regulator and this is not straight forward because there exist regenerative power in the system, but also because the ICE can recharge the ESS with the help of the generator.

Summary of the control strategy

- 1) **Satisfy power demand:** This is probably the most important part in the control strategy. If this is not satisfied at all time this would lead to an excavator not operating properly and it will not be able to perform its assignments.
- 2) **Minimize fuel consumption:** One further step when the power demand is fulfilled is to make the excavator consume as little fuel as possible with an optimal combination of the ICE and the ESS. This can be achieved with various strategies and in this work two different strategies are considered. One is to minimize the losses in the system to get as low fuel consumption as possible. The other strategy is to minimize the fuel consumption directly, i.e. to minimize a parameter defining the fuel consumption at each sampling interval. These two are detailed presented in section 6.2.1-6.2.2.
- 3) **Specific interval for the rotational speed on engine:** For each work mode, the rotational speed should be bounded in a specific interval because it is a physical property corresponding to an EGM in the excavator. For example, if the user chooses to run the HCEV in a work mode that comprehends "dig and dump", the HCEVs rotational speed is always in a specific interval.
- 4) **Level on SoE:** A battery's lasting effect depends on how it is used. If a battery is drained or fully charged continuously, the lasting effect is lowered and this should be avoided. The power capacity in the battery is denoted SoE and is a number between 0-1. Zero means that the battery is drained and one means fully charged. The SoE should be in a preferable interval during the complete simulation.
- 5) **Constraint handling:** The possibility to define limitations on different variables due to physical constraints in the system. For example, the control signal (torque on engine and generator), should not exceed a value comprehended to the maximal torque in reality for the engine and generator.

The first stated control objective, denoted 'satisfy power demand', is indirectly controlled by the third control objective. This is because the rotational acceleration is depended on the difference between the produced and demanded mechanical power in the excavator.

6.2. Cost function

The MPC control algorithm is based on the cost function defined in Section 4.2, but can be seen with some changes as well below (see the same section for theory enlightenment). From here on, the norm of the cost function is set to be quadratic and there exists penalty on both the states as well as on the outputs and inputs. The reason why a quadratic norm is used is because a quadratic representation of the cost function generally yields controllers of lower complexity than their $1/\infty$ -norm counterparts.

$$J(k) = \sum_{k=1}^{H_p-1} \left(\hat{y}(k+i|k) \cdot Q_y \cdot \hat{y}(k+i|k) + \hat{x}(k+i|k) \cdot Q \cdot \hat{x}(k+i|k) \right) + \sum_{i=0}^{H_u-1} \hat{u}(k+i|k) \cdot R \cdot \hat{u}(k+i|k) \quad (61)$$

This equation is a very essential part of the ECA, because it tells how the dynamics should be controlled. There exists a great amount of different control strategies based on how the control problem is formulated, i.e. if the control structure is based on a conventional hybrid vehicle or if in this case, a HCEV. As described before, a HCEV can withdraw power from two power supplying units, i.e. the ICE and the ESS, and this enables a feature to reduce the fuel consumption with an energy control strategy, but also monitoring other variables of interest.

The first approach is to develop an MPC regulator to control a PWA model of the real plant and after that replaces this model with the real plant. To start with in this strategy, two linear models need to be created, one inside the MPC block and one that acts as the plant. These two models do not have to be the same, in fact it is much more convenient to let the “MPC model” (i.e. the model used by the MPC regulator) be less complicated than the plant model to minimize computational time. The states and the inputs to both models must be the same, but changes can be made on the outputs. Outputs in the plant model in our case exist because these signals should be inside physical boundaries (constraints) and to see how the process behaves. To minimize the complexity in the MPC model, a lot of these outputs are removed in the beginning. Only those output signals that are included in the control strategy are defined in the MPC model. When successive simulations with this model have been done, the outputs included in the plant model are introduced in order to create a regulator that takes all the constraints in the system into account.

As can be seen in the definition of the cost function previously; states, inputs and outputs can be included. The variable denoted \hat{y} in the cost function is the outputs that are to be controlled, which includes both the states and the outputs, because all states are included in the output vector.

Theoretically states, inputs and outputs can be introduced in the cost function as stated earlier, but in the MPT toolbox, the state vector is removed in the cost function when introducing penalizes on the outputs. That is why the state vector should be included in the output vector in order to cope with the control objectives stated in Section 6.1.

The plant has outputs that only got a visualization purpose, i.e. outputs that are created to see how the dynamics behave and with “nice” physical constraints. For example, an output signal from the plant model (and the real plant) is the total power demand from the HCEV (P_{DEM}). It is of no interest to let this signal be a controllable signal, i.e. let the signal be a part of the cost function, due to the fact that this signal alone can not create a functional control strategy. With other words, this signal alone is insufficient to define one piece of the control strategy and it does not make any sense if this signal should be controlled to a specific reference trajectory (because it is generated by the drive cycle). This signal includes only variables that can not be changed by the regulator, i.e. the total power demand is given as a known disturbance, and the constraints corresponding to this signal is therefore always fulfilled, which is another reason to not include it in the MPC model.

Which variables that should be included in the cost function defines the control strategy and there exists not any straightforward approach to these kinds of problems. There exist infinite many ways when creating the controllable vector (\hat{y}) in the cost function and this is because new signals can be applied to the MPC model and old signals from the plant model can be removed. One thing to bear in mind when creating the MPC model is to minimize the number of outputs, due to the computational time.

The control objectives in the MPC controller are to satisfy the power demand from the pumps, SWEM and the constant auxiliary in the system. In Figure 28 the flow chart of the power is shown, where P_{Eng} and P_{pumps} represents the mechanical power and the variables P_{ESS} , P_{Gen} , P_{SWEM} , P_{AUX} represents the electrical power in the system. Furthermore, the equations for P_{ESS} , P_{Gen} and P_{Eng} all include control signals and the signals denoted P_{SWEM} , P_{AUX} , P_{pumps} represents the disturbances.

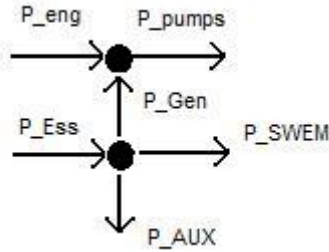


Figure 28. A simple chart of the how the different power suppliers and demanders are oriented. Note that some of the power arrows can go in the opposite direction, i.e. P_{SWEM} and P_{GEN} .

Due to the fact that this power flow is already included in the dynamics stated in Section 5.2, no new controllable outputs need to be created to satisfy the power demand in the excavator. This is because, for example, the state-update equation for the rotational speed (22) is given by the sum mechanical torques. This variable should be in some certain interval corresponding to a specific engine mode in the excavator (more on engine mode in Section 6.3). When a new value is calculated for this state update, this value must be in the defined constraint and therefore satisfy the mechanical power demand within certain limits. The same is it for the electrical power output from the ESS, which should satisfy the electrical power demand.

As also can be seen in the flow chart in Figure 28 is how the electrical power is distributed. The mathematical term of this has already been defined in Section 5.2 which is defined through Kirchoffs current law. This expression tells how much the battery should produce in power to satisfy the AUX system, the swing system and if the pumps must have additional power from the ESS. Due to this, this expression should only be considered as a constraint where the output (or input) power to the battery should be in some intervals defined by a physical constraint.

Other control objectives in the controller are to minimize the fuel consumption in some way and to keep specific variables in desirable intervals. For example, to control the rotational speed in the ICE to make the ICE work around a preferable operating point.

The cost function in (61) penalizes the input signals from a reference value of zero. Generally and stated in the example of Section 4.2.1, cost functions uses an incremented control signal instead of the ordinary control signal. But in this work the ordinary control signal is used and this creates problems in the cost function. These incremented control signals must be introduced and follows in the next subsection.

6.2.1. Introduction of new control signal

As presented in this work, the control signals in this system are the torque on the ICE and the generator and are denoted (u_1, u_2) . A very common way when introducing the control signal in the cost function is to replace them with the difference between the current control signal sample and the previous sampled signal. With other words, instead of penalizes the control signal, the penalty is set to the increments (or decrements) of the control signal between one sample and the next. The definition on this signal is Δu and the expression can be seen in (62). Notice here that the signal is given in discrete time.

$$\Delta \bar{u}(k) = \bar{u}(k) - \bar{u}(k-1) \quad (62)$$

Accordingly to how the presented control problem is defined, this approach has several advantages. One of these is to penalized large increments (or decrements) on the control signal, which was one of the stated goals in the Section 3.3, i.e. to minimize rapid power changes in the system. Another advantage follows from the use of zero reference signals in the cost function. With zero reference trajectories in the cost function, all variables are forced as close to zero as possible. This is not preferable on the control signal, i.e. to keep this signal as small as possible. Instead the control signal should have the freedom to generate a value in the interval between the physical boundaries defined by the ICE and the generator.

Instead of changing the input signal to the one in (62), the state vector is extended further to create output signals that represent these incremented values. Then these values are penalized more in the cost function and the control signal is penalized less. The additional states that need to be introduced are the control signals on the previous sample in order to form these preferable output signals and the new state vector is presented in (63);

$$\bar{x}(k) = \begin{Bmatrix} \omega_{Eng}(k) \\ P_{boost}(k) \\ SoE(k) \\ P_{pumps}^{mech}(k) \\ P_{SWEM}^{el}(k) \\ T_{Eng}(k-1) \\ T_{Gen}(k-1) \end{Bmatrix} \quad (63)$$

In Section 5.5, when the state vector was extended due to the disturbances, the state space representation had to be changed in order to create the appropriate signals. It is likewise here and the new extended matrices can be found in (64) and (65). In the extended matrices denoted $(A_{ext}^{tot}, B_{ext}^{tot}, F_{ext}^{tot})$ in (64), one could see that the last state in the state vector at the next sample is equal to the control signal at the current sample. Then the new outputs can be formed from (62) with the help of the new extended state vector.

$$\begin{Bmatrix} \bar{x}(k+1) \\ \bar{d}(k+1) \\ \bar{u}(k+1) \end{Bmatrix} = \begin{bmatrix} A & Bd & 0 \\ 0 & I & 0 \\ 0 & 0 & 0 \end{bmatrix} \cdot \bar{x}(k) + \begin{bmatrix} B \\ 0 \\ I \end{bmatrix} \cdot \bar{u}(k) + \begin{bmatrix} F \\ 0 \\ 0 \end{bmatrix} = A_{ext}^{tot} \cdot \bar{x}(k) + B_{ext}^{tot} \cdot \bar{u}(k) + F_{ext}^{tot} \quad (64)$$

$$\begin{Bmatrix} \bar{y}(k) \\ \Delta \bar{u}(k) \end{Bmatrix} = \begin{bmatrix} C & Dd \\ 0 & -I \end{bmatrix} \cdot \bar{x}(k) + \begin{bmatrix} D \\ I \end{bmatrix} \cdot \bar{u}(k) + \begin{bmatrix} G \\ 0 \end{bmatrix} = C_{ext}^{tot} \cdot \bar{x}(k) + D_{ext}^{tot} \cdot \bar{u}(k) + G_{ext}^{tot} \quad (65)$$

With this approach the weighting matrix on the control signal can be set to a very small value, i.e. a small penalty which leads to a greater freedom on this signal.

6.2.2. Approach 1: Minimizes the fuel consumption

The first approach uses a signal corresponding to the fuel consumption for the ICE, denoted (m_{fuel}) .

This signal is introduced as an output signal to be minimized in the cost function. As stated previously, the MPC model should include as few signals as possible and therefore, in the beginning, the output vector has only three signals. These are besides the fuel consumption on the ICE, also the incremented control signals introduced in Section 6.2.1. The output vector for this control approach can be found in (66).

$$\bar{y}(k)_{MPC1} = \begin{cases} y_1(k) = m_{fuel} = \Omega_{11}(x_1(k), u_1(k)) \\ y_2(k) = \omega_{Eng} = x_1(k) \\ y_3(k) = pboost = x_2(k) \\ y_4(k) = SoE = x_3(k) \\ y_5 = \Delta u_1 = u_1(k) - u_1(k-1) \\ y_6 = \Delta u_2 = u_2(k) - u_2(k-1) \end{cases} \quad (66)$$

The thought is to only minimize the fuel consumption over the prediction horizon with of course handling all constraints and the other control objectives stated in Section 6.1. When minimizing the fuel consumption directly as this approach does, the prediction horizon should be fairly long in order take advantage of this control strategy. Due to the rapidly increase of computational time when the prediction horizon is set to be longer, this approach can be a poor ECA compare to other possibilities.

When the MPC model has been defined and the controllable signals have been included in the output vector, the MPC controller should be defined. This means that the prediction and control horizon as well as the weighting matrices should be defined. The weighting matrices are denoted R and Q_y for the input vector and the output vector, respectively.

Due to the use of a quadratic norm, the weighting matrices must be semi-definite in order to guarantee a minimum in the cost function. This means that the diagonal elements in (67-68) must be equal or greater then zero, i.e. $R_{(i)} > 0$ and $Q_{(i)} \geq 0$, in order to guarantee a minimum.

$$\text{Weighting matrix for the input signals: } R = \begin{bmatrix} R_1 & 0 \\ 0 & R_2 \end{bmatrix} \quad (67)$$

$$\text{Weighting matrix for the output signals: } Q_y = \begin{bmatrix} Q_1 & 0 & 0 & 0 & 0 & 0 \\ 0 & Q_2 & 0 & 0 & 0 & 0 \\ 0 & 0 & Q_3 & 0 & 0 & 0 \\ 0 & 0 & 0 & Q_4 & 0 & 0 \\ 0 & 0 & 0 & 0 & Q_5 & 0 \\ 0 & 0 & 0 & 0 & 0 & Q_6 \end{bmatrix} \quad (68)$$

The prediction and control horizon is a parameter that is tuned to a value for this approach further in this work, in Section 6.4. The elements in the weighting matrices are also tuned in that Section.

6.2.3. Approach 2: Minimizes the losses in the system

When talking about the control strategy for hybrid electrical vehicles in general the efficiency factors play an important part when the objective is to optimize fuel saving. This second approach uses a new output signal in the cost function which represents the total amount of losses in the system. No other output signals or inputs are included in the cost function besides the incremented control signals.

The strategy is to create a signal that represents the difference between the total amount of power out from the system and the total amount of power into the system. This is the definition of the total power losses in this system. Mathematically this is shown in equation (69) where P_{fuel} defines the transformed power from the consumed diesel fuel, P_{ESS}^{inner} stands for the withdrawn power from the battery with the efficiency factor included and P_{DEM} is the total power demand.

$$P_{losses} = P_{fuel} + P_{ESS}^{inner} - P_{DEM} = y_3 \quad (69)$$

In (69) there is only one variable that has been defined earlier and it is the total power demand, which is included in the plant model.

The P_{ESS}^{inner} is defined in (70) where both P_{ESS} and η_{ESS} are stated in (33) and (35) respectively.

$$P_{ESS}^{inner} = P_{ESS} \cdot \eta_{ESS} \quad (70)$$

The last variable to define in (69) is the transformed power from the diesel fuel and here the use of a transformation factor is needed (Q_{diesel}).

$$P_{fuel} = \frac{getfuelcons(\omega_{eng}, T_{eng})}{1000} \cdot Q_{diesel} = \frac{\Omega_{11}(\omega_{eng}, T_{eng})}{1000} \cdot Q_{diesel} \quad (71)$$

The map included in (71) gives the amount of diesel per second, i.e. the fuel consumption in [mg/s]. As probably know to the reader, all diesel engines have an efficiency factor which is fairly bad and these vary from vehicle to vehicle and fabrication brand to another brand. The transformation factor used here has been taken from a Volvo report written last year which they have taken from table at the website *Wikipedia* [16], *Volvo report* [17].

$$Q_{diesel} = 4.3 \cdot 10^4 J / g$$

A straight-forward manipulation on the map value (milligram to gram) is done to bring it to [g/s] in order for it to be compatible with this transformation factor and the resulting output signal in which to be controlled is as followed;

$$y_3 = \frac{\Omega_{11}(\omega_{eng}, T_{eng})}{1000} \cdot Q_{diesel} + \frac{(x_1 \cdot u_2 \cdot \Omega_5(x_1, u_2) + P_{AUX} + d_2)}{(1 - \frac{const \cdot (x_1 \cdot u_2 \cdot \Omega_5(x_1, u_2) + P_{AUX} + d_2)}{\Omega_{10}^2(x_3)})} \quad (*)$$

$$-d1 - d2 - P_{AUX}$$

$$y_3 = \frac{\Omega_{11}(\omega_{eng}, T_{eng})}{1000} \cdot Q_{diesel} + (x_1 \cdot u_2 \cdot \Omega_5(x_1, u_2) + P_{AUX} + d_2) \cdot \quad (**)$$

$$(1 + \frac{const \cdot (x_1 \cdot u_2 \cdot \Omega_5(x_1, u_2) + P_{AUX} + d_2)}{\Omega_{10}^2(x_3)}) - d1 - d2 - P_{AUX}$$

(72)

$$y_3 = \frac{\Omega_{11}(\omega_{eng}, T_{eng})}{1000} \cdot Q_{diesel} + \frac{(\frac{x_1 \cdot u_2}{\Omega_5(x_1, u_2)} + P_{AUX} + d_2)}{(1 - \frac{const \cdot (\frac{x_1 \cdot u_2}{\Omega_5(x_1, u_2)} + P_{AUX} + d_2)}{\Omega_{10}^2(x_3)})} \quad (***)$$

$$-d1 - d2 - P_{AUX}$$

$$y_3 = \frac{\Omega_{11}(\omega_{eng}, T_{eng})}{1000} \cdot Q_{diesel} + (\frac{x_1 \cdot u_2}{\Omega_5(x_1, u_2)} + P_{AUX} + d_2) \cdot \quad (***)$$

$$(1 + \frac{const \cdot (\frac{x_1 \cdot u_2}{\Omega_5(x_1, u_2)} + P_{AUX} + d_2)}{\Omega_{10}^2(x_3)}) - d1 - d2 - P_{AUX}$$

The PWA model's outputs for the MPC controller can now be defined and can be seen in (73).

$$y_2^{MPC}(k) = \begin{cases} y_1(k) = P_{Losses}(k) \\ y_2(k) = x_1(k) \\ y_3(k) = x_2(k) \\ y_4(k) = x_3(k) \\ y_5(k) = \Delta u_1(k) \\ y_6(k) = \Delta u_2(k) \end{cases} \quad (73)$$

The new matrices created in this way are defined as followed; $C_1 = \begin{bmatrix} c_{11}^{MPC} & c_{12}^{MPC} & 0 & 0 \end{bmatrix}$, $Dd_1 = \begin{bmatrix} dd_{11}^{MPC} & dd_{12}^{MPC} \end{bmatrix}$, $D_1 = \begin{bmatrix} d_{11}^{MPC} & d_{12}^{MPC} \end{bmatrix}$. The elements in the matrices are partial derivatives of P_{losses} . The constants created with the linearization of the new output signal (P_{losses}) are gathered in G_1 likewise as in Section 4.1, equ (10).

The weighting matrices are defined as in previous subsection (6.2.2) and are tuned in Section 6.4.

6.3. Constraints

Handling physical constraints in a system are a very important part in the ECA and the MPC approach makes this possible.

As mentioned in section 6.1 the applied control strategy is to minimize the fuel consumption, but at the same time satisfy the power demand from the pumps and swing system. These conditions are controlled with the MPC approach when defining different hard constraints on the included variables.

In Figure 14, the constraints on the rotational speed for the ICE and the SoE level are shown and here it can be seen the effect on having hard constraints on those variables preferable to control. Also in this figure is how these constraints are defined and in the figure the reader can see the upper and lower limits on the rotational speed and the SoE level in the system. This means, for example, that the mechanical power demand from the pumps (and also from the generator if it should transform mech. power to elec. power) should be satisfied indirectly with the limits on the rotational speed due to the dynamic described in Section 5.2.



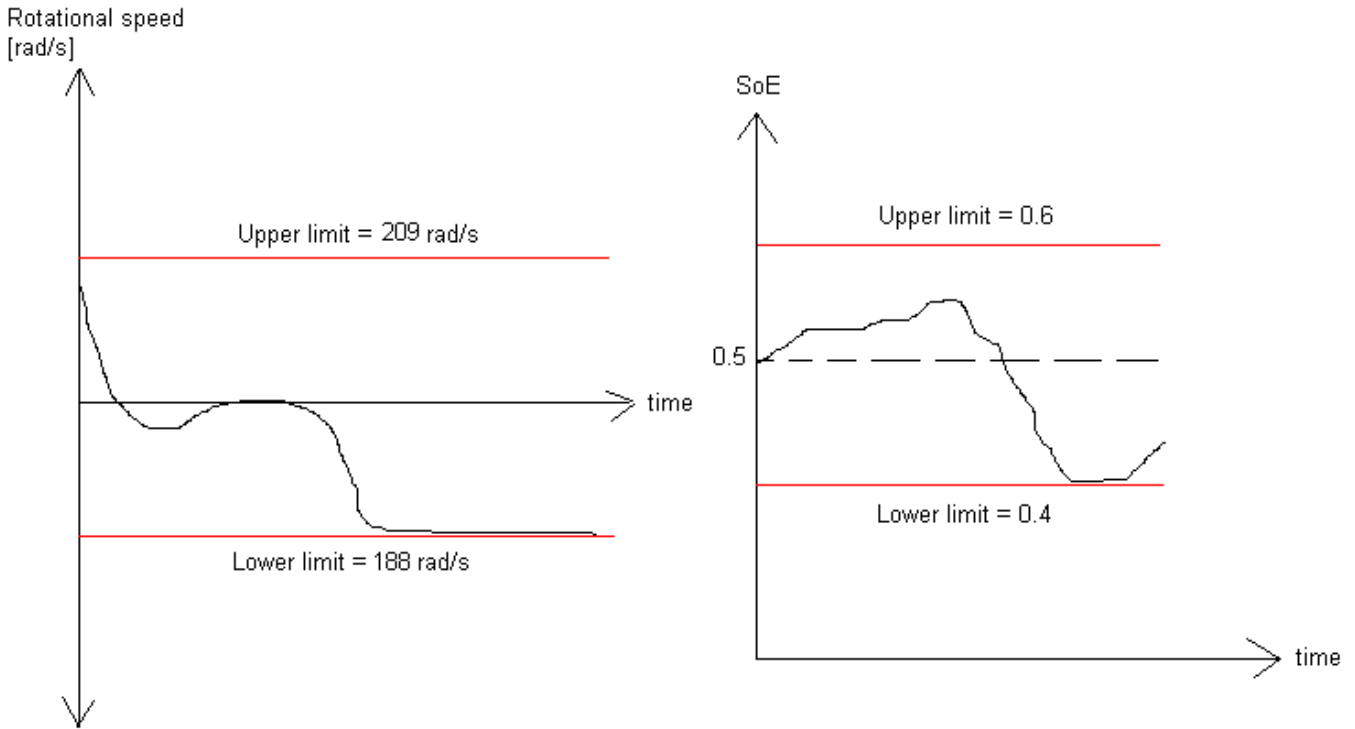


Figure 29. Example of constraints handling the ECA.

The mentioned constraint on the rotational speed can not be set to constant boundaries during the complete simulation. This is due to the time-varying preferences and this is because the operator in the HCEV chooses engine mode by a switch in the cabin and therefore chooses how the rotational speed should be bounded. These engine modes are denoted EGM. High engine speeds are desired for power demanding operation. Lower engine speeds are used for more convenient operation and normally results in lower fuel consumption. In Table 9 the EGM modes are defined and there rotational speed interval on the ICE.

Engine mode	I2	I1	F1	G2	G1	H	P
Engine speed range (rad/s)	84	105	136-152	162-173	168-188	178-199	188-209

Table 9. Defining the different EGM modes and corresponding rotational speed interval. Table taken from [14] but with conversion to rad/s.

This time-varying constraint on the rotational speed on the ICE leads to some problems in the MPT toolbox due to the fact that only constant constraints can be defined there. As mention earlier, constraints can be set on states, inputs and outputs, but these constraints are the same in the whole simulation and can not be changed. In the simulation with the presented driving cycle, some different EGM:s are introduced and this needs an alternative approach.

In Figure 30 the solution is presented for this problem and it uses multiple MPC regulators with different constant constraint on the rotational speed. From the driving cycle defined in Section 5.1, the EGM value is generated and with a so called “switch unit”, the correct MPC regulator is operating with the rotational speed within correct boundaries.

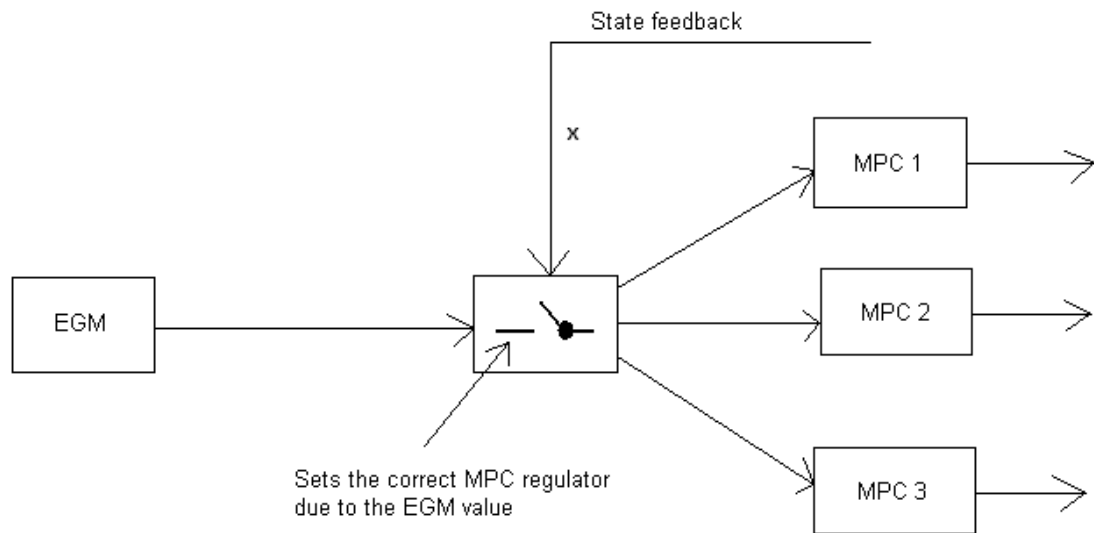


Figure 30. Shows the solution to the time-varying constraint. The EGM box generates an EGM mode that makes the box in the center to choose appropriate regulator with correct constraint on the rotational speed on the ICE.

For example, with this solution, MPC 1 in Figure 30 corresponds to EGM *P* (see table 3) and if this is the case, this regulator has hard constraints between 188-209 rad/s on the rotational speed on the ICE. The same method is applied to the other regulators to cover all EGM:s. Due to the lack of time, only the MPC controller representing engine mode *P* was created and used in the simulations.

6.3.1. Physical constraints in the system

In Appendix 9.9 all physical constraints in the system are defined such as for example the boundaries on the torque on the ICE or the generator (has a limitation on how much it can produce). Below a table can be seen on the used constraints in the system and all of the constraints defined in Appendix 9.9 are not include due to a fairly simple starting model.

Signals	Lower limit	Upper limit	Hard/Soft constraint
Input signal: T_{Eng} [Nm]	0	750	Hard
Input signal: T_{Gen} [Nm]	-500	500	Hard
State 1: ω_{Eng} [rad/s] ¹⁾	188.5	209	Hard/Soft
State 2: p_{boost} [Pa]	0	600	Hard
State 3: SoE [1]	0.4	0.6	Hard/Soft
State 4: P_{pumps}^{mech} [W]	0	$1.3 \cdot 10^5$	Hard
State 5: P_{SWEM}^{el} [W]	$-9 \cdot 10^4$	$9 \cdot 10^4$	Hard
State 6: $T_{Eng}(k-1)$ [Nm]	0	750	Hard
State 7: $T_{Gen}(k-1)$ [Nm]	-500	500	Hard
Output 1: m_{fuel} [mg/s]	0	Inf	Hard
Output 1: P_{losses} [W]	0	Inf	Hard
Output 2: ΔT_{Eng} [Nm]	-750	750	Hard

Output 3: ΔT_{Gen} [Nm]	-500	500	Hard
---------------------------------------------------	------	-----	------

Table 10. The definition on the constraints use in the MPC regulator. ¹⁾ Note that the constraints on state 1 can be changed if it is a different EGM, but this leads to a new regulator.

6.4. Tuning

Due to the highly computational preferences in this control problem some simple different MPC regulators were created and evaluated. The controllers are denoted MPC 1, MPC 2 and MPC 3. All these controllers are based on the strategy stated in Section 6.2.2, i.e. minimizes the fuel consumption directly. The sampling time is set to 0.5 and the prediction horizon is set to only 1 due to the computational burden for MPC 1 and MPC 2, and prediction horizon 2 for MPC 3.

Soft constraints are introduced on the most critical variables, which is the rotational speed and the battery level. The constraint on the rotational speed can be violated by most of 10 rad/s and 0.05 for the battery level constraint.

All three controllers have the same penalty on the control signals as can be seen in (74).

$$R = \begin{bmatrix} 10^{-8} & 0 \\ 0 & 10^{-8} \end{bmatrix} \quad (74)$$

In Table 11, the three controllers can be found with different weighting values and prediction horizons.

MPC	Pred. horizon	Penalty on y_1	Penalty on y_2	Penalty on y_4
1	1	$Q_1 = 10^{-14}$	$Q_2 = 10$	$Q_2 = 10^4$
2	1	$Q_1 = 10^{-6}$	$Q_2 = 10$	$Q_2 = 10^4$
3	2	$Q_1 = 10^{-6}$	$Q_2 = 10$	$Q_2 = 10^4$

Table 11. Shows three different MPC controllers with different control preferences.

- **MPC 1:** The purpose with MPC 1 is to control the outputs (y_2, y_4) to a given reference trajectory during the presented driving cycle. This means that some important variables are almost ignored in the control strategy to get a feasible running model due to the short prediction horizon. For example, the fuel consumption is almost not penalized at all in the cost function, i.e. it has the freedom to be a high value. The most critical variables to be in their intervals are the rotational speed on the motor and the battery level, which are penalize hard in the weighting matrices, as can be seen in Table 11.
- **MPC 2:** The control strategy in MPC 2 is to apply a greater penalty on the fuel consumption in order to make it as low as possible. This leads to a shorter simulation because of the infeasibility on the rotational speed and the battery level after a while. The penalty on the first output in (76), i.e. fuel consumption, is here set to a smaller value then in MPC 1 to bring the fuel consumption to a low value.
- **MPC 3:** The last controller is identical to MPC 2 but with a prediction horizon of 2. Due to the computational time when the prediction horizon is increased by one, the simulation is also shorter with this controller. Theoretically, this controller should be able to achieve better results than MPC 2.

All other outputs are penalized equally for the three controllers and these weighting values are very low. This is due to that these variables should not be controlled to a specific reference trajectory and therefore could be any value within the defined constraints.

6.5. Experienced problems

In this section the main problems occurred are described which can be limitations on the MPT toolbox or other flaws.

6.5.1. MPT limitations

There is a possibility to create an off-line MPC controller in the MPT toolbox, which leads to a much lower complexity and hence lower computational time in the simulations. This is a preferable option when simulating complex problems, where the MPC model needs to include a big PWA system with a low sampling time due to the hybrid plant. But unfortunately, creation of an explicit controller in the MPT toolbox with this dynamics is infeasible. This is because some of the variables in the system are defined between great intervals, i.e. for example $0 \leq P_{pumps} \leq 1.3 \cdot 10^5 W$ and $-9 \cdot 10^4 \leq P_{SWEM} \leq 9 \cdot 10^4 W$.

When the MPT creates a controller with these signals (large intervals in the constraints), unwanted artificial constraints are produced by the toolbox and makes the explicit controller only defined in a few models of the PWA system. With the existence of this “bug” the explicit controller’s control laws are only pre-calculated on some of the linear models in the PWA system and do not cover all. With some of the models in the PWA system omitted, which describes a certain dynamic behavior in the system, leads to worthless model in a hybrid perspective. One solution to this problem would be to scale the signals in the MPC model that have big interval preferences and then rescale them to recreate the right units. This was tested during the work with no successes, which can not be explained.

The conclusion is to ignore the explicit controller option and create an on-line controller. This leads to more computational demanding simulations, which results in bigger approximations on the plant, longer sampling time etc.

Another problem that occurred is in the MPT cost function. Due to the presented control strategy, the outputs need to be introduced in the cost function and this is an optional feature in the toolbox. But when the outputs are included in the cost function, the toolbox removes the state vector in the function, i.e. the states are not penalized in the cost function. This is because the MPT assumes that the states are included in the output vector when the user wants to penalize the outputs and hence removes the state vector from the cost function. It took a while before I realized this and this is one reason why the states are included in the output vector.

6.5.2. Computational time

The main issue that is created with the MPC approach for these systems needs truly an engineering handling. Due to switches and nonlinearities in the system, different state-space models must be applied and one trade off is created between minimize the number of models to be included compare to how good the approximation of the nonlinear plant should be. With a higher amount of different linear models in the system a higher computational time is required. Also as mentioned in the previous subsection, the compulsory use of the on-line MPC controller leads to an easy MPC model and control structure.

Due to this, the PWA 2 model was used as the MPC model in all the presented result when the MPC controller is operating. This PWA system has, as denoted before, six linear models which one could see as a very easy PWA system with a pretty high approximation level.

When it comes to sampling time and prediction horizon (and control horizon), these parameters have a very high dependence on the computational time. This was noted when different control structures were simulated. For example, when the prediction horizon was greater then 3-4 samples, the simulation lead to a crash in Matlab due to the insufficient memory.

7. RESULTS

In this section, results are shown for the three MPC controllers defined in Section 6.4 and a MPC controller operating on the nonlinear plant. Due to the lack of time, all simulations were executed with a constant disturbance during the prediction horizon. The simulink file used for these simulations can be seen in Appendix 10.12. In this Simulink chart, the driving cycle is located at the bottom and the MPC controller in the center. Notice here that the MPC controller has a state feedback as stated in Section 5.5 and that this feedback includes the states, the disturbances and the previous control signals. The previous control signals are needed to create the incremental control signals defined in Section 6.2.1. In the upper part in Appendix 10.12 the linear model of the plant can be found. This is an approximation of the nonlinear plant and this was used for MPC 1-3. Last in this section, a MPC controller similar to the controller MPC 3 was applied to operate the nonlinear plant. This was done by replacing the linear plant with the nonlinear plant in the Simulink file in Appendix 10.12.

7.1. MPC operating (disturbance constant in Hp)

The MPC controller's prediction ability on the known disturbance is removed and replaced with a constant disturbance value in the prediction horizon. With other words, at the current sample in the controller, the disturbance is set to the same value during the prediction horizon as it had at the current sample. This was stated in Section 5.5.

Furthermore, the MPC model inside the MPC controller is fairly simple due to minimize the computational time during the simulations. This is done by removing some of the unimportant output signals stated in Section 5.2.

7.1.1. MPC 1

In this controller the simulation could go to 50 sec, but with a sacrificing performance on the fuel consumption as can be seen in Figure 31, which is due to the low weight on the consumed fuel variable. This is because of the low penalty value in the weighting matrix for the fuel consumption. If the penalty on this signal would be increased, the fuel consumption should decrease and this is described in the next subsection, i.e. MPC 2.

The soft constraint on the rotational speed as well as for the battery level is violated during the simulation. This lead to a greater penalty on these variables and results in the controller forces them in inside the feasible intervals, as can be seen in Figure 31.

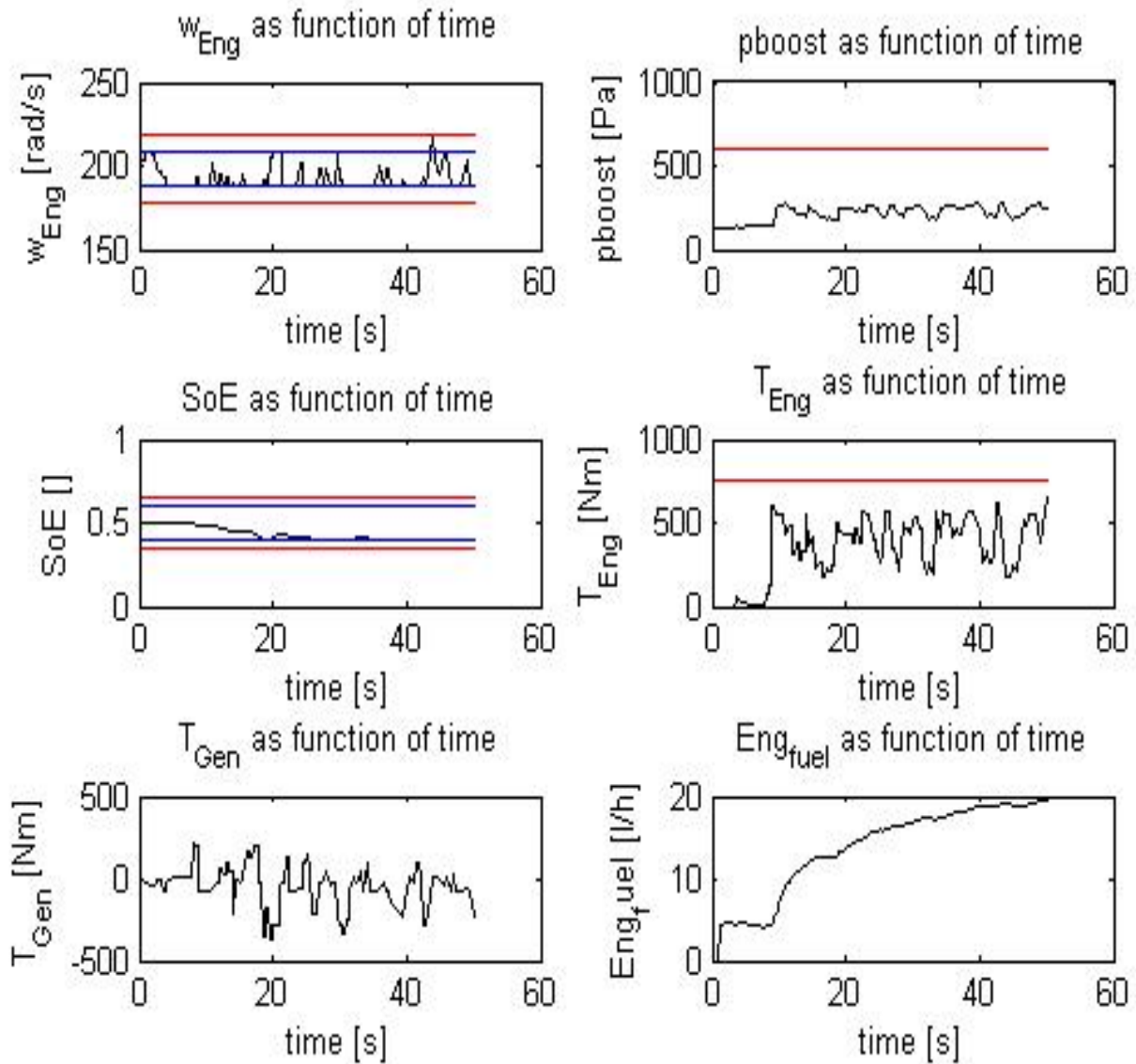


Figure 31. Results from MPC 1.

A power plot can be seen in Figure 32 for MPC 1. This plot shows the total power demand (P_{dem}), the output power from the ICE (P_{Eng}) and the output (or input if the variable is negative) on the ESS (P_{ESS}). The physical behavior on the power distribution can be seen here. For example, when the power demand is low and the output power from the ICE is high, then some of the power from the ICE is transferred into the ESS to recharge the battery. Due to the efficiency factor on the ICE, the total power supply from the engine and the ESS is almost always greater than the power demand. One example of this can be in Figure 32 at roughly 43 sec, where the total power supply is greater than the power demand.

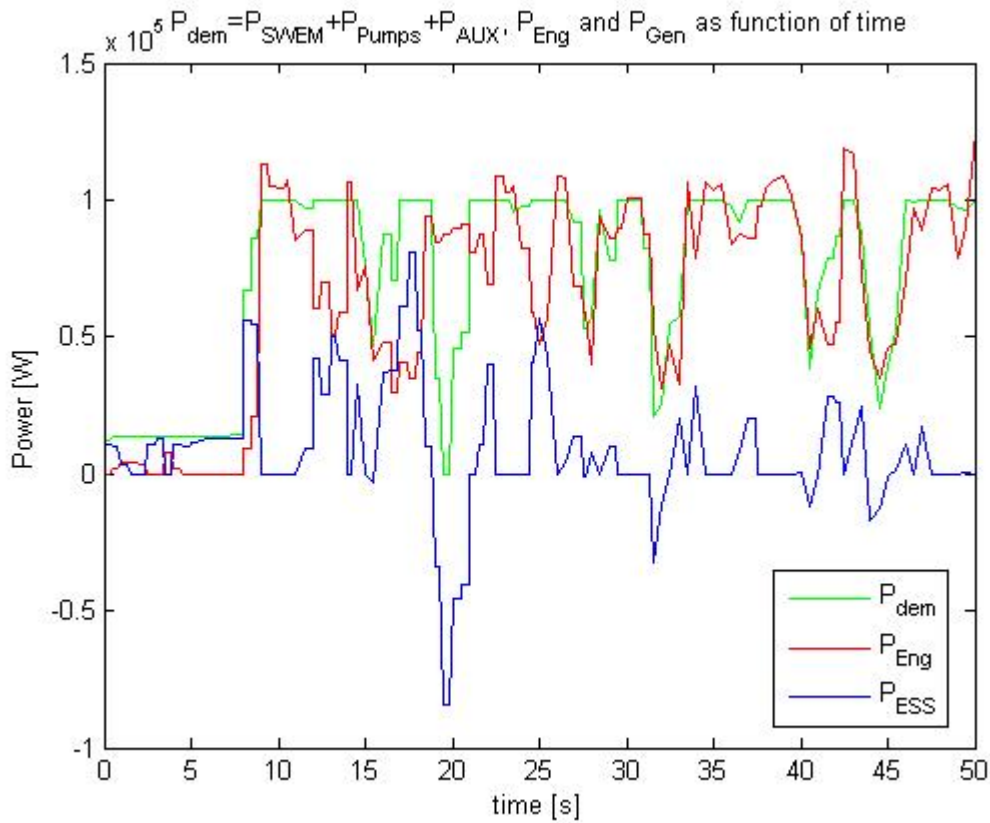


Figure 32. Power plot for MPC 1.

The efficiency map for the ICE can be seen in Figure 33. Due to the control strategy, the rotational speed is almost always in the interval 188-209 rad/s which correspond to the engine mode operating (EGM). The result because of this is that the ICE efficiency only depends on the engine torque which can be seen in the figure. A summary on this chart is that the ICE operates most efficient when the torque has a high value.

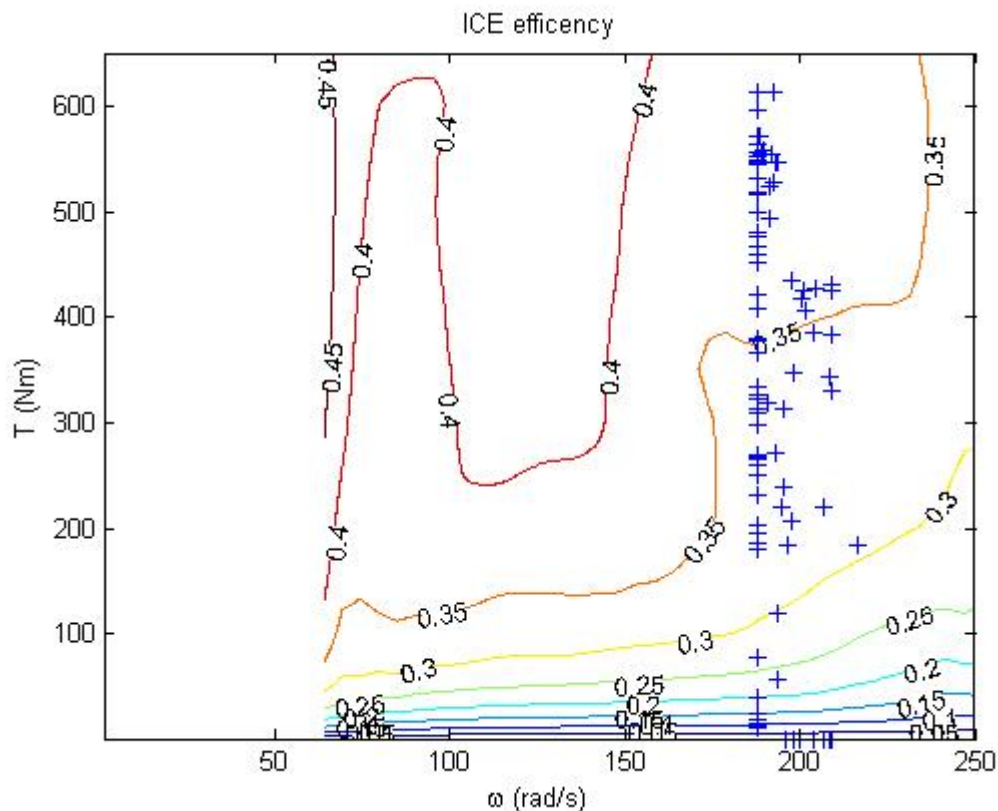


Figure 33. Efficiency plot for MPC 1.

7.1.2. MPC 2

The main goal with a HCEV is to minimize the fuel consumption and in the previous controller, this was ignored. In MPC 2 the output representing the fuel consumption is penalized much more. The result of this can be seen in the lower-right subplot in Figure 34. Compare to the fuel consumption in MPC 1 at 15 sec, where it is roughly 12-13 l/h, this controller makes the fuel consumption to roughly 10 l/h at 15 sec. But due to the low prediction horizon, some of the other constraints can not be fulfilled after 15 sec. in the simulation, as can be realized when investigating the value for the rotational speed in Figure 34. This is because the controller drives the SoE level to its lower limit and after that, the controller can not find a feasible control law.

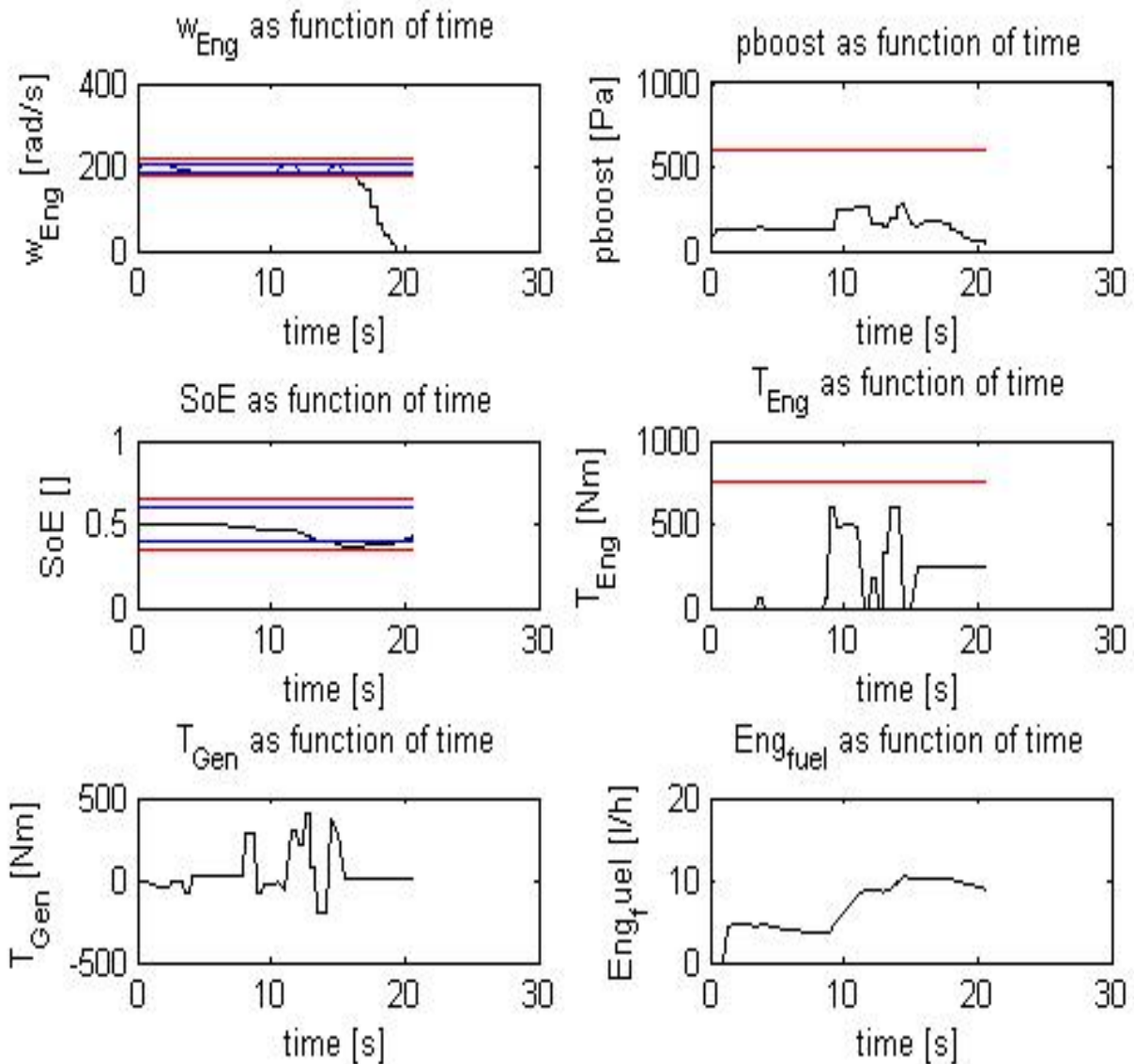


Figure 34. Result from MPC 2.

The power plot for MPC 2 is denoted Figure 35 and the difference here compare to the power plot for MPC 1 is the P_{ESS} behavior. The output power from the ESS is much higher then in Figure 32 and this

means that the battery drives the power demanding units more, which leads to a lower fuel consumption. Notice also that the output power from the ICE (P_{Eng}) is lower in this simulation than in Figure 32.

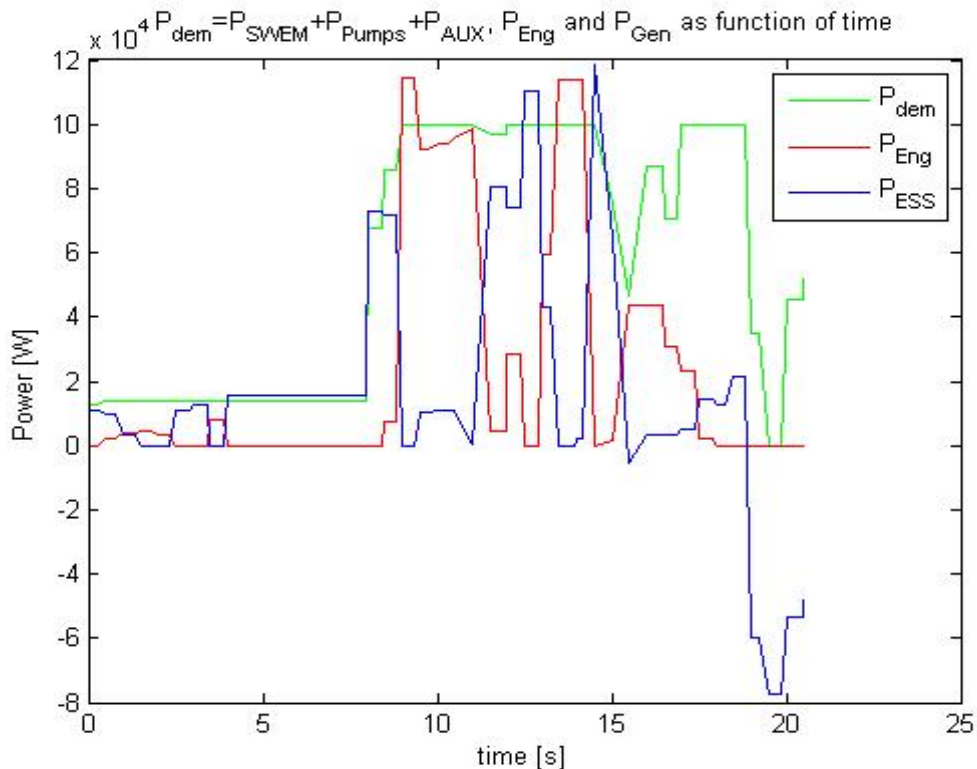


Figure 35. Power plot for MPC 2.

The efficiency map has almost the same appearance as in the previous controller, but with the difference when the rotational speed goes outside its boundaries. This is not a feasible result and can be ignored, i.e. the rotational speed violates its constraint when the controller can not satisfy to achieve low fuel consumption and at the same time have the rotational speed around 200 rad/s.

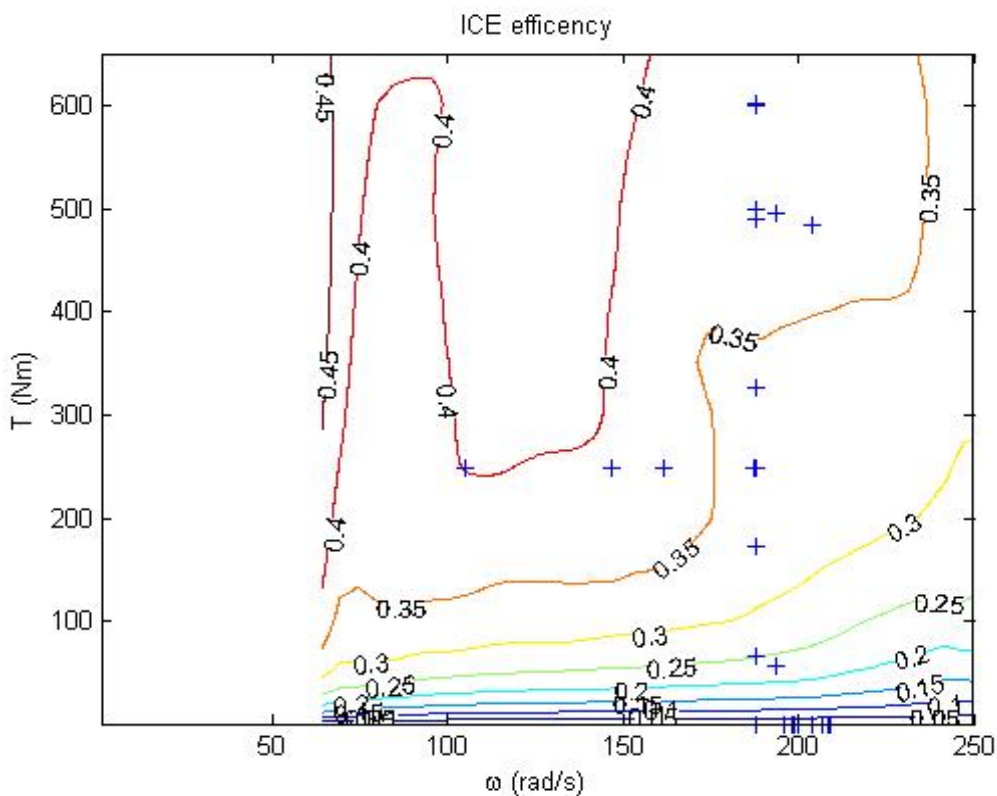


Figure 36. Efficiency plot for MPC 2.

7.1.3. MPC 3

The last controller evaluated is denoted MPC 3. This controller is identical as MPC 2 but with a prediction horizon of 2. The result on the most important variables is shown in Figure 37 with a very good result on the rotational speed and the battery level. Due to a longer prediction horizon, the controller can be more intelligent and construct control signal which satisfy the included variables constraints in a better way than in MPC 2. Also the fuel consumption is taken into account in the cost function as can be seen in the lower left subplot. But this controller pays more attention to getting the rotational speed and the battery level their references, that is why the fuel consumption is higher here than in the results for MPC 2.

A prediction horizon of 2 leads to a very long computational time and that is why the simulation only goes to 20 sec.

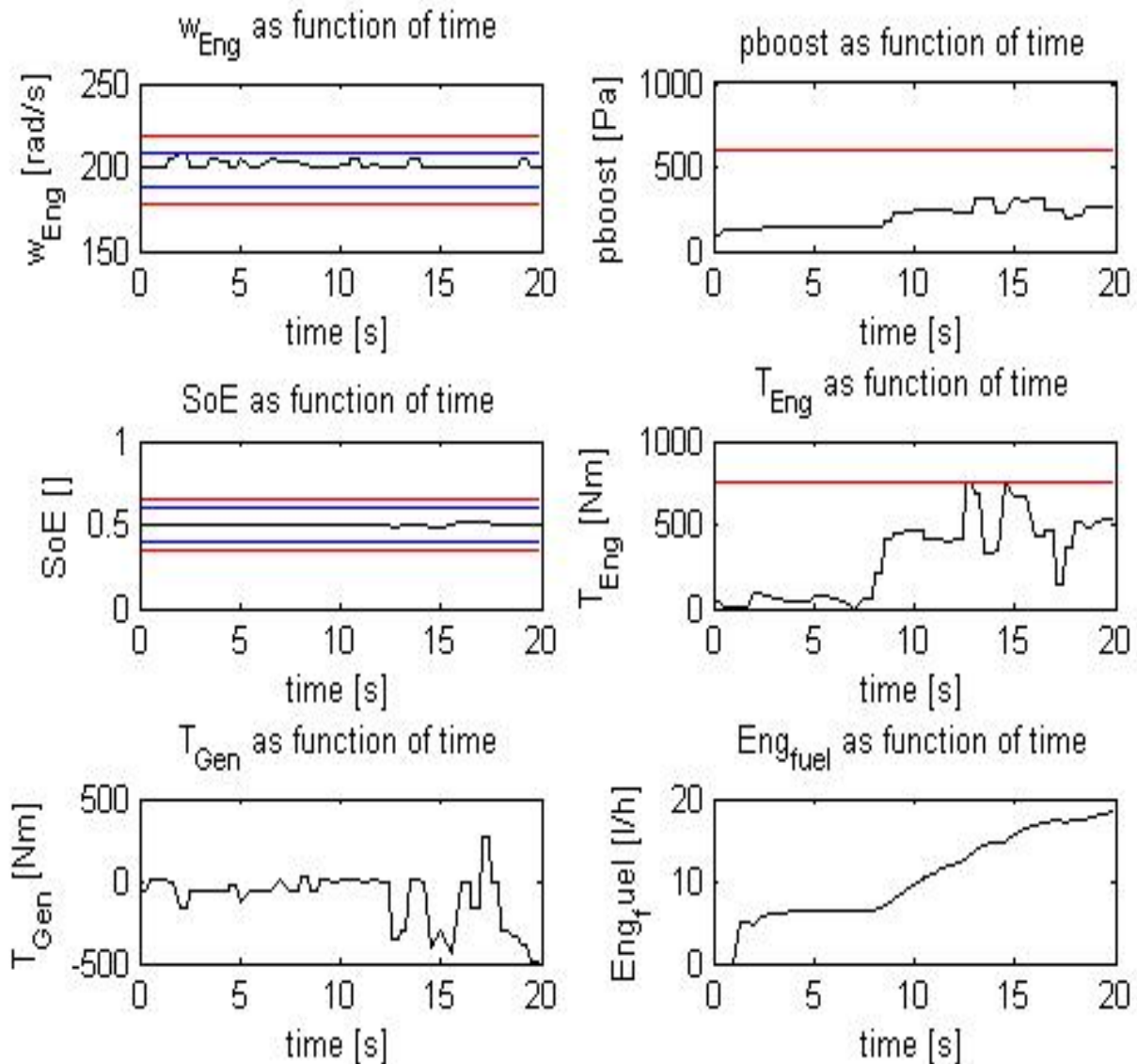


Figure 37. Result from MPC 3.

The power plot for MPC 3 can be seen in Figure 38. Due to the control strategy this plot shows a great average value on the power output on the ICE, which leads to a high fuel consumption.

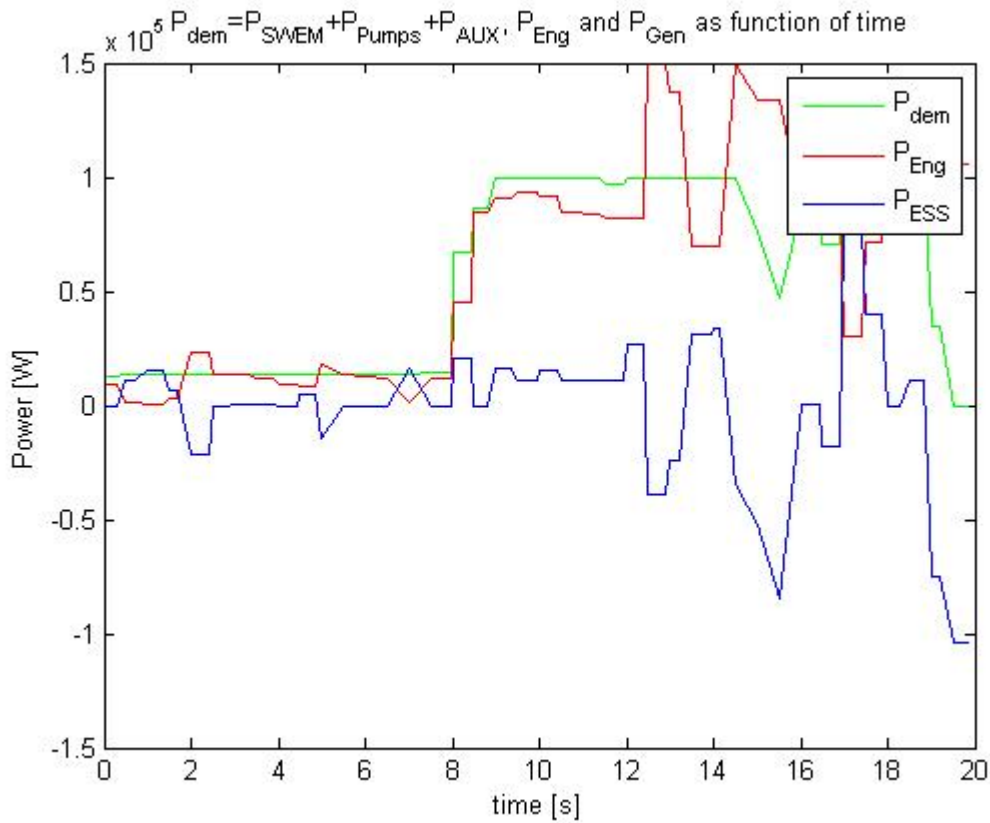


Figure 38. Power plot for MPC 3.

The efficiency map for MPC 3 can be seen in Figure 39. Notice here that the rotational speed is in a very tight interval, which is a good result.

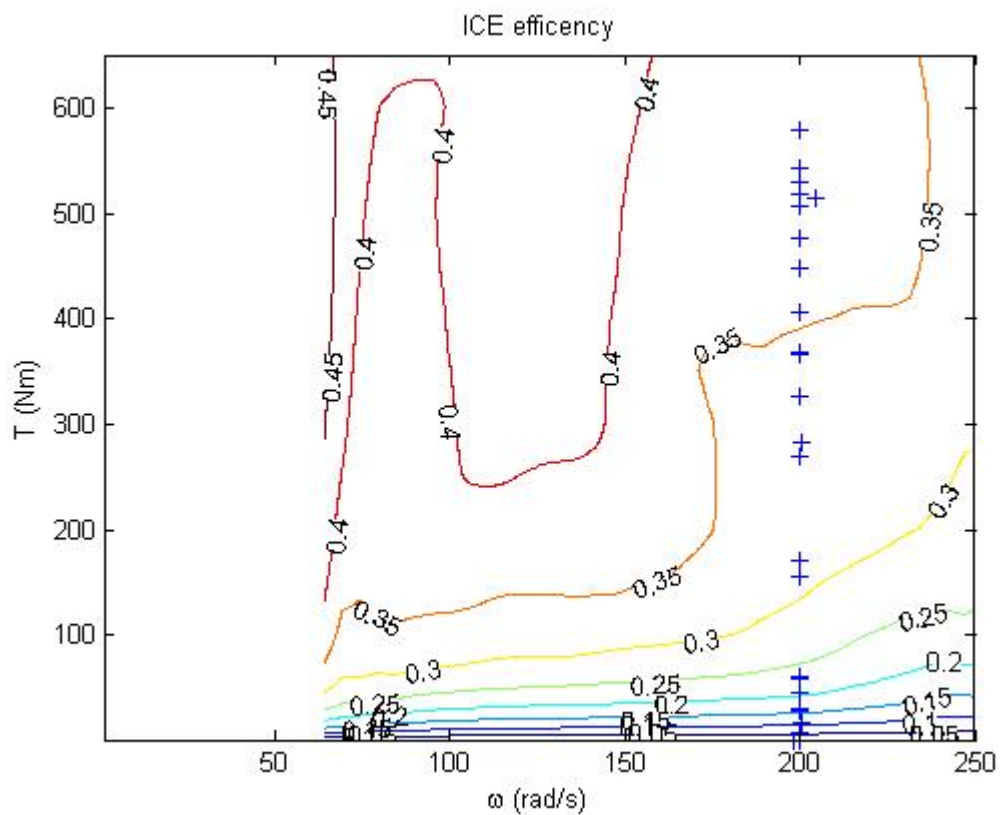


Figure 39. Efficiency plot for MPC 3.

7.1.4. MPC operating on the nonlinear plant

The last experiment in this thesis work was to simulate the MPC controller operating on the nonlinear hybrid plant, which was the stated goal from the beginning. Due to the lack of time, the only MPC controller introduced in this experiment had some similar characteristics with MPC 3, but with a lower penalty on the fuel consumption. The reason why this controller did not penalized the fuel consumption more, was to achieve a controller that could simulate an entire interval for an engine mode. A high penalty was therefore used for the rotational speed and the SoE to not bring these critical variables to its limitations, i.e. make assure that a feasible control law can be found. Also the prediction horizon was set to 2. The results from this experiment can be seen in Figure 40-42.

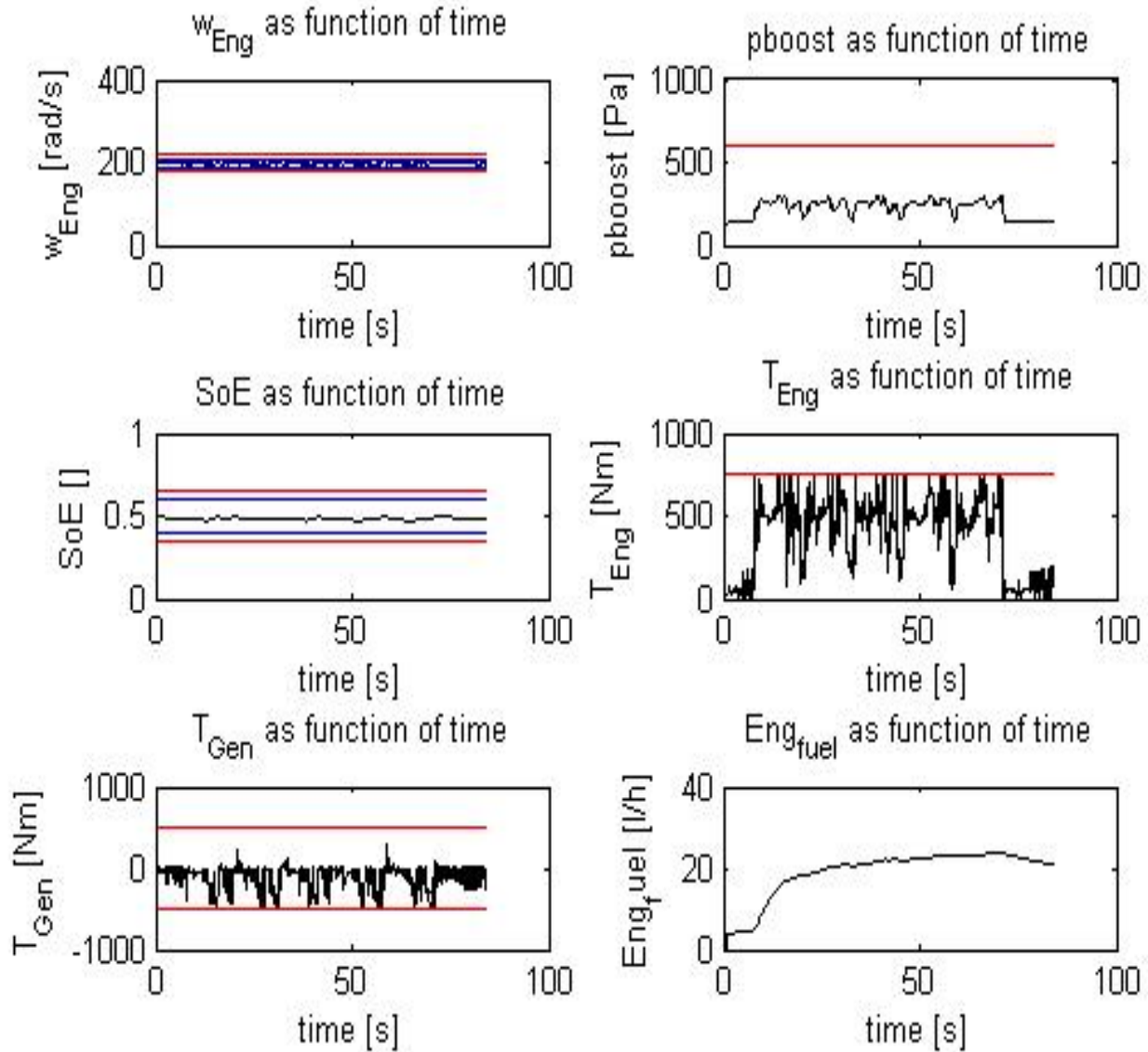


Figure 40. Results with the nonlinear plant

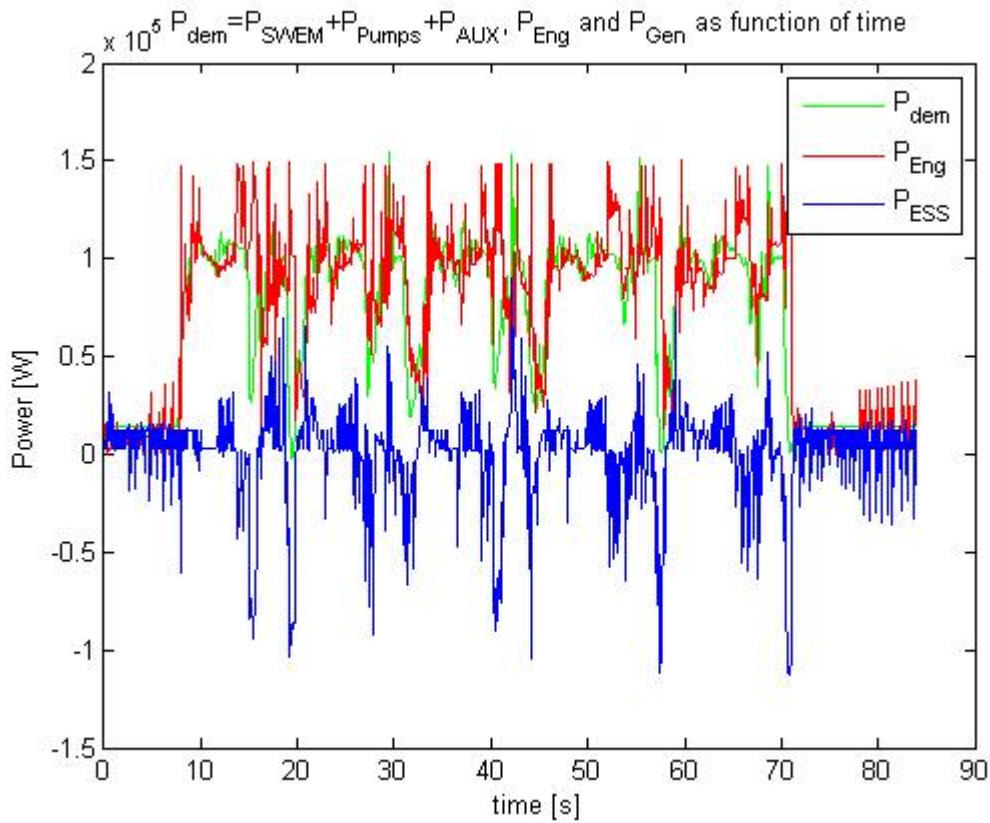


Figure 41. Powerplot for a MPC controller operating on the nonlinear plant.

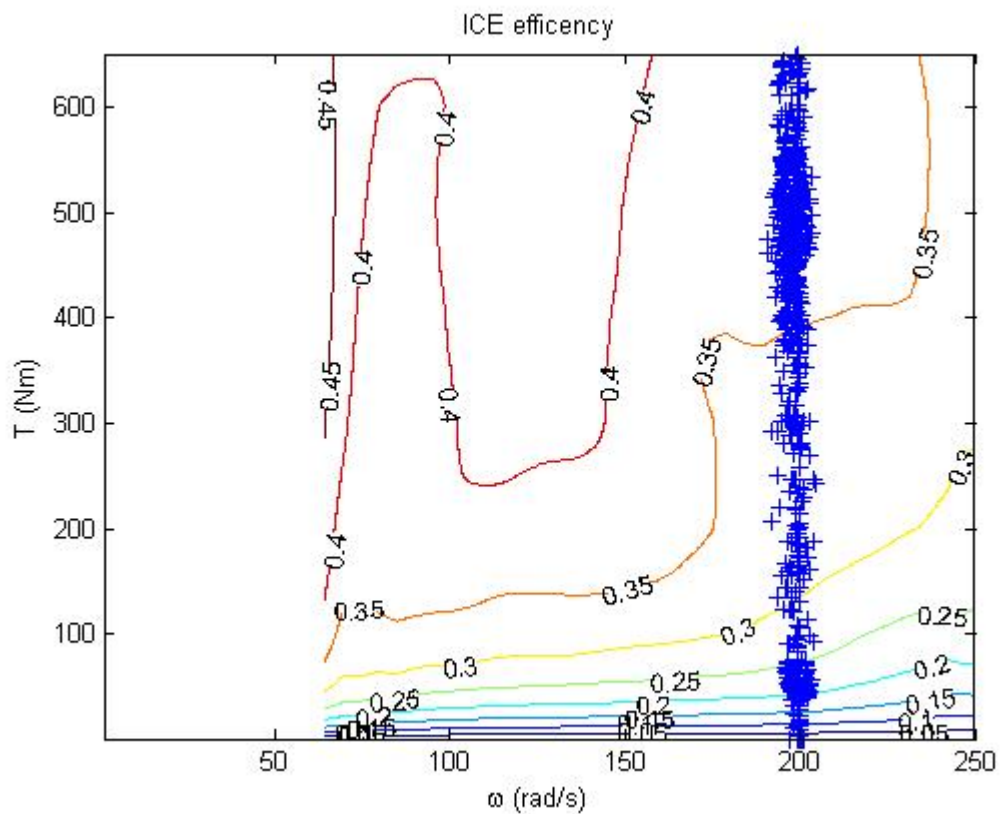


Figure 42. Efficiency plot for a MPC controller operating on the nonlinear plant.

What is notable from these results are that the power output from the generator, in the lower-right graph in Figure 40, almost always is negative. This means that the ICE helps to operate the SWEM and AUX

power demand or to recharge the ESS. Evidence regarding this is that the SoE level is kept at the preferable level 0.5 during the simulation. This also means that the fuel consumption becomes higher compared to some of the other simulations (MPC 1-2), where the battery level is forced down to its lower limit. In Figure 41, the power output from the ESS is negative a large part during the simulation, which means that power is brought into the battery, to keep it at the battery level 0.5.

There existed a big difference between the nonlinear plant and the PWA plant simulation. This was the simulation time, which was a lot smaller when the MPC controller operated on the nonlinear plant than the linear plant. The difference in simulation time shows that there are some uncertainties when using the MPT toolbox. For example, an error denoted 'Algebraic loop' occurred throughout the experiments in Simulink when the linear plant was used, but this error was removed when the nonlinear plant was operating.



8. CONCLUSIONS

As a summary, the conclusions in this work are fairly positive. This conclusion section is divided as this work is divided. First, conclusions on the linearization of the nonlinear plant is made, i.e. creation of the PWA system. Then the control strategy is evaluated with conclusions on the MPT toolbox. Last, prospects and future work are summarized and presented.

- **Creating model of the nonlinear plant:** Three different PWA systems were created in this work with different levels of approximation. The results shown in Section 5.6 are not that important and do not tell so much of the model validation versus the nonlinear plant. But with the results achieved in Section 7.1.4, i.e. when the nonlinear plant was introduced, shows that the model validation was very satisfying with only one set of linearization points. This tells that the PWA system can be created with a fairly simple structure and still make the MPC controller compute optimal control signals to control the dynamics.
- **Control strategy:** If the work had been divided into sections representing most advanced problems, the creation of a feasible MPC controller would be the dominating part. This is partly due to the development of the different control strategies, but mostly due to the MPT toolbox. Some misunderstandments followed by some “bugs” in the MPT toolbox slowed the work down and some of the pre-set simulation goals had to be removed. One example of this is the simulation with a known disturbance during the prediction horizon.

Due to the use of an on-line MPC controller, the prediction horizon was forced to be low. It was only feasible with a maximal pred. horiz. of 2 before the simulation became unreasonable time consuming. For example, if the MPC controller had a prediction horizon of 2, a simulation of only 20 seconds with the presented driving cycle took over 12 hours to complete. This is why most of my results are shown with a prediction horizon of 1. The conclusion on this matter is that the MPC preferences are almost not used and with a short horizon, the controller can not minimize the fuel consumption to agreeable values and at the same time satisfy all constraints in the system.

- **Future work:** MPC control strategy for a HCEV is much undeveloped and according to this work, much more attention could be applied to create a good MPC controller for this problem structure. As mentioned in the previous subsection, the computational factor leads to simulations with a short prediction horizon. Indications have been shown that great improvement in the overall results can be made with a longer prediction horizon with the same control strategy as presented in this work. Then again, results have been shown that the PWA model can be of a simple structure and if the prediction horizon is to be increased, then the fuel consumption can be lowered.

Future work also includes trying different control strategies to see which variables that need most attention. This could be evaluated faster if some of the limitations in the MPT toolbox can be removed, such as the bug when creating an explicit MPC controller. With the use of an explicit controller, longer prediction horizon could be possible and a more convenient trouble solving approach is introduced.

9. REFERENCES

9.1. References

- [1] Jonas Hellgren, "Conceptual power split control functionality - Power system modeling.doc", HEMP report, 2008.
 - [2] Jonas Hellgren, "Conceptual power split control functionality - Equivavelent Consumption Minimization Strategy.doc", HEMP report 2008.
 - [3] Jonas Hellgren and Jonas Ottosson, "Conceptual power split control functionality - EMA technique ideas and overview.doc", HEMP report 2007
 - [4] J.M. Maciejowski, "Predictive Control with constraints", Pearson Education Limited 2002
 - [5] M. J. West, C. M. Bingham, and N. Schofield, "Predictive control for energy management in all/more electric vehicles with multiple energy storage units," in Proc. IEEE Int. Electric Machines and Drives Conf., vol. 1, Jun. 2003, pp. 222-228.
 - [6] Jonas Hellgren, "Total system optimization - Load profile generation.doc", Report 2008.
 - [7] M. Kvasnica, P. Grieder, M. Baotic and F.J. Christophersen, Multi-Parametric Toolbox (MPT), 2006, <http://control.ee.ethz.ch/~mpt/>
 - [8] Jonas Ottosson, "Conceptual power split control functionality - Dynamic programming.doc", Report 2008
 - [9] <http://www.komatsu.com/CompanyInfo/press/2008051315113604588.html>, Komatsus press release page, 2008/05/13
 - [10] Johan Åkesson, "MPCtools 1.0 – Reference Manual", January 2006, <http://www.control.lth.se/database/publications/article.pike?artkey=ake06mpctools>
 - [11] Jonas Hellgren, "Hybrid excavator fuel consumption analysis.doc", Hybrid excavator concepts analysis report, 2007-12-19
 - [12] J.T.B.A Kessels, P.P.J. van den Bosch, Michiel Koot, Bram de Jager, "Energy Management for vehicle power net with flexible electric load demand", 2005.
 - [13] Karl J. Åström, Björn Wittenmark, "Computer controlled systemst", Third edition 1997
 - [14] Jonas Hellgren, Jonas Ottosson, "Conceptual power split control functionality - EMA technique ideas and overview.doc", Report 2007.
 - [15] M.J. West C. M. Bingham N. Schofield, "Predictive control for energy management in all/more electric vehicles with multiple energy storage units", IEEE 2003.
 - [16] The MathWorks, www.mathworks.com, 1984-2007.
 - [17] Maple, www.maplesoft.com
-
-

10. APPENDIX

10.1. Pumps

$$(A.1) \quad T_{\text{pumps}} = \begin{cases} 0 & (\text{isengon} = \text{False} \Leftrightarrow \text{ENG} = \text{off}) \\ \frac{P_{\text{pumps}}}{\omega_{\text{ENG}}} & (\text{isengon} = \text{True} \Leftrightarrow \text{ENG} = \text{on}) \end{cases}$$

$$(A.2) \quad \omega_{\text{pumps}} = \omega_{\text{GEN}}$$

10.2. Engine system

$$(A.3) \quad \dot{m}_{\text{fuel}} = \frac{d}{dt} m_{\text{fuel}}(T_{\text{ENG}}, \omega_{\text{ENG}}) = \begin{cases} 0 & (\text{isengon} = \text{false}) \\ \text{getfuelcons}(T_{\text{ENG}}, \omega_{\text{ENG}}) & (\text{isengon} = \text{true}) \end{cases}$$

$$(A.4) \quad P_{\text{ENG}} = T_{\text{ENG}} \cdot \omega_{\text{ENG}}$$

$$(A.5) \quad \omega_{\text{ENG}} = \omega_{\text{GEN}}$$

$$(A.6) \quad (T_{\text{ENG}} + T_{\text{boost}} + T_{\text{GEN}} - T_{\text{pumps}}) = I_{\text{ENG}} \cdot \dot{\omega}_{\text{ENG}} \approx 0$$

$$(A.7) \quad dp = \text{getboost}(T_{\text{ENG}}, \omega_{\text{ENG}}) - p_{\text{boost}}$$

$$(A.8) \quad p_{\text{boost}} = \int \dot{p}_{\text{boost}} \cdot dt$$

$$(A.9) \quad \dot{p}_{\text{boost}} = \begin{cases} \frac{dp}{\text{getboosttimeconstA}(\omega_{\text{ENG}})} - \frac{K_{\text{corr}} \cdot \dot{\omega}_{\text{ENG}} \cdot p_{\text{boost}}}{\omega_{\text{ENG}}} & (dp > 0) \\ \frac{dp}{\text{getboosttimeconstB}(\omega_{\text{ENG}})} - \frac{K_{\text{corr}} \cdot \dot{\omega}_{\text{ENG}} \cdot p_{\text{boost}}}{\omega_{\text{ENG}}} & (dp \leq 0) \end{cases}$$

$$(A.10) \quad T_{\text{boost}} = \text{getboosttorque}(dp, \omega_{\text{ENG}}) = -k_1(\omega_{\text{ENG}}) \cdot dp^2 - k_2(\omega_{\text{ENG}}) \cdot dp$$

$$T_{\text{SMOKE}} = \text{getsmokelimit}(\omega_{\text{ENG}}, p_{\text{boost}}) = \dots$$

$$(A.11) \quad \left(x + (1-x) \cdot \frac{(p_{\text{boost}} - 100)}{\text{getboost}(\omega_{\text{ENG}}, T_{\text{ENG}}^{\text{max}}(\omega_{\text{ENG}})) - 100} \right) \cdot T_{\text{ENG}}^{\text{max}}(\omega_{\text{ENG}})$$

$$(A.12) \quad T_{\text{ENG}}^{\text{max}}(\omega_{\text{ENG}}) = \text{getmaxtorque}(\omega_{\text{ENG}})$$

$$(A.13) \quad T_{\text{ENG}}^{\text{max, smoke}} = \min(T_{\text{ENG}}^{\text{max}}(\omega_{\text{ENG}}), T_{\text{SMOKE}}(\omega_{\text{ENG}}, p_{\text{boost}}))$$

10.3. Electrical system

$$(A.14) \quad I_{ESS} - I_{GEN} - I_{aux} - I_{SWEM} = 0$$

$$(A.15) \quad I_{ESS} = \frac{P_{ESS}}{U_{ESS}}$$

$$(A.16) \quad I_{GEN} = \frac{P_{GEN}^{el}}{U_{ESS}}$$

$$(A.17) \quad I_{AUX} = \frac{P_{AUX}}{U_{ESS}}$$

$$(A.18) \quad I_{SWEM} = \frac{P_{SWEM}^{el}}{U_{ESS}}$$

10.4. Generator

$$(A.19) \quad \omega_{GEN} = \omega_{ENG}$$

$$(A.20) \quad P_{GEN}^{mech} = T_{GEN} \cdot \omega_{GEN}$$

$$(A.21) \quad P_{GEN}^{el} = P_{GEN}^{mech} \cdot \varphi_{GEN}$$

$$(A.22) \quad \varphi_{GEN}(P_{GEN}^{mech}, \eta_{GEN}) \approx \begin{cases} \eta_{GEN} & (P_{GEN} < 0 \Leftrightarrow \text{generator mode}) \\ 1/\eta_{GEN} & (P_{GEN} > 0 \Leftrightarrow \text{motor mode}) \end{cases}$$

$$(A.23) \quad \eta_{GEN} = \text{getgeneff}(T_{GEN}, \omega_{GEN})$$

10.5. ESS

$$(A.24) \quad \frac{d}{dt} SoE = S\dot{o}E = -\frac{\varphi_{ESS} \cdot P_{ESS}}{E_{ESS \max}}$$

$$(A.25) \quad \varphi_{ESS}(P_{ESS}, \eta_{ESS}) \approx \begin{cases} 1/\eta_{ESS} & (P_{ESS} > 0 \Leftrightarrow \text{discharge mode}) \\ \eta_{ESS} & (P_{ESS} < 0 \Leftrightarrow \text{charge mode}) \end{cases}$$

$$(A.26) \quad \eta_{ESS} = \eta_{ESS}(P_{ESS}) = \dots^1$$

$$(A.27) \quad U_{ESS} = \text{getucell}(SoE) \cdot N_{\text{cellsser}}$$

¹ Derived from following relations:

$$\eta_{ESS} = \frac{|P_{ESS}| - |P_{ESS}^{\text{loss}}|}{|P_{ESS}|}; \quad P_{ESS}^{\text{loss}} = R_{ESS} \cdot \left(\frac{P_{ESS}}{U_{ESS}} \right)^2; \quad R_{ESS} = \frac{N_{\text{cell}}^{\text{ser}}}{N_{\text{cell}}^{\text{par}}} \cdot R_{\text{cell}}$$

10.6. Swing system

$$(A.28) \quad (T_{\text{SWEM}} \cdot r_{\text{SWGEAR}} - T_{\text{SWING}} - T_{\text{SWING}}^{\text{frict}}) = I_{\text{SWING}} \cdot \dot{\omega}_{\text{SWING}}$$

$$(A.29) \quad T_{\text{SWING}}^{\text{frict}} = \text{sign}(\omega_{\text{SW}}) \cdot \text{getswingfriction}(|\omega_{\text{SW}}|)$$

$$(A.30) \quad P_{\text{SWEM}}^{\text{el}} = P_{\text{SWEM}}^{\text{mech}} \cdot \varphi_{\text{SWEM}}$$

$$(A.31) \quad \varphi_{\text{SWEM}}(P_{\text{SWEM}}^{\text{mech}}, \eta_{\text{SWEM}}) \approx \begin{cases} \eta_{\text{SWEM}} & (P_{\text{SWEM}} < 0 \Leftrightarrow \text{generator mode}) \\ 1/\eta_{\text{SWEM}} & (P_{\text{SWEM}} > 0 \Leftrightarrow \text{motor mode}) \end{cases}$$

$$(A.32) \quad \eta_{\text{SWEM}} = \text{getswemeff}(T_{\text{SWEM}}, \omega_{\text{SWEM}})$$

10.7. Mapping definitions

$$(A.33) \quad \Omega_1(\omega_{\text{ENG}}) = \text{getboosttimeconstA}(\omega_{\text{ENG}})$$

$$(A.34) \quad \Omega_2(\omega_{\text{ENG}}) = \text{getboosttimeconstB}(\omega_{\text{ENG}})$$

$$(A.35) \quad \Omega_3(T_{\text{ENG}}, \omega_{\text{ENG}}) = \text{getboost}(T_{\text{ENG}}, \omega_{\text{ENG}})$$

$$(A.36) \quad \Omega_4(T_{\text{GEN}}, \omega_{\text{ENG}}, \eta_{\text{GEN}}) = \begin{cases} \eta_{\text{GEN}} & (P_{\text{GEN}} < 0 \Leftrightarrow \text{generator mode}) \\ 1/\eta_{\text{GEN}} & (P_{\text{GEN}} > 0 \Leftrightarrow \text{motor mode}) \end{cases}$$

$$(A.37) \quad \Omega_5(T_{\text{GEN}}, \omega_{\text{ENG}}) = \eta_{\text{GEN}} = \text{getgeneff}(T_{\text{GEN}}, \omega_{\text{ENG}})$$

$$(A.38) \quad \Omega_6(\omega_{\text{ENG}}) = k_1(\omega_{\text{ENG}})$$

$$(A.39) \quad \Omega_7(\omega_{\text{ENG}}) = k_2(\omega_{\text{ENG}})$$

$$(A.40) \quad \Omega_8(P_{\text{ESS}}) = \begin{cases} 1/\eta_{\text{ESS}} & (P_{\text{ESS}} > 0 \Leftrightarrow \text{discharge mode}) \\ \eta_{\text{ESS}} & (P_{\text{ESS}} < 0 \Leftrightarrow \text{charge mode}) \end{cases}$$

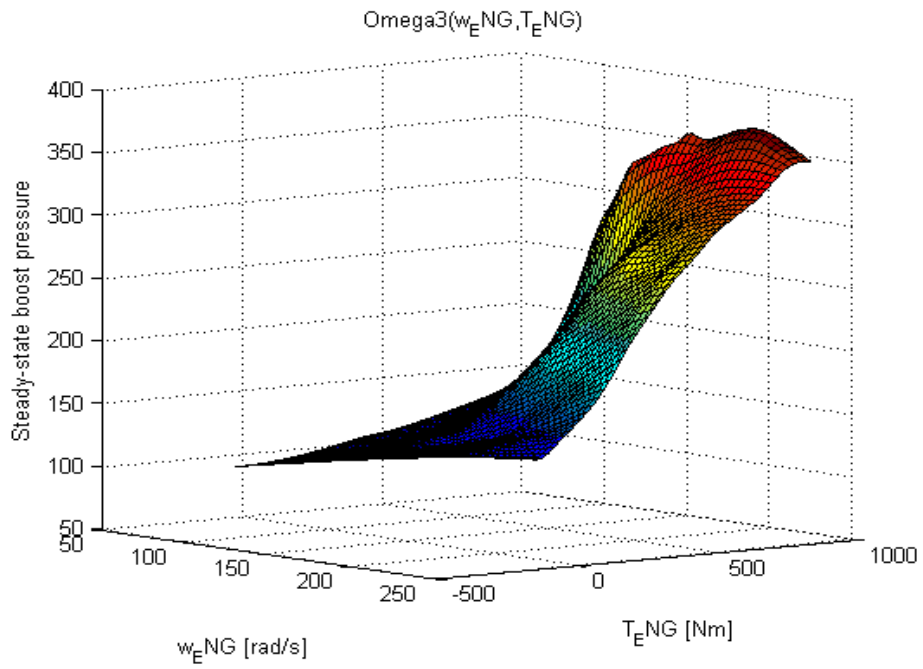
$$(A.41) \quad \Omega_9(P_{\text{ESS}}) = \eta_{\text{ESS}}(P_{\text{ESS}}) = \frac{|P_{\text{ESS}}| - \left| \frac{N_{\text{cell}}^{\text{ser}}}{N_{\text{cell}}^{\text{par}}} \cdot R_{\text{cell}} \cdot \left(\frac{P_{\text{ESS}}}{U_{\text{ESS}}} \right)^2 \right|}{|P_{\text{ESS}}|}$$

$$(A.42) \quad \Omega_{10}(\text{SoE}) = U_{\text{ESS}} = \text{getucell}(\text{SoE})$$

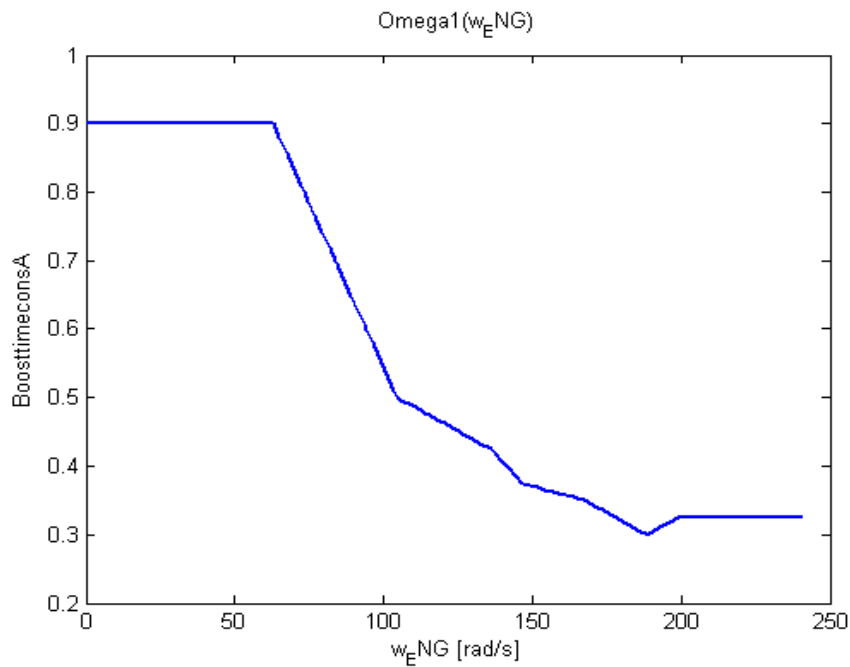
$$(A.43) \quad \Omega_{11}(T_{\text{ENG}}, \omega_{\text{ENG}}) = \text{getfuelcons}(T_{\text{ENG}}, \omega_{\text{ENG}})$$

10.8. Graphical illustration of maps

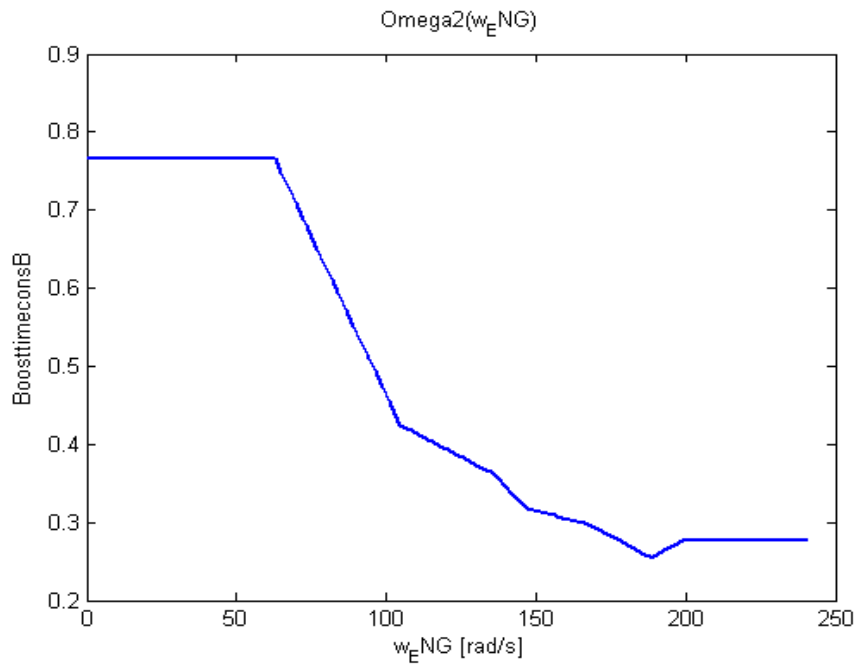
Graphical illustration of the steady-state turbo boost map: $\Omega_3(\omega_{ENG}, T_{ENG})$



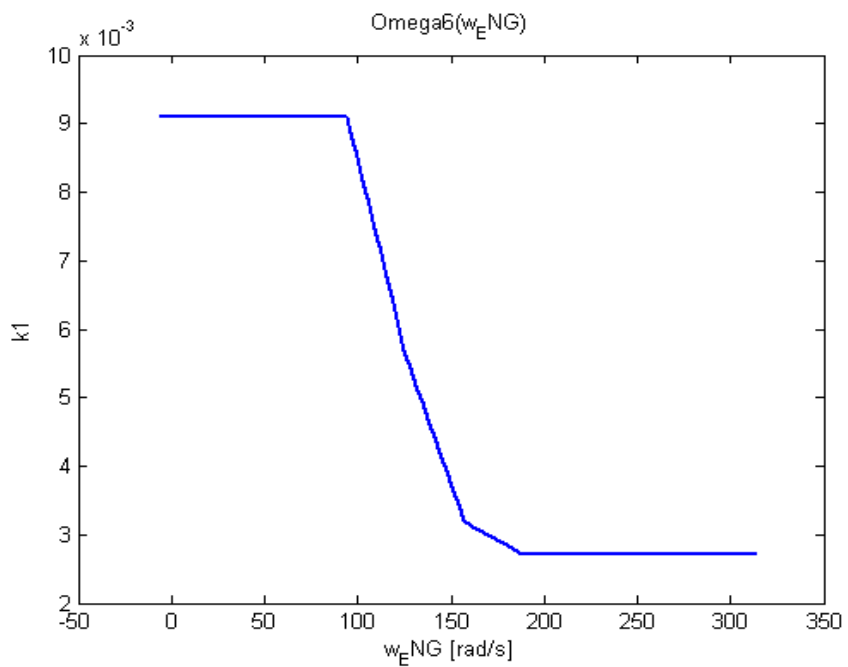
Graphical illustration of the timeboostconstantA: $\Omega_1(\omega_{ENG})$



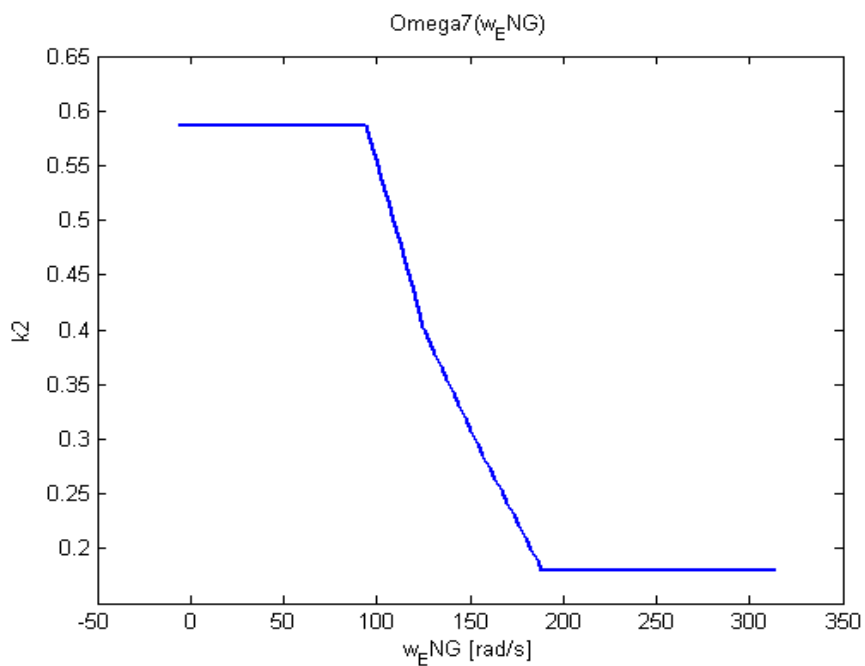
Graphical illustration of the timeboostconstantB: $\Omega_2(\omega_{ENG})$



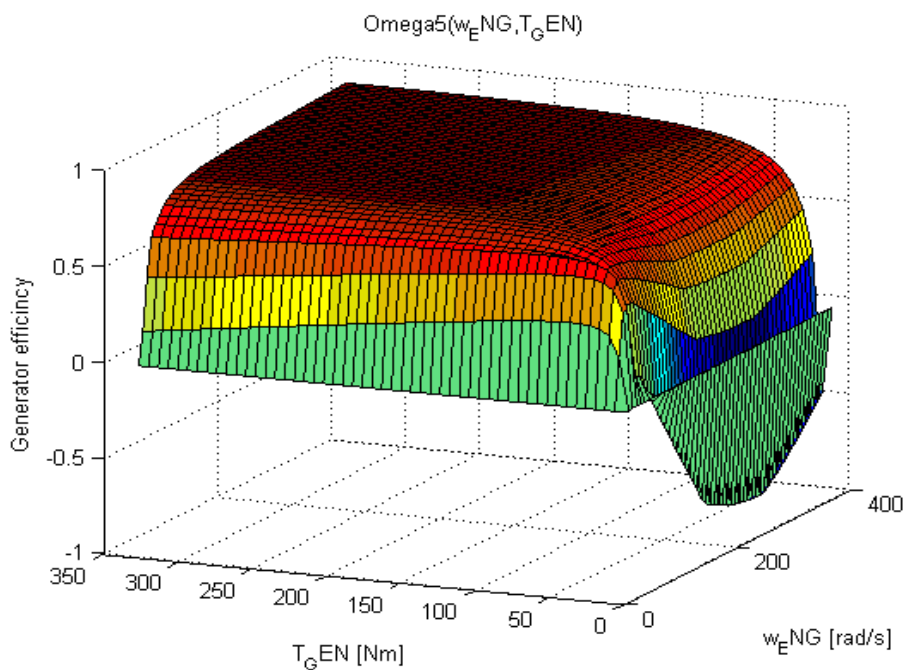
Graphical illustration of the k1 function in the boosttorque: $\Omega_6(\omega_{ENG})$



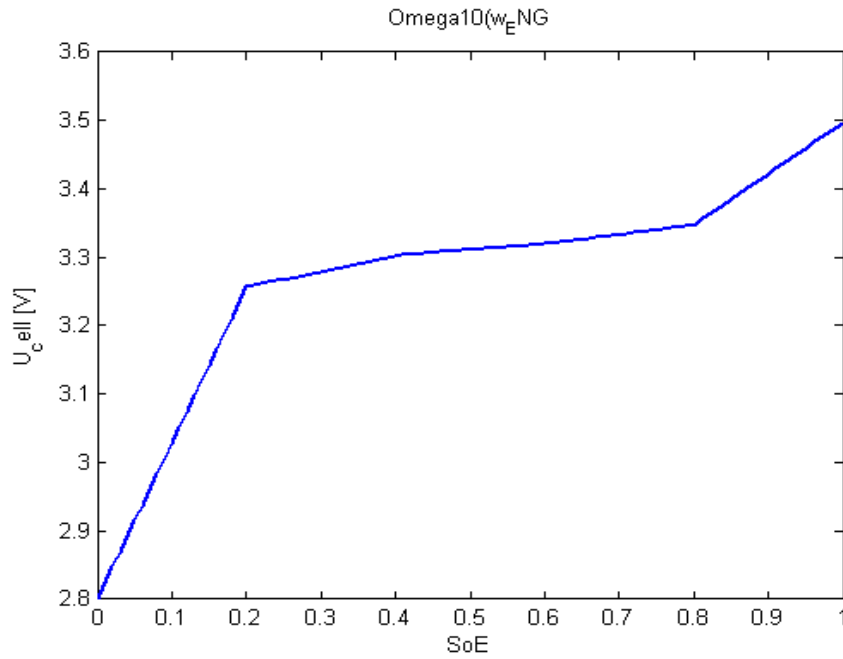
Graphical illustration of the k2 function in the boosttorque: $\Omega_7(\omega_{ENG})$



Graphical illustration of generator efficiency map: $\Omega_5(\omega_{ENG}, T_{GEN})$



Graphical illustration of the ucell map: $\Omega_{10}(\omega_{ENG})$



10.9. Switch

$$(A.44) \quad isengon = true / false$$

$$(A.45) \quad dp = getboost(T_{ENG}, \omega_{ENG}) - p_{boost} \geq 0 \text{ or } < 0$$

$$(A.46) \quad P_{GEN}^{mech} = \omega_{ENG} \cdot T_{GEN} \geq 0 \text{ or } < 0$$

$$(A.47) \quad P_{ESS} = \omega_{ENG} \cdot T_{GEN} \cdot getgeneff(T_{GEN}, \omega_{ENG}) + P_{AUX} + P_{SWEM}^{el} \geq 0 \text{ or } < 0$$

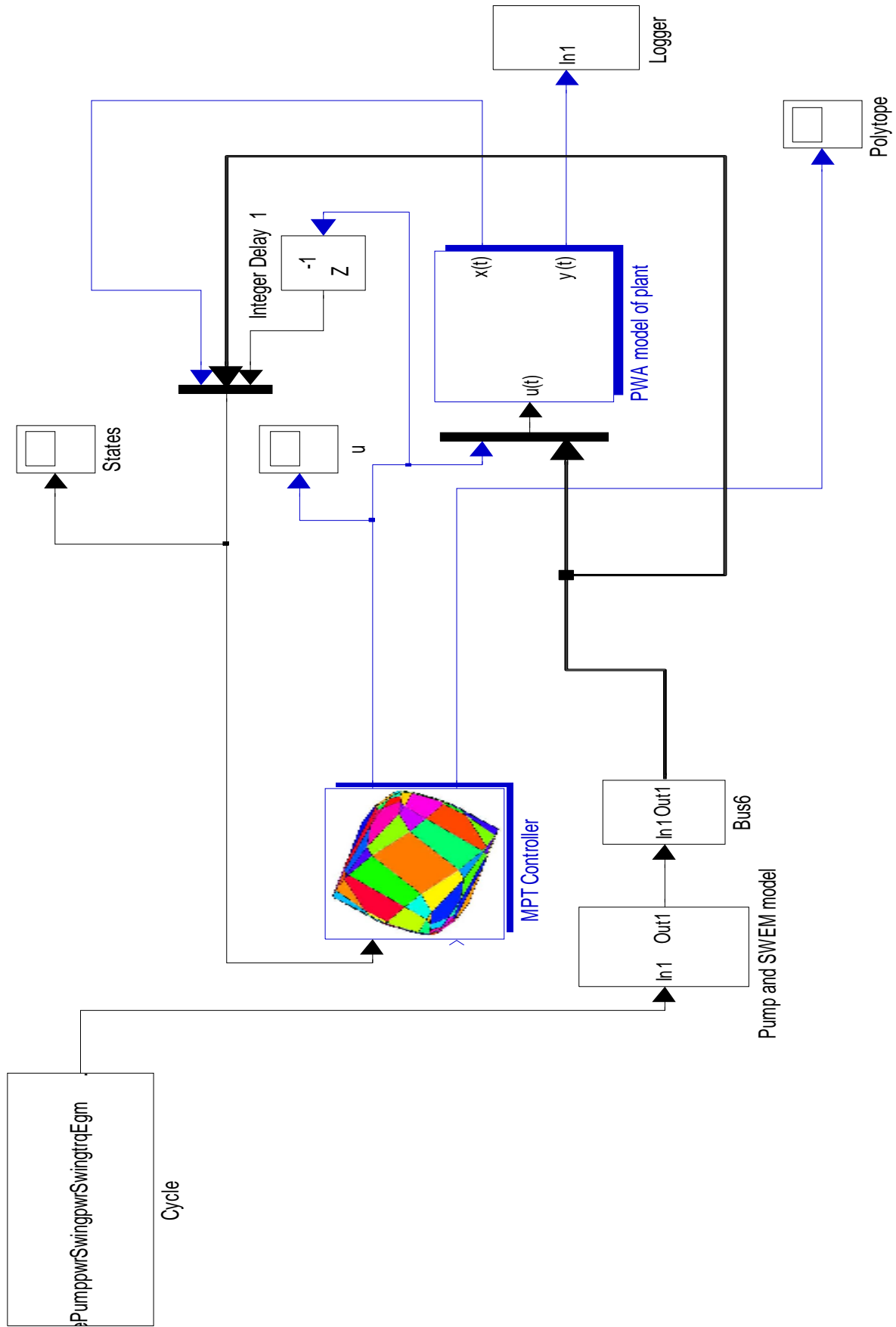
10.10. Constraints

- C1. $T_{\text{ENG}}^{\text{max}}(\omega_{\text{ENG}}) = \text{getmaxenginotorque}(\omega_{\text{ENG}})$
- C2. $T_{\text{ENG}} < T_{\text{ENG}}^{\text{max, smoke}}(\omega_{\text{ENG}})$
- C3. $P_{\text{ENG}} > 0$
- C4. $\omega_{\text{ENG}} < \omega_{\text{ENG}}^{\text{max}}(\text{EGM}) = \text{getminenginespeedforworkmode}(\text{EGM})$
- C5. $\omega_{\text{ENG}} > \omega_{\text{ENG}}^{\text{min}}(\text{EGM}) = \text{getmaxenginespeedforworkmode}(\text{EGM})$ ²
- C6. $|P_{\text{GEN}}| < P_{\text{GEN}}^{\text{max}}$
- C7. $|T_{\text{GEN}}| < T_{\text{GEN}}^{\text{max}}$
- C8. $|\omega_{\text{GEN}}| < \omega_{\text{GEN}}^{\text{max}}$
- C9. $|P_{\text{SWEM}}| < P_{\text{SWEM}}^{\text{max}}$
- C10. $|T_{\text{SWEM}}| < T_{\text{SWEM}}^{\text{max}}$
- C11. $|\omega_{\text{SWEM}}| < \omega_{\text{SWEM}}^{\text{max}}$
- C12. $P_{\text{ESS}} < P_{\text{ESS}}^{\text{max}}$
- C13. $P_{\text{ESS}} > -|P_{\text{ESS}}^{\text{min}}|$ ³
- C14. $U_{\text{ESS}} > U_{\text{ESS}}^{\text{min}}$
- C15. $U_{\text{ESS}} < U_{\text{ESS}}^{\text{max}}$
- C16. $|I_{\text{ESS}}| < I_{\text{ESS}}^{\text{max}}$
- C17. $\text{SoE} < 1$
- C18. $\text{SoE} > 0$
- C19. $|T_{\text{pumps}}| < T_{\text{pumps}}^{\text{max}}$
- C20. $\text{engineOn}(t) = \text{engineOn}(t - dt)$, when $T_{\text{InEngineMode}} < T_{\text{minInEngineMode}}$

² Only valid when engine is on

³ For some battery types $|P_{\text{ESS min}}| \gg P_{\text{ESS max}}$

10.12. Simulink file for MPC control



10.13. Coefficients in the jacobian matrices

States

If $dp \geq 0$:

$$(A.48) \quad a_{11} = \frac{dl}{xl^2 I_{ENG}}$$

$$(A.49) \quad a_{12} = 0$$

$$(A.50) \quad b_{11} = \frac{1}{I_{ENG}}$$

$$(A.51) \quad b_{12} = \frac{1}{I_{ENG}}$$

$$(A.52) \quad bd_{11} = -\frac{1}{xl I_{ENG}}$$

$$(A.53) \quad a_{21} = \frac{\frac{\partial}{\partial xl} \Omega_3(xl, ul)}{\Omega_2(xl)} - \frac{(\Omega_3(xl, ul) - x2) \left(\frac{d}{dxl} \Omega_2(xl) \right)}{\Omega_2(xl)^2} + \frac{K_{corr} x2 \left(ul + u2 - \frac{dl}{xl} \right)}{xl^2 I_{ENG}} - \frac{K_{corr} x2 dl}{xl^3 I_{ENG}}$$

$$(A.54) \quad a_{22} = -\frac{1}{\Omega_2(xl)} - \frac{K_{corr} \left(ul + u2 - \frac{dl}{xl} \right)}{xl I_{ENG}}$$

$$(A.55) \quad b_{21} = \frac{\frac{\partial}{\partial ul} \Omega_3(xl, ul)}{\Omega_2(xl)} - \frac{K_{corr} x2}{xl I_{ENG}}$$

$$(A.56) \quad a_{91} = -\frac{K_{corr} x2}{xl I_{ENG}}$$

$$(A.57) \quad bd_{21} = \frac{K_{corr} x2}{xl^2 I_{ENG}}$$

If $dp < 0$:

$$(A.58) \quad a_{11} = \frac{1}{I_{ENG}} \left(-\left(\frac{d}{dxl} \Omega_6(xl) \right) (\Omega_3(xl, ul) - x2)^2 - 2 \Omega_6(xl) (\Omega_3(xl, ul) - x2) \left(\frac{\partial}{\partial xl} \Omega_3(xl, ul) \right) - \left(\frac{d}{dxl} \Omega_7(xl) \right) (\Omega_3(xl, ul) - x2) - \Omega_7(xl) \left(\frac{\partial}{\partial xl} \Omega_3(xl, ul) \right) + \frac{dl}{xl^2} \right)$$

$$a_{12} = \frac{2 \Omega_6(xl) (\Omega_3(xl, ul) - x2) + \Omega_7(xl)}{I_{ENG}}$$

(A.59)

$$b_{11} = \frac{1}{I_{ENG}} \left(1 - 2 \Omega_6(xl) (\Omega_3(xl, ul) - x2) \left(\frac{\partial}{\partial ul} \Omega_3(xl, ul) \right) - \Omega_7(xl) \left(\frac{\partial}{\partial ul} \Omega_3(xl, ul) \right) \right)$$

(A.60)

$$b_{12} = \frac{1}{I_{ENG}}$$

(A.61)

$$bd_{11} = -\frac{1}{xl I_{ENG}}$$

(A.62)

$$a_{21} = \frac{\frac{\partial}{\partial xl} \Omega_3(xl, ul)}{\Omega_1(xl)} - \frac{(\Omega_3(xl, ul) - x2) \left(\frac{d}{dxl} \Omega_1(xl) \right)}{\Omega_1(xl)^2} + \frac{1}{xl^2 I_{ENG}} \left(K_{corr} x2 \left(ul - \Omega_6(xl) (\Omega_3(xl, ul) - x2)^2 - \Omega_7(xl) (\Omega_3(xl, ul) - x2) + u2 - \frac{dl}{xl} \right) \right) - \frac{1}{xl I_{ENG}} \left(K_{corr} x2 \left(- \left(\frac{d}{dxl} \Omega_6(xl) \right) (\Omega_3(xl, ul) - x2)^2 - 2 \Omega_6(xl) (\Omega_3(xl, ul) - x2) \left(\frac{\partial}{\partial xl} \Omega_3(xl, ul) \right) - \left(\frac{d}{dxl} \Omega_7(xl) \right) (\Omega_3(xl, ul) - x2) - \Omega_7(xl) \left(\frac{\partial}{\partial xl} \Omega_3(xl, ul) \right) + \frac{dl}{xl^2} \right) \right)$$

(A.63)

$$a_{22} = -\frac{1}{\Omega_1(xl)} - \frac{1}{xl I_{ENG}} \left(K_{corr} \left(ul - \Omega_6(xl) (\Omega_3(xl, ul) - x2)^2 - \Omega_7(xl) (\Omega_3(xl, ul) - x2) + u2 - \frac{dl}{xl} \right) \right) - \frac{K_{corr} x2 (2 \Omega_6(xl) (\Omega_3(xl, ul) - x2) + \Omega_7(xl))}{xl I_{ENG}}$$

(A.64)

$$b_{21} = \frac{\frac{\partial}{\partial ul} \Omega_3(xl, ul)}{\Omega_1(xl)} - \frac{1}{xl I_{ENG}} \left(K_{corr} x2 \left(1 - 2 \Omega_6(xl) (\Omega_3(xl, ul) - x2) \left(\frac{\partial}{\partial ul} \Omega_3(xl, ul) \right) - \Omega_7(xl) \left(\frac{\partial}{\partial ul} \Omega_3(xl, ul) \right) \right) \right)$$

(A.65)

$$b_{22} = -\frac{K_{corr} x2}{xl I_{ENG}}$$

(A.66)

$$bd_{21} = \frac{K_{corr} x2}{xl^2 I_{ENG}}$$

(A.67)

$$a_{31} = - \frac{u2 \Omega_5(x1, u2) + u2 x1 \left(\frac{\partial}{\partial x1} \Omega_5(x1, u2) \right)}{\left(1 - \frac{R_{cell} (u2 x1 \Omega_5(x1, u2) + P_{AUX} + d2)}{N_{ser} N_{par} \Omega_{10}(x3)^2} \right) E_{MAX}} \\ - \left((u2 x1 \Omega_5(x1, u2) + P_{AUX} + d2) R_{cell} (u2 \Omega_5(x1, u2) + \iota \right. \\ \left. - \frac{R_{cell} (u2 x1 \Omega_5(x1, u2) + P_{AUX} + d2)}{N_{ser} N_{par} \Omega_{10}(x3)^2} \right) \\ \left. E_{MAX} N_{ser} N_{par} \Omega_{10}(x3)^2 \right)$$

$$a_{33} = \left(2 (u2 x1 \Omega_5(x1, u2) + P_{AUX} + d2)^2 R_{cell} \left(\frac{d}{dx3} \Omega_{10}(x3) \right) \right) \\ \left(\left(1 - \frac{R_{cell} (u2 x1 \Omega_5(x1, u2) + P_{AUX} + d2)}{N_{ser} N_{par} \Omega_{10}(x3)^2} \right) \right) \\ \left. E_{MAX} N_{ser} N_{par} \Omega_{10}(x3)^3 \right)$$

(A.68)

$$b_{32} = - \frac{x1 \Omega_5(x1, u2) + u2 x1 \left(\frac{\partial}{\partial u2} \Omega_5(x1, u2) \right)}{\left(1 - \frac{R_{cell} (u2 x1 \Omega_5(x1, u2) + P_{AUX} + d2)}{N_{ser} N_{par} \Omega_{10}(x3)^2} \right) E_{MAX}} \\ - \left((u2 x1 \Omega_5(x1, u2) + P_{AUX} + d2) R_{cell} (x1 \Omega_5(x1, u2) + \iota \right. \\ \left. - \frac{R_{cell} (u2 x1 \Omega_5(x1, u2) + P_{AUX} + d2)}{N_{ser} N_{par} \Omega_{10}(x3)^2} \right) \\ \left. E_{MAX} N_{ser} N_{par} \Omega_{10}(x3)^2 \right)$$

(A.69)

$$bd_{32} = - \frac{1}{\left(1 - \frac{R_{cell} (u2 \ x1 \ \Omega_5(x1, u2) + P_{AUX} + d2)}{N_{ser} N_{par} \Omega_{10}(x3)^2} \right) E_{MAX}} - \left((u2 \ x1 \ \Omega_5(x1, u2) + P_{AUX} + d2) R_{cell} \right) / \left(\left(1 - \frac{R_{cell} (u2 \ x1 \ \Omega_5(x1, u2) + P_{AUX} + d2)}{N_{ser} N_{par} \Omega_{10}(x3)^2} \right) E_{MAX} N_{ser} N_{par} \Omega_{10}(x3)^2 \right)$$

(A.70)

If $P_{ESS} < 0$ and $T_{GEN} * w_{ENG} < 0$:

$$a_{31} = - \frac{1}{E_{MAX}} \left(\left(u2 \ \Omega_5(x1, u2) + u2 \ x1 \ \left(\frac{\partial}{\partial x1} \Omega_5(x1, u2) \right) \right) \left(1 + \frac{R_{cell} (u2 \ x1 \ \Omega_5(x1, u2) + P_{AUX} + d2)}{N_{ser} N_{par} \Omega_{10}(x3)^2} \right) \right) - \frac{1}{N_{ser} N_{par} \Omega_{10}(x3)^2 E_{MAX}} \left((u2 \ x1 \ \Omega_5(x1, u2) + P_{AUX} + d2) R_{cell} \left(u2 \ \Omega_5(x1, u2) + u2 \ x1 \ \left(\frac{\partial}{\partial x1} \Omega_5(x1, u2) \right) \right) \right)$$

(A.71)

$$a_{33} = \frac{2 (u2 \ x1 \ \Omega_5(x1, u2) + P_{AUX} + d2)^2 R_{cell} \left(\frac{d}{dx3} \Omega_{10}(x3) \right)}{N_{ser} N_{par} \Omega_{10}(x3)^3 E_{MAX}}$$

(A.72)

$$b_{32} = - \frac{1}{E_{MAX}} \left(\left(x1 \ \Omega_5(x1, u2) + u2 \ x1 \ \left(\frac{\partial}{\partial u2} \Omega_5(x1, u2) \right) \right) \left(1 + \frac{R_{cell} (u2 \ x1 \ \Omega_5(x1, u2) + P_{AUX} + d2)}{N_{ser} N_{par} \Omega_{10}(x3)^2} \right) \right) - \frac{1}{N_{ser} N_{par} \Omega_{10}(x3)^2 E_{MAX}} \left((u2 \ x1 \ \Omega_5(x1, u2) + P_{AUX} + d2) R_{cell} \left(x1 \ \Omega_5(x1, u2) + u2 \ x1 \ \left(\frac{\partial}{\partial u2} \Omega_5(x1, u2) \right) \right) \right)$$

(A.73)

$$bd_{32} = - \frac{1 + \frac{R_{cell} (u2 \ x1 \ \Omega_5(x1, u2) + P_{AUX} + d2)}{N_{ser} N_{par} \Omega_{10}(x3)^2}}{E_{MAX}} - \frac{(u2 \ x1 \ \Omega_5(x1, u2) + P_{AUX} + d2) R_{cell}}{N_{ser} N_{par} \Omega_{10}(x3)^2 E_{MAX}}$$

(A.74)

If $P_{ESS} \geq 0$ and $T_{GEN} * w_{ENG} \geq 0$:

$$\begin{aligned}
a_{31} = & - \frac{\frac{u_2}{\Omega_5(x_1, u_2)} - \frac{u_2 x_1 \left(\frac{\partial}{\partial x_1} \Omega_5(x_1, u_2) \right)}{\Omega_5(x_1, u_2)^2}}{\left(1 - \frac{R_{cell} \left(\frac{u_2 x_1}{\Omega_5(x_1, u_2)} + P_{AUX} + d_2 \right)}{N_{ser} N_{par} \Omega_{10}(x_3)^2} \right) E_{max}} \\
& - \left(\left(\frac{u_2 x_1}{\Omega_5(x_1, u_2)} + P_{AUX} + d_2 \right) R_{cell} \left(\frac{u_2}{\Omega_5(x_1, u_2)} - \frac{u_2 x_1}{\Omega_5(x_1, u_2)^2} \right. \right. \\
& \left. \left. - \frac{R_{cell} \left(\frac{u_2 x_1}{\Omega_5(x_1, u_2)} + P_{AUX} + d_2 \right)}{N_{ser} N_{par} \Omega_{10}(x_3)^2} \right) \right) \\
& \left. E_{max} N_{ser} N_{par} \Omega_{10}(x_3)^2 \right)
\end{aligned}
\tag{A.75}$$

$$\begin{aligned}
a_{33} = & \left(2 \left(\frac{u_2 x_1}{\Omega_5(x_1, u_2)} + P_{AUX} + d_2 \right)^2 R_{cell} \left(\frac{d}{dx_3} \Omega_{10}(x_3) \right) \right) / \\
& - \left(\frac{R_{cell} \left(\frac{u_2 x_1}{\Omega_5(x_1, u_2)} + P_{AUX} + d_2 \right)}{N_{ser} N_{par} \Omega_{10}(x_3)^2} \right) \\
& \left. E_{max} N_{ser} N_{par} \Omega_{10}(x_3)^3 \right)
\end{aligned}
\tag{A.76}$$

$$\begin{aligned}
b_{32} = & - \frac{\frac{x_1}{\Omega_5(x_1, u_2)} - \frac{u_2 x_1 \left(\frac{\partial}{\partial u_2} \Omega_5(x_1, u_2) \right)}{\Omega_5(x_1, u_2)^2}}{\left(1 - \frac{R_{cell} \left(\frac{u_2 x_1}{\Omega_5(x_1, u_2)} + P_{AUX} + d_2 \right)}{N_{ser} N_{par} \Omega_{10}(x_3)^2} \right) E_{max}} \\
& - \left(\left(\frac{u_2 x_1}{\Omega_5(x_1, u_2)} + P_{AUX} + d_2 \right) R_{cell} \left(\frac{x_1}{\Omega_5(x_1, u_2)} - \frac{u_2 x_1}{\Omega_5(x_1, u_2)^2} \right. \right. \\
& \left. \left. - \frac{R_{cell} \left(\frac{u_2 x_1}{\Omega_5(x_1, u_2)} + P_{AUX} + d_2 \right)}{N_{ser} N_{par} \Omega_{10}(x_3)^2} \right) \right) \\
& \left. E_{max} N_{ser} N_{par} \Omega_{10}(x_3)^2 \right)
\end{aligned}
\tag{A.77}$$

$$(A.78) \quad bd_{32} = - \frac{1}{\left(1 - \frac{R_{cell} \left(\frac{u2 \ x1}{\Omega_5(x1, u2)} + P_{AUX} + d2 \right)}{N_{ser} N_{par} \Omega_{10}(x3)^2} \right) E_{max} \left(1 - \frac{R_{cell} \left(\frac{u2 \ x1}{\Omega_5(x1, u2)} + P_{AUX} + d2 \right)}{N_{ser} N_{par} \Omega_{10}(x3)^2} \right)^2 E_{max} N_{ser} N_{par} \Omega_{10}(x3)^2}$$

If $P_{ESS} < 0$ and $T_{GEN} * W_{ENG} >= 0$:

$$(A.79) \quad bd_{32} = - \frac{1}{\left(1 - \frac{R_{cell} \left(\frac{u2 \ x1}{\Omega_5(x1, u2)} + P_{AUX} + d2 \right)}{N_{ser} N_{par} \Omega_{10}(x3)^2} \right) E_{max} \left(1 - \frac{R_{cell} \left(\frac{u2 \ x1}{\Omega_5(x1, u2)} + P_{AUX} + d2 \right)}{N_{ser} N_{par} \Omega_{10}(x3)^2} \right)^2 E_{max} N_{ser} N_{par} \Omega_{10}(x3)^2}$$

$$(A.80) \quad a_{33} = \frac{2 \left(\frac{u2 \ x1}{\Omega_5(x1, u2)} + P_{AUX} + d2 \right)^2 R_{cell} \left(\frac{d}{dx3} \Omega_{10}(x3) \right)}{N_{ser} N_{par} \Omega_{10}(x3)^3 E_{MAX}}$$

$$(A.81) \quad b_{32} = - \frac{1}{E_{MAX}} \left(\left(\frac{x1}{\Omega_5(x1, u2)} - \frac{u2 \ x1 \left(\frac{\partial}{\partial u2} \Omega_5(x1, u2) \right)}{\Omega_5(x1, u2)^2} \right) \left(1 + \frac{R_{cell} \left(\frac{u2 \ x1}{\Omega_5(x1, u2)} + P_{AUX} + d2 \right)}{N_{ser} N_{par} \Omega_{10}(x3)^2} \right) \right) - \frac{1}{N_{ser} N_{par} \Omega_{10}(x3)^2 E_{MAX}} \left(\left(\frac{u2 \ x1}{\Omega_5(x1, u2)} + P_{AUX} + d2 \right) R_{cell} \left(\frac{x1}{\Omega_5(x1, u2)} - \frac{u2 \ x1 \left(\frac{\partial}{\partial u2} \Omega_5(x1, u2) \right)}{\Omega_5(x1, u2)^2} \right) \right)$$

$$(A.82) \quad bd_{32} = - \frac{1 + \frac{R_{cell} \left(\frac{u2 \ x1}{\Omega_5(x1, u2)} + P_{AUX} + d2 \right)}{N_{ser} N_{par} \Omega_{10}(x3)^2}}{E_{MAX}} - \frac{\left(\frac{u2 \ x1}{\Omega_5(x1, u2)} + P_{AUX} + d2 \right) R_{cell}}{N_{ser} N_{par} \Omega_{10}(x3)^2 E_{MAX}}$$

Outputs

$$(A.83) \quad c_{11} = 1$$

$$(A.84) \quad d_{21} = 1$$

If $dp > 0$

$$(A.85) \quad c_{31} = 0$$

$$(A.86) \quad c_{32} = 0$$

$$(A.87) \quad d_{31} = 0$$

If $dp \leq 0$

$$(A.88) \quad c_{31} = - \left(\frac{d}{dxl} \Omega_6(xl) \right) \left(\Omega_3(xl, ul) - x2 \right)^2 - 2 \Omega_6(xl) \left(\Omega_3(xl, ul) - x2 \right) \left(\frac{\partial}{\partial xl} \Omega_3(xl, ul) \right) - \left(\frac{d}{dxl} \Omega_7(xl) \right) \left(\Omega_3(xl, ul) - x2 \right) - \Omega_7(xl) \left(\frac{\partial}{\partial xl} \Omega_3(xl, ul) \right)$$

$$(A.89) \quad c_{32} = 2 \Omega_6(xl) \left(\Omega_3(xl, ul) - x2 \right) + \Omega_7(xl)$$

$$(A.90) \quad d_{31} = -2 \Omega_6(xl) \left(\Omega_3(xl, ul) - x2 \right) \left(\frac{\partial}{\partial ul} \Omega_3(xl, ul) \right) - \Omega_7(xl) \left(\frac{\partial}{\partial ul} \Omega_3(xl, ul) \right)$$

$$(A.91) \quad c_{42} = 1$$

$$(A.92) \quad c_{51} = - \frac{dl}{xl^2}$$

$$(A.93) \quad dd_{51} = \frac{1}{xl}$$

$$(A.94) \quad c_{61} = \frac{\partial}{\partial xl} \Omega_{11}(xl, ul)$$

$$(A.95) \quad d_{61} = \frac{\partial}{\partial ul} \Omega_{11}(xl, ul)$$

$$(A.96) \quad c_{83} = 1$$

$P_{Gen} < 0$

$$(A.97) \quad c_{71} = u2 \Omega_5(xl, u2) + u2 xl \left(\frac{\partial}{\partial xl} \Omega_5(xl, u2) \right)$$

$$(A.98) \quad d_{72} = xl \Omega_5(xl, u2) + u2 xl \left(\frac{\partial}{\partial u2} \Omega_5(xl, u2) \right)$$

$$(A.99) \quad dd_{72} = 1$$

$P_{Gen} \geq 0$

$$(A.100) \quad c_{71} = \frac{u2}{\Omega_5(x1, u2)} - \frac{u2 x1 \left(\frac{\partial}{\partial x1} \Omega_5(x1, u2) \right)}{\Omega_5(x1, u2)^2}$$

$$(A.101) \quad d_{72} = \frac{x1}{\Omega_5(x1, u2)} - \frac{u2 x1 \left(\frac{\partial}{\partial u2} \Omega_5(x1, u2) \right)}{\Omega_5(x1, u2)^2}$$

$$(A.102) \quad dd_{72} = 1$$

$P_{ESS} \geq 0$ and $P_{Gen} < 0$

$$(A.103) \quad c_{91} = - \frac{const \left(u2 \Omega_5(x1, u2) + x1 u2 \left(\frac{\partial}{\partial x1} \Omega_5(x1, u2) \right) \right)}{\Omega_{10}(x3)^2}$$

$$(A.104) \quad c_{93} = \frac{2 const \left(x1 u2 \Omega_5(x1, u2) + P_{AUX} + d2 \right) \left(\frac{d}{dx3} \Omega_{10}(x3) \right)}{\Omega_{10}(x3)^3}$$

$$(A.105) \quad d_{92} = - \frac{const \left(x1 \Omega_5(x1, u2) + x1 u2 \left(\frac{\partial}{\partial u2} \Omega_5(x1, u2) \right) \right)}{\Omega_{10}(x3)^2}$$

$$(A.106) \quad dd_{92} = - \frac{const}{\Omega_{10}(x3)^2}$$

$P_{ESS} \geq 0$ and $P_{Gen} \geq 0$

$$(A.107) \quad c_{91} = \frac{const \left(u2 \Omega_5(x1, u2) + x1 u2 \left(\frac{\partial}{\partial x1} \Omega_5(x1, u2) \right) \right)}{\Omega_{10}(x3)^2}$$

$$(A.108) \quad c_{93} = - \frac{2 const \left(x1 u2 \Omega_5(x1, u2) + P_{AUX} + d2 \right) \left(\frac{d}{dx3} \Omega_{10}(x3) \right)}{\Omega_{10}(x3)^3}$$

$$(A.109) \quad d_{92} = \frac{const \left(x1 \Omega_5(x1, u2) + x1 u2 \left(\frac{\partial}{\partial u2} \Omega_5(x1, u2) \right) \right)}{\Omega_{10}(x3)^2}$$

$$(A.110) \quad dd_{92} = \frac{const}{\Omega_{10}(x3)^2}$$

$P_{ESS} < 0$ and $P_{Gen} < 0$

$$(A.111) \quad c_{91} = - \frac{const \left(\frac{u2}{\Omega_5(x1, u2)} - \frac{x1 u2 \left(\frac{\partial}{\partial x1} \Omega_5(x1, u2) \right)}{\Omega_5(x1, u2)^2} \right)}{\Omega_{10}(x3)^2}$$

$$(A.112) \quad c_{93} = \frac{2 \text{ const} \left(\frac{x1 u2}{\Omega_5(x1, u2)} + P_{AUX} + d2 \right) \left(\frac{d}{dx3} \Omega_{10}(x3) \right)}{\Omega_{10}(x3)^3}$$

$$(A.113) \quad d_{92} = - \frac{\text{const} \left(\frac{x1}{\Omega_5(x1, u2)} - \frac{x1 u2 \left(\frac{\partial}{\partial u2} \Omega_5(x1, u2) \right)}{\Omega_5(x1, u2)^2} \right)}{\Omega_{10}(x3)^2}$$

$$(A.114) \quad dd_{92} = - \frac{\text{const}}{\Omega_{10}(x3)^2}$$

$P_{ESS} < 0$ and $P_{Gen} \geq 0$

$$(A.115) \quad c_{91} = \frac{\text{const} \left(\frac{u2}{\Omega_5(x1, u2)} - \frac{x1 u2 \left(\frac{\partial}{\partial x1} \Omega_5(x1, u2) \right)}{\Omega_5(x1, u2)^2} \right)}{\Omega_{10}(x3)^2}$$

$$(A.116) \quad c_{93} = - \frac{2 \text{ const} \left(\frac{x1 u2}{\Omega_5(x1, u2)} + P_{AUX} + d2 \right) \left(\frac{d}{dx3} \Omega_{10}(x3) \right)}{\Omega_{10}(x3)^3}$$

$$(A.117) \quad d_{92} = \frac{\text{const} \left(\frac{x1}{\Omega_5(x1, u2)} - \frac{x1 u2 \left(\frac{\partial}{\partial u2} \Omega_5(x1, u2) \right)}{\Omega_5(x1, u2)^2} \right)}{\Omega_{10}(x3)^2}$$

$$(A.118) \quad dd_{92} = \frac{\text{const}}{\Omega_{10}(x3)^2}$$